Bulletin No. 58

Hydrogeology of the Swan Hills Area, Alberta: Evaluation for deep waste injection

Brian Hitchon,
Claude M. Sauveplane,
Stefan Bachu, Emlyn H. Koster
and Andre T. Lytviak

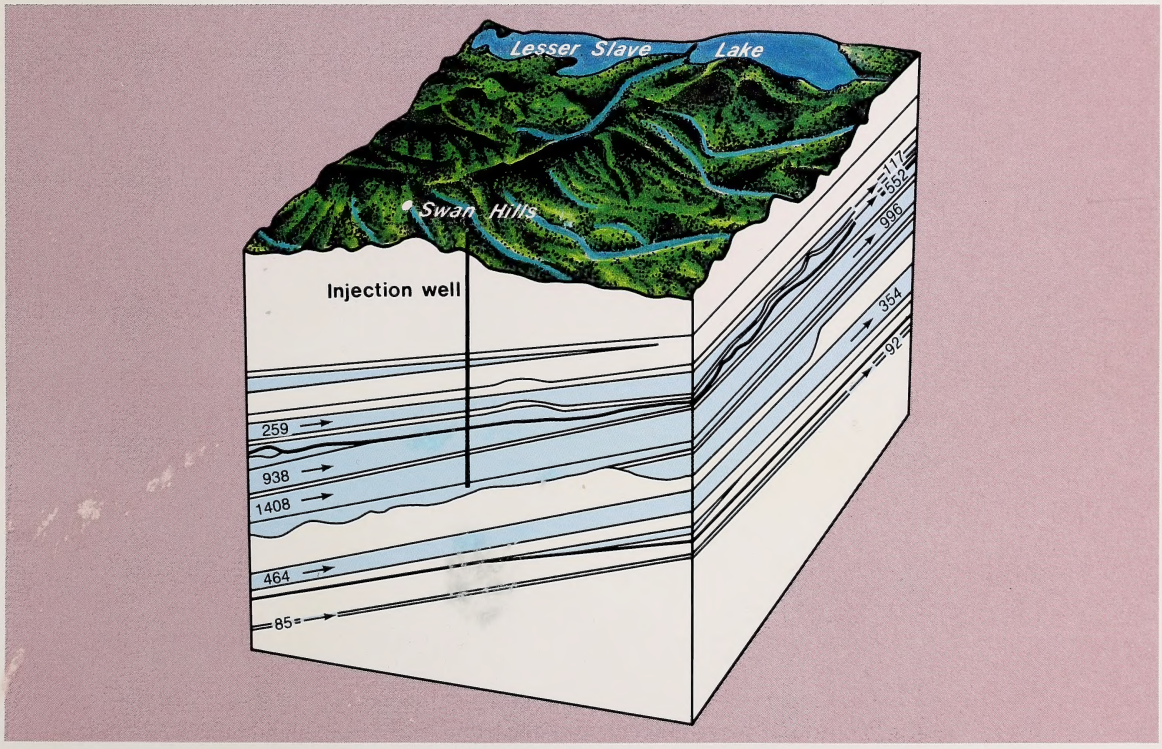

ALBERTA RESEARCH COUNCIL

Geological Survey Department

Hydrogeology of the Swan Hills Area, Alberta: Evaluation for deep waste injection

Brian Hitchon, Claude M. Sauveplane, Stefan Bachu, Emlyn H. Koster and Andre T. Lytviak

Cover:
Block diagram of the Phanerozoic succession in the northwest half of the Swan Hills model area, showing input and output flow rates and the rates of cross-formational flow for the entire block; (flow rates in m^3/d).

GEOLOGICAL SURVEY DEPARTMENT, ALBERTA RESEARCH COUNCIL
EDMONTON, ALBERTA, CANADA 1989

Acknowledgments

The work on which this study is based was funded by the Alberta Special Waste Management Corporation, and the writers thank John P.C. Elson (formerly Chairman and Chief Executive Officer) and Ken J. Simpson (Senior Vice President, System Development and Operations) for their cooperation and understanding in what eventually became a major technical undertaking. Dr. S.R. Moran (Terrain Sciences Department) provided project liaison between the Alberta Research Council and the Corporation. The extensive technical computer support necessary to carry out the study was ably provided by Michel E. Brulotte. The massive data entry requirements were carried out by Kelly D. Roberts and Parminder K. Sahota. For the regional geology, the determination of the detailed stratigraphy of the Cambrian was made by Anne Ing, of the Banff shales by Tom Ross, and of the Grosmont-Upper Ireton by Mark Prefontaine. An initial GEODIAL literature search on the Swan Hills region was conducted by J.R. MacGillivray; Ernie Perkins was responsible for the water-rock interaction study at the injection well site. W.N. Hamilton made useful editorial comments. Major technical reviews were provided by G.D. Mossop (Alberta Geological Survey) and Albert Vonhof, Consultant, Calgary, and the authors record their thanks for many valuable comments. English editing was done by Pat F. Stothart. Appreciation is expressed to Lorne Bradley, Dale Hite, Dan Magee, Jim Matthie and Karen Parrish of Publishing and Graphics. Special thanks are due to Mika M. Madunicky, technical assistant to the senior author, who played a major role in coordinating various aspects of the work. The typing and production of the consultant report for the Corporation and the typing of this bulletin were ably provided by Kathie J. Skogg.

Copies of this report are available from:

Edmonton:
Alberta Research Council
Publications Sales
250 Karl Clark Road
Edmonton, Alberta
Canada

Phone: (403)450-5390

Mailing address:
Alberta Research Council
Publications Sales
PO Box 8330
Postal Station F
Edmonton, Alberta
Canada T6H 5X2

Calgary:
Alberta Research Council
Publications Sales
3rd Floor
6815 - 8 Street NE
Calgary, Alberta
Canada T2E 7H7

Phone (403)297-2600

Contents

Tables

Figures

Appendices

Abstract

A detailed hydrogeological study was carried out in a region defined as Tp 62-74 R 1-13 W5M, comprising 15 760 km^2 effectively centered on the Special Waste Injection Site of the Alberta Special Waste Management Corporation. The objective was the selection of aquifers for environmentally safe disposal of waste water from treatment processes. The approach included: (1) identification of the major hydrogeological and economic constraints; (2) analysis of the natural flow system for all hydrostratigraphic units between the Lower Cretaceous Viking aquifer and the Precambrian basement; (3) numerical simulation of the flow in, effectively, the entire Phanerozoic succession to obtain conformance with the natural flow system; and (4) steady-state perturbation of the system at an injection rate of 225 m^3/d in two potential injection aquifers to evaluate the importance of the hydraulic head buildups at a theoretically infinite time of injection. The study was based on examination and interpretation of stratigraphic information from 3276 wells, and on 635 drillstem tests, 3477 core analyses, and 645 formation water analyses, all from the files of the Energy Resources Conservation Board, using specialized software developed by the Basin Analysis Group, and the three-dimensional finite element groundwater model FE3DGW. The preferred injection aquifer is the basal portion of the Wabamun-Winterburn aquifer system. The Basal Cambrian aquifer was selected as a less desirable backup injection aquifer. After completing this study, a well was drilled to the top of the Ireton aquitard and successfully tested and completed in the Wabamun-Winterburn aquifer system.

Introduction

Since 1979 the Province of Alberta has been developing a program for the proper management of more than 92 000 t of special waste generated annually in the province. Through a series of expert committees, public hearings and technical reports, a policy was formulated which would result in the development of a central treatment facility. A Policy Statement on Industrial and Hazardous Waste, issued January 1982 noted three key concepts:

1. A central treatment facility would be built in Alberta on land owned by the Crown to augment existing and proposed on-site treatment facilities.
2. The private sector would be encouraged to build and operate the central facility.
3. A new Crown Agency would be formed to oversee the operation of the management system.

On 1 April 1984 the Alberta Special Waste Management Corporation was formed to develop the Alberta System and to oversee the construction of the central facility as well as ancillary services, the installation of surface and groundwater monitoring systems, and a series of collection and transfer stations within a transportation network. More complete details of the development of the Alberta System can be found in Simpson (1985).

The present study was carried out under contract to the Alberta Special Waste Management Corporation, to whom the Alberta Research Council acts as an advisor with respect to selected earth science aspects related to their special waste treatment site near Swan Hills, Alberta (W half, Sec 6, Tp 67 R 8 W5M). A brief interim report of the results of this investigation has been published by Hitchon et al. (1985).

The site includes both surface treatment facilities and a deep waste injection system. Although site selection was based on a wide variety of criteria (Simpson 1985), these did not include a detailed hydrogeological evaluation for deep waste injection. Accordingly, although the specific injection site was predetermined, the problem was approached from a regional perspective to ensure that all pertinent investigations were carried out in light of the sensitive nature of the issues involved. Extreme care and prudence were exercised with respect to data collection and interpretation, as well as to the conclusions drawn from this evaluation.

Before describing the work accomplished and the conclusions drawn, it is important to point out a number of significant caveats which are well known to the authors, but which may not be obvious on reading this bulletin:

1. Effectively all data used in compiling this bulletin originated in the public files of the Energy Resources Conservation Board (ERCB) up to 1983; although additional information may exist in the files of private corporations it was not available for study.
2. Data distribution is highly variable within the study area. First, there is no well information from the northwest corner of the study area under Lesser Slave Lake, and there are few wells in a critical area between the Special Waste Injection Site and the Mitsue oilfield. Second, the amount of information available decreases sharply with depth, so that although 3276 wells have been drilled in the study area to 1983, only 54 penetrate

the Precambrian basement. The size of the area selected for study takes both of these factors into account.

3. The raw data used for the hydrogeological and hydrochemical input require a significant degree of interpretation before they can be used for a study of this type. Some of this interpretation is, of necessity, rather subjective and is based heavily on the experience of the researchers concerned. Computer contouring using software packages which depend on distribution in a fixed grid helps to resolve this problem. At the same time, the contouring package overcomes the difficulty of very irregular data distribution, although some grid manipulation is necessary. As a result of the techniques used, all maps are representative of the parameters contoured, but exact values are available only for specific wells.
4. The numerical simulation model used in this study is limited to 3000 nodes and elements due to the configuration of the computer system. This meant that in the Swan Hills study area, with its very complex hydrostratigraphic geometry, it was necessary to approach the numerical simulation of the fluid flow regime in stages. For very simple hydrostratigraphic situations, the problem of systematic variation in regional permeability within any aquifer can be handled, theoretically, by dividing the aquifer into discrete domains with specific permeabilities; this is not possible in an area as hydrogeologically complex as Swan Hills, with random variability of hydraulic parameters within each hydrostratigraphic unit.

Approach

The objective of this study was the identification of aquifers for environmentally safe disposal of waste water from treatment processes. This meant approaching the evaluation in eight separate steps:

1. Identification of the major hydrogeological and economic constraints.
2. Selection of the study area and stratigraphic units requiring evaluation.
3. Determination of the geometry of the stratigraphic units.
4. Determination of the hydraulic parameters of the fluid and porous matrix by stratigraphic units.
5. Combination into hydrostratigraphic units.
6. Selection of the areas for numerical simulation.
7. Calibration of the numerical model.
8. Perturbation of the system for the given injection rate.

The regional geology was compiled by Emlyn H. Koster; Claude M. Sauveplane and Brian Hitchon determined the hydrogeology, and Stefan Bachu was responsible for the numerical simulation. All software was developed by Andre T. Lytviak. With respect to the data base and data processing techniques the reader is referred to Bachu et al. (1987) to appreciate the caveats cited in the introduction.

Major hydrogeological and economic constraints

In evaluating any region for deep waste injection, three types of major constraints need to be considered. These may be broadly classified as relating to: (1) the natural steady-state flow regime; (2) the possible contamination of existing and potentially economic resources; and (3) the mechanical properties of the injection aquifer and adjacent hydrostratigraphic units. The following sections are general in nature and are applicable throughout Alberta; their implications to the study area are considered elsewhere in this bulletin.

Ideally, site selection should be based on the presence of a thick, porous and permeable, mechanically strong aquifer overlain and underlain by thick aquicludes such as halite beds. Depending on the hydrogeological flow regime, a satisfactory alternative would be a similar aquifer overlain and underlain by continuous major regional aquitards. Assuming adequate well completion techniques, contamination of the near-surface potable groundwater resources may be avoided by injection into an aquifer in the regional flow regime that is effectively semiconfined by continuous major regional aquitards. The amount of cross-formational flow that occurs naturally, and which will be enhanced through the injection process, can be calculated by means of numerical modelling. Provided the amount of cross-formational flow is within limits acceptable to those carrying out the injection operation, environmentally safe disposal can be achieved.

Once injection has commenced, there is a potential environmental problem related to the transport in the modified flow field of any specific substance dissolved in the injected fluid. Provided chemical reactions do not occur, this substance will be moved away from its point of introduction by the combined mechanisms of convection, dispersion, molecular diffusion and sorption. In practice, the injected and native fluids are miscible and commonly of different density, viscosity and salinity. A transition zone will develop at their interface; the main mechanism in the movement of this front is hydrodynamic dispersion. Because detailed analyses of the native and injected fluids were not available, this important aspect of deep waste injection could not be considered.

In addition to potable groundwater, economic resources include existing and potential accumulations of crude oil and natural gas, potential geothermal energy resources, potential halite resources, and recoverable resources of Ca, Mg, Br, I and Li in formation waters.

With respect to potable groundwater, a combination of adequate well completion techniques and deep injection into the regional flow regime are sufficient to avoid contamination problems. Because the bulk of the Paleozoic and Mesozoic rocks of Alberta fall within the so-called 'oil window', consideration must be given to the entire range of conventional hydrocarbon occurrences, from shallow natural gas, through conventional crude oil and condensate, to deep gas. It is recognized that evaluation of strata for potential hydrocarbon accumulations is very subjective.

An additional possible energy resource is the heat recovered from formation waters. This resource is presently utilized on an experimental scale at Regina, but there are no large-scale commercial operations such as those in the Paris Basin where thousands of apartments and offices are supplied with space heating from low-grade geothermal energy resources. Much of the Canadian research done on this resource has been supported by the Earth Physics Branch of Energy, Mines and Resources, and the interested reader is referred to this organization for a complete list of pertinent publications. There is, however, no comprehensive evaluation of the low-grade geothermal energy resources of Alberta. Accordingly, at a reconnaissance level, we have followed the criteria used by the U.S. Geological Survey and defined low temperature resources as less than 90°C, to depths of 2 km. In addition, we have defined the 50°C isotherm as the lower economic limit because temperatures less than 50°C may be significant for some purposes. Modern heat exchangers, together with proper fluid composition control, mean that saline waters (110 000 mg/L in the Regina experiment) can be tapped; hence, salinity is not a major determining factor, although it will be for some potential users.

Intermediate-grade geothermal energy resources are arbitrarily defined as between 90 and 150°C. Only published data on reservoir temperatures of conventional crude oil and natural gas reserves in the undisturbed part of the Alberta Basin were used to evaluate the potential for intermediate-grade geothermal energy. Distribution of the data plotted by individual stratigraphic units suggests that some of the values are erroneous. Bearing this in mind, the information is summarized as follows. No reserves with temperatures greater than 90°C occur east of the fifth meridian. Maximum reservoir temperatures are found close to the disturbed belt along the axis of the Alberta Syncline. In this region, Upper Cretaceous rocks seldom reach 90°C, and Lower Cretaceous, Jurassic and Triassic strata are generally less than 100°C. It is not until Mississippian rocks are reached that maximum temperatures are in the range 100 to 110°C. These features occur along the length of the syncline west of the fifth meridian. With some notable exceptions (for example the Westpem Field), most 'hot' reservoirs in the Middle and Upper Devonian are related to the carbonate reefs of the Swan Hills-Windfall complex and the overlying, effectively continuous, carbonate succession in the Winterburn and Wabamun Groups. Data are therefore limited to the central portion of the deepest part of the Alberta Basin. Maximum temperatures close to 125°C occur in the Wabamun and Winterburn Groups, although 135°C was recorded for the latter group at the Obed Field. It is in the underlying carbonate complexes of the Leduc Formation and Beaverhill Lake Group, however, where the effects of depth and hydraulic continuity to strata adjacent to the disturbed belt are best illustrated (see discussion in Hitchon 1984a). Here, at depths of about 4.5 km, reservoir temperatures reach 145°C, with an extraordinary recording of 166°C for the Leduc Formation at the Banshee Field. Maximum temperatures in the deepest portion of the Alberta Basin are estimated at 180°C.

In addition to energy resources, there are also proven and potential resources of economic minerals. The most important are halite and Ca-Mg brines, both of which are commercially exploited in Alberta.

Hamilton (1971) has evaluated the halite resources of east-central Alberta and noted that increasing industrial development undoubtedly will lead to increasing demand for salt, mainly to meet the expanding requirements of the chemical industry. Greater indirect use of salt beds for storage of liquefied petroleum gas (LPG) and natural gas (in man-made caverns) was also foreseen. Hamilton (1971) suggested that improved solution mining techniques may ultimately lead to extraction of Mg and Br through selective brining of beds rich in these elements. Although thick salt beds are regarded as effective aquicludes, the impact of fluid injection in an adjacent aquifer on them is obvious. Not only might the integrity of the aquiclude be damaged, but the potential for selective brining might be destroyed.

More direct impact of fluid injection may occur through contamination of formation waters which contain recoverable mineral resources. Hitchon (1984b) has summarized the potential of Alberta formation waters as a source of industrial minerals. Table 1 is from this summary, and shows the minimum concentration limits for Ca, Mg, Br, I and Li that are used

Table 1. Minimum concentration limits of selected elements in formation waters to assist in defining areas for exploration for sources of industrial minerals.

Element sought	Minimum regional Exploration limit (mg/L)	Minimum detailed Exploration limit (mg/L)
Ca	20 000	60 000
Mg	3 000	9 000
Br	1 000	3 000
I	40	100
Li	50	?

From Hitchon (1984b)

to define areas for regional and detailed study during exploration. The limits are based on present commercial technology for successful exploitation. Detailed studies of Ca and Mg (Hitchon and Holter 1971) and Br, I and B (Hitchon et al. 1977) in Alberta formation waters have been carried out, but the content of Li is known only from a few selected hydrocarbon-producing reservoirs (Hitchon et al. 1971). With respect to deep waste injection, only Ca, Mg, Br and possibly Li are of concern because B is probably below commercial potential and I resources occur most extensively in the relatively shallow Lower Cretaceous Viking and Bow Island Formations, and the basal beds of the Upper Cretaceous Belly River Formation.

The mechanical properties of the disposal aquifer and adjacent hydrostratigraphic units are the third major constraint that must be considered in order to evaluate the risk of hydrofracturing the rocks. This is effectively an engineering problem and was not addressed in this study.

Selection of study area and stratigraphic units

Preliminary evaluation of the information in the ERCB well data system showed that examination of a region of about six townships around the injection site would be necessary if computer manipulations of all pertinent data were to be used, bearing in mind that a minimum of ten well-distributed data points are required for satisfactory contouring. Accordingly, the study area was defined as Tp 62-74 R 1-13 W5M, comprising 15 760 km^2 effectively centered on the Special Waste Injection Site. Prior published reports on the regional hydrodynamics and hydrochemistry of the Alberta Basin (Hitchon 1963, 1964, 1969a, 1969b, and 1984a) suggested that the entire stratigraphic succession from the Precambrian basement to the Upper Cretaceous Lea Park and Wapiti Formations should be considered. In effect, only the Tertiary strata capping the Swan Hills and the surficial deposits were not studied in detail.

Bachu et al. (1987) have described the data base management system used by the Basin Analysis Group to process and integrate the various parameters from formation water analyses, drillstem tests, cores, and bottom hole temperature measurements which are required for the analysis of fluid and heat regimes in sedimentary basins. The interested reader is referred to Bachu et al. (1987) for more details of the data processing and synthesis techniques used in this study.

Regional geology

Introduction

This section of the bulletin summarizes the Phanerozoic history of the Swan Hills study area in the context of regional depositional and erosional events that affected this part of the Western Canada Sedimentary Basin. In keeping with modern practice in basin analysis (Miall 1984), the local formation stratigraphy (table 2) is unraveled by tracing paleogeographic developments. This involves viewing the depositional framework of successive formations and the paleogeomorphic development of unrepresented intervals in the context of major tectonic events and sea level changes (viz. table 1 in Nelson et al. 1964). In turn, this provides the background information necessary for understanding the relative depth (table 3), overall geometry (table 4) and lithological character of hydrostratigraphic units evaluated in subsequent parts of this bulletin.

The study area (figure 1) lies mostly within the physiographic region known as the Swan Hills Upland, a subdivision of the Alberta High Plains. This sparsely populated, forested area reaching 1328 m above sea level has a radial drainage network feeding the Smoky, Slave and Athabasca Rivers, which border the upland. The upland is a broad outlier of the early Tertiary Paskapoo Formation that extends about 90 km northeastward from the main updip edge of this unit. The northern and eastern borders of the study area occupy the Lesser Slave Lowland which is underlain by Upper Cretaceous strata. Surficial deposits of glacial, glaciofluvial and glaciolacustrine origin (St. Onge and Richard 1975) overlie a plateau gravel sheet of Oligocene age (Vonhof 1965; Fischbuch 1968). The glacially-related deposits are generally thinner than 20 m over the upland, but they exceed 50 m along parts of the peripheral preglacial valleys.

Attempting to reconstruct the paleogeographical evolution for an area requires a good understanding of the sedimentology of the local stratigraphic sequence. For the Swan Hills study area, this varies for each formation generally according to the distribution of oil and gas. In this regard, a particularly dense network of core and geophysical log data exists for the Middle and Upper Devonian reef carbonate reservoirs. However, the continuing attention in research literature to refining depositional models for this interval emphasizes the point that subsurface data rarely yield unequivocal interpretations.

Stratigraphic nomenclature in the study area (table 2) has arisen from studies using both local subsurface data and outcrop work on deformed, correlative strata within the Rocky Mountains. Against this framework, this summary of the regional geology strives toward a synthesis of studies spanning the last twenty or so years. General works of McCrossan and Glaister (1964), Parsons (1973) and Porter et al. (1982) on the geological history of Alberta, supplement, where necessary, the more specific research work. Stearn et al. (1979) is a good reference for viewing the study area in the context of the continent-wide geological history.

Western Canada Sedimentary Basin

Background

The Western Canada Sedimentary Basin is a westward-thickening wedge of Phanerozoic strata, up to 6 km thick (figure 2), that underlies all but the extreme northeast corner of Alberta where Precambrian crystalline basement rocks are exposed in the Canadian Shield. The southwest margin of the basin is the deformed terrain of the Rocky Mountain Foothills and Front Ranges; parallel to its trend, the basin continues northward across the western Northwest Territories and southward into the Western Interior of the U.S.A. Because of the mild regional dip (5 to 10 m/km) and low relative relief, the present-day erosion level truncates the sedimentary fill of the basin over a relatively narrow stratigraphic range. Upper Cretaceous rocks predominate at the surface, the exceptions being lower Tertiary strata over the highest plains and outer foothills and Lower Cretaceous and Devonian strata near the exposed Canadian Shield.

Sedimentary sequences

Only 40% of the 570 Ma duration of Phanerozoic time is preserved as strata within the study area. In table 2, the terms Sauk, Tippecanoe, Kaskaskia, Absaroka and Zuni relate to work by Sloss (1963) who introduced these tribal names to refer to the major unconformity-bounded sedimentary sequences across the North American interior. As reviewed by Miall (1984), later work has confirmed that this concept has global application. These sequences reflect large-scale, long-term fluctuations in sea level relative to the elevation of the craton surface. Sloss (1963) recognized that the transgressive phase of each sequence is better preserved than the terminal regressive phase because of protection by later, onlapping strata and the erosional development of paleoplains (Martin 1966) represented by the capping unconformity. Commonly, the emergent periods were also times of mild epeirogenic deformation so that subjacent sequences now show minor discordance in southwestward regional tilt.

Four of the six sequences of Sloss (1963) are represented in the stratigraphy of the Swan Hills study area (table 2). In chronological order, these relate to Middle-Upper Cambrian (Sauk), Lower-Upper Devonian

Table 2. Stratigraphic nomenclature and hydrostratigraphy.

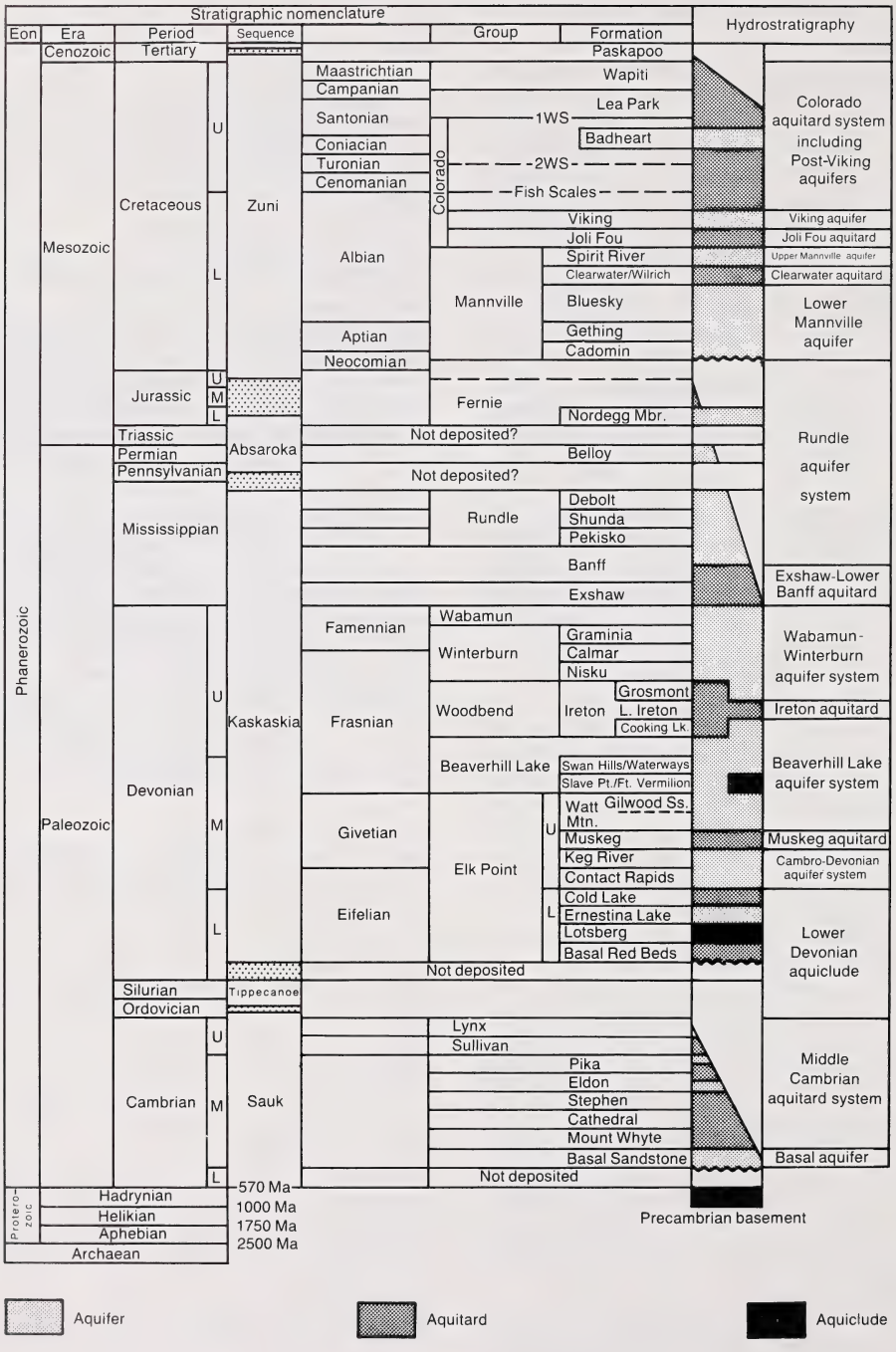

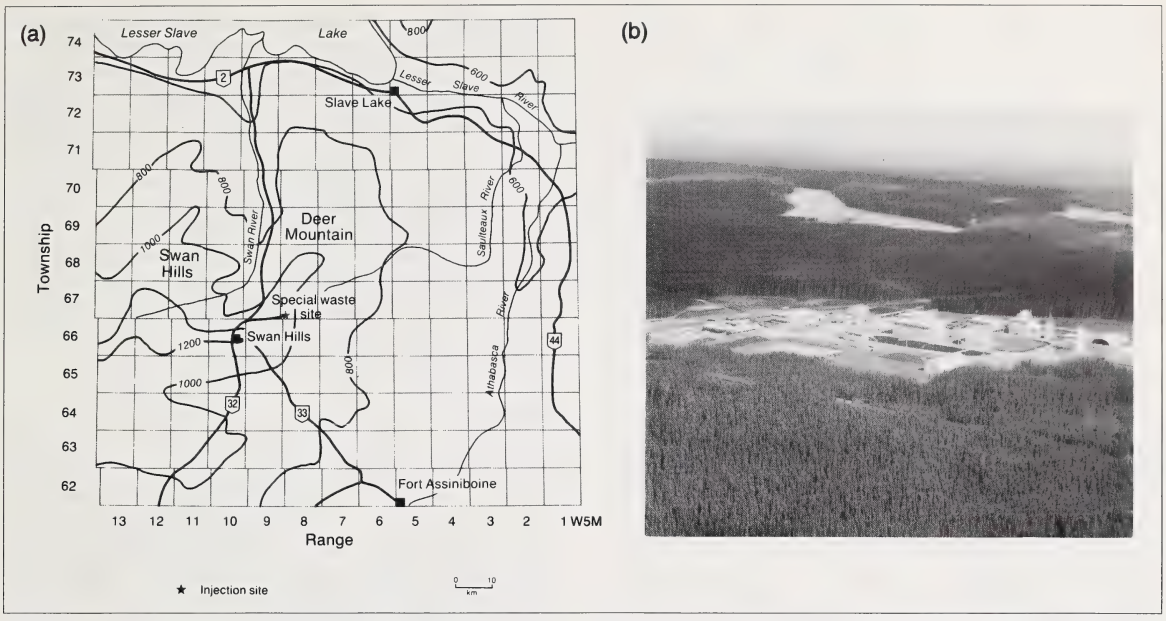

Figure 1. a) topography (m) and major surface drainage of the Swan Hills study area in relation to the Special Waste Injection Site; b) areal view of the special waste treatment and storage facility, Swan Hills, Alberta (photograph courtesy Chem-Security Ltd.).

and Mississippian (Kaskaskia), Upper Pennsylvanian to Lower Jurassic (Absaroka) and uppermost Jurassic to lower Tertiary (Zuni). These stratigraphic intervals and their bounding unconformities are used in summarizing the regional geology of the study area, although the summary is separated into two parts corresponding to the major two-stage tectonic evolution of this region.

Tectonic settings

During the development of the first three stratigraphic sequences, the Alberta region was a preorogenic continental margin within a lithospheric plate comparable to the modern east coast of the Americas. Between the exposed crystalline nucleus of the continent to the northeast (the Canadian Shield, now stripped of its former sedimentary cover) and an expanding proto-Pacific Ocean to the west, a westward-thickening wedge comprising three sedimentary sequences accumulated over this 'passive' continental margin. The paleogeography and resulting geometry of stratigraphic units, however, became increasingly affected by slow tectonic activity along basement structures through the Paleozoic Era. The general result was that the continental margin became internally differentiated into a changing network of sub-basins between more slowly subsiding linear areas. More specifically, this caused variation in the sources, lithology and transport directions of sediments, the thickness of strata representing a given sequence, and the distribution of relief and denudation between sequence accumulations. A distinctive feature of Paleozoic strata is the common occurrence of carbonates and evaporites.

Paleogeographic events in the Swan Hills study area were particularly influenced by the northeast-

Table 3. Elevation (relative to sea level datum) of selected surfaces.

Surface	Elevation (m) Minimum	Mean	Maximum
Ground	531	787	1328
Zuni sequence			
Base of Post-Colorado Group	-100	309	579
Base of Colorado Group	-600	-37	279
Base of Mannville Group/ Pre-Zuni unconformity	-837	-303	76
Absaroka sequence			
Base of Fernie Group	-898	-736	-586
Kaskaskia sequence			
Base of Mississippian	-1137	-500	8
Base of Wabamun Group	-1361	-679	-112
Base of Winterburn Group	-1526	-813	-254
Base of Woodbend Group	-1815	-1145	-582
Base of Beaverhill Lake Group	-1945	-1315	-793
Base of Upper Elk Point Group	-1672	-1296	-963
Base of Lower Elk Point Group/ Pre-Kaskaskia unconformity	-2033	-1492	-1225
Sauk sequence			
Base of Lynx Group	-2074	-1743	-1462
Base of Middle Cambrian/ Pre-Sauk unconformity	-2335	-1642	-1168

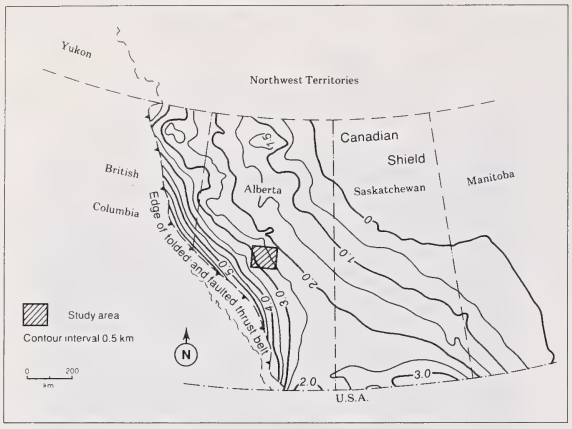

Figure 2. Total preserved thickness of Phanerozoic strata east of the Cordillera (based on figure 2 in Porter et al. 1982), showing the Swan Hills study area.

trending Peace River Arch which lay about 125 km to the northwest. Porter et al. (1982, p. 173) refer to examples in southern Alberta and central Montana of "aulacogen-type rifts" that extended into the craton from the former rifted margin, and which were probably controlled by older structures in the Precambrian basement. D.J. Cant (pers. comm.), Alberta Geological Survey (now with the Atlantic Geoscience Centre), has been involved in a comprehensive subsurface study of the Peace River Arch and interprets it as a failed rift extending from the Paleozoic continental margin.

The uppermost Zuni sequence accumulated under a contrasting set of paleogeographical conditions related to the onset, in the Late Jurassic, of Cordilleran deformation. This signifies that the once 'passive' continental margin had now become a complex western boundary of the North American plate. In general terms, the present British Columbia area is regarded (e.g. by Porter et al. 1982) as having developed from oblique accretion of exotic terrains and extensive igneous activity. From the standpoint of the Swan Hills study area, orogenic development of the Rocky Mountains straddling the B.C.-Alberta border had greater significance. This orogenic event resulted in isolation of the Alberta region from the Pacific Ocean, whereby the former distal edge of the Western Canada Sedimentary Basin became uplifted, deformed and the source of detrital sediments to the Zuni sequence. In fact, palinspastic reconstruction by Price (1981) shows that the original rifted western margin of the Precambrian craton lies about 200 km west of the present axis of the Alberta Basin. This convergence of terrains was incremental with successive thrusting, thereby causing a gradual eastward shift in the line of maximum basin subsidence and an increasing amount of sediment recycling.

Stott (1983, 1984) has pointed out that this new foreland basin adopted an eastward transport direction in the Middle-Late Jurassic, and that a poorly documented unconformity of this age marks the reversal. The ensuing Cretaceous succession has evoked particular interest (Caldwell 1975) because of its widespread surface distribution over the Western Interior, abundant hydrocarbon and coal resources, and its markedly cyclical character. The latter takes the form of eastward-thinning clastic wedges, each relating to accelerated denudation in the Cordillera due to a new deformational phase, that interfinger with westward-thinning marine shaley intervals associated with the fluctuating Western Interior Seaway.

Depositional systems

A chronological summary of a stratigraphic succession that stresses general lithological character tends to obscure the fact that the original sediments accumulated in a limited variety of 'depositional systems' (e.g. alluvial coastal plain, delta, carbonate shelf; viz. Miall 1984; Walker 1984). Given the successful application of the depositional systems concept in the Gulf Coast region of the U.S.A., where it was necessary to assimilate huge quantities of stratigraphic data for systematic oil and gas exploration, Miall (1984) advocates its more general use. He describes the approach (p. 277)

Table 4. Range in thickness of selected hydrostratigraphic units.

Hydrostratigraphic unit	Range in thickness (m)
Post-Viking aquitard	300 – 613
Zuni sequence	
Viking aquifer	3 – 67
Joli Fou aquitard	5 – 23
Upper Mannville aquifer system	79 – 241
Clearwater-Wilrich aquitard	12 – 61
Lower Mannville aquifer	11 – 168
Kaskaskia sequence	
Debolt aquifer	0 – 67
Shunda aquifer	0 – 132
Pekisko aquifer	0 – 88
Upper Banff aquifer	0 – 257
Exshaw-Lower Banff aquitard	0 – 50
Wabamun aquifer	76 – 333
Winterburn aquifer	46 – 269
Grosmont aquifer	0 – 255
Ireton aquitard	37 – 438
Swan Hills-Slave Point aquifer	5 – 153
Fort Vermilion aquiclude	0 – 23
Muskeg aquitard	19 – 125
Keg River-Contact Rapids aquifer	0 – 134
Cold Lake aquiclude	0 – 58
Ernestina Lake aquifer	0 – 15
Lotsberg-Basal Red Beds aquiclude	0 – 163
Sauk sequence	
Pika aquifer	0 – 63
Eldon aquifer	0 – 23
Basal Cambrian aquifer	0 – 54

as "...essentially genetic stratigraphy, in which the focus of the analysis is on the interpretation of the interrelationships of large sediment bodies, based on an understanding of the depositional environments and syndepositional tectonics which controlled their formation."

The following stratigraphic summary of the Swan Hills study area incorporates the depositional systems approach, in that it helps to emphasize that:

1. A limited number of tectono-sedimentary settings prevailed during the 'passive' Paleozoic and 'active' Mesozoic stages of basin development; and
2. Formation boundaries commonly represent the shifting, diachronous boundaries between laterally coexistent systems.

Passive development of the continental margin

Pre-Sauk unconformity

The Sauk sequence rests with major unconformity (1200 Ma) on the subsurface extension of the Canadian Shield which forms the basement of the Western Canada Sedimentary Basin. This part of the Precambrian craton is assigned to the Churchill Province, and consists mainly of Archean crystalline rocks and Aphebian (2500 to 1750 Ma) supracrustal rocks that underwent deformation, metamorphism and magmatism during the Early Proterozoic (1750 Ma) Hudsonian Orogeny (Porter et al. 1982). Beyond the updip erosional edge to the sedimentary cover the Churchill Province has a strong northeast-southwest trend (Stockwell 1969); parallel orientation of the Peace River Arch is good evidence that this structural grain continues into the subsurface. Based on the work of Burwash et al. (1964), the Swan Hills study area lies near the southern margin of the Peace River Arch division of the basement where deep wells have shown that metamorphic rocks of granitic composition predominate.

As noted in the foregoing tectonic overview, the pre-Cordillera rifted margin of the Proterozoic continent lay about 200 km to the west of the present axis of the Alberta Basin. Preserved strata from this initial stage of the passive margin are limited to the Purcell Supergroup now exposed along the Main Ranges. Within the study area, the Precambrian surface steepens southwestward, with an average dip of 5.9 m/km, from 1168 to 2335 m below sea level (figure 3). At the injection site, it lies about 2.84 km below ground. van Hees (1959) noted some marked relief on this unconformity, including isolated hills up to 200 m high although no such relief has been specifically recorded for the study area.

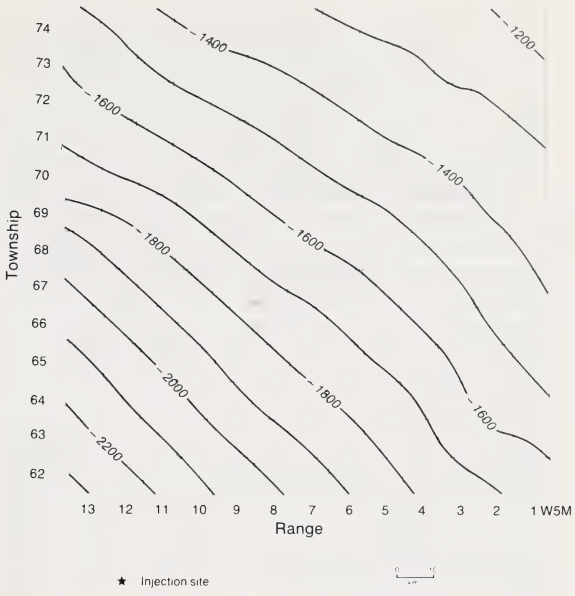

Figure 3. Structure contours (100 m interval) on top of the Precambrian basement.

Sauk sequence

This first sequence of Middle to Late Cambrian age (figure 4) records the eastward transgression of an open shelf sea over the deeply denuded surface of the Precambrian craton. Due to erosional bevelling associated with the pre-Kaskaskia unconformity, this sequence thickens from 50 to 300 m south-southwestward across the study area.

Early terminology (e.g. Baillie 1956) referred to the basal Paleozoic rocks as Granite Wash, a term intended to encompass sandy detritus derived from the crystalline basement. Pugh (1973) discouraged further use of this term because later drill cuttings from northern Alberta allowed discrimination of two facies of different age. The first relates to the in situ regolith at the basement surface which is best developed under the Middle Cambrian basal sandstone (Gog Group equivalent), but also occurs beyond the erosional edge of Cambrian strata where Kaskaskia-age formations directly overlie the reexposed basement. The second relates to reworked cleaner sandstone, mostly devoid of igneous rock fragments, which characterizes the basal clastic unit of the Kaskaskia sequence (figure 5).

Marine conditions became established in the study area by Middle Cambrian time. van Hees (1959), van Hees and North (1964) and Pugh (1973, 1975) all agree that Cambrian sedimentation over the craton margin consisted of four shore-parallel facies belts, corresponding to deltaic, inner shelf, shelf edge, and deeper basin environments. The basal sandstone of

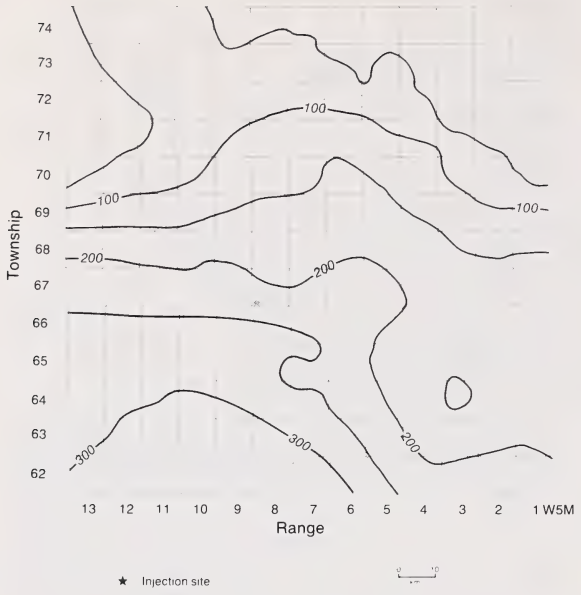

Figure 4. Isopachs (50 m interval) of preserved Cambrian strata, corresponding to the Sauk sequence.

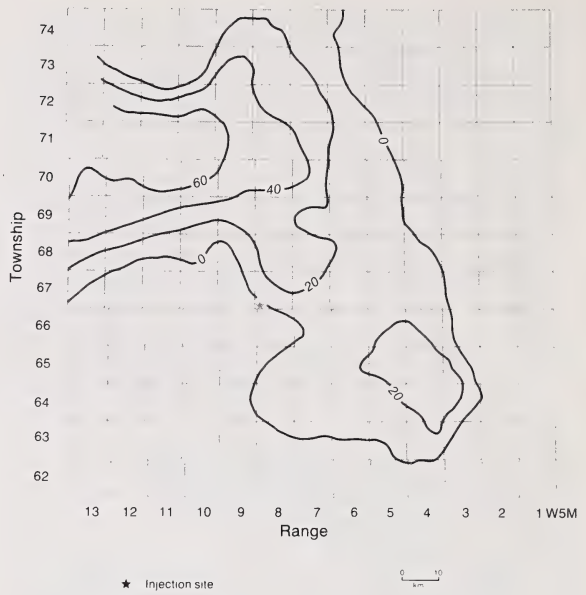

Figure 5. Isopachs (20 m interval) of basal clastic unit of Kaskaskia sequence overlying Cambrian strata.

deltaic origin gave way offshore to a glauconitic silty-shale belt which, according to van Hees and North (1964), dominates the Middle Cambrian succession in the study area. Beyond the reach of Shield-derived sediment, thick carbonates accumulated near the shelf margin and black graphitic shales were deposited, with interbedded lavas, on the slope and rise below the shelf. Review of evidence by Porter et al. (1982) suggests that this carbonate bank remained relatively fixed in position over the rifted craton margin. The work of Aitken (1966, 1968) on formation nomenclature and sedimentology of this carbonate succession at outcrop in the Rocky Mountains was applied to the subsurface by Pugh (1975). The Mount Whyte-Cathedral, Stephen-Eldon, Pika, and Sullivan-Lynx units above the basal sandstone in the study area represent upward-shallowing successions. Pugh (1975) interpreted these as evidence of cyclic crustal movements, whereas a more recent view (James 1984) holds that these developed simply because shelf carbonate systems have an inherent tendency to aggrade up to sea level before subsiding. The first two cycles both comprise shales with minor glauconitic, micaceous arenites (Mount Whyte, Stephen) passing upward into dolomite (Cathedral, Eldon). The third cycle (Pika) contains a similar trend, although when traced southward the upper dolomite becomes a coarser, oolitic limestone. Pugh (1975) viewed this lateral facies change as evidence that the Peace River Arch had already taken the form of a broad peninsula. The minor disconformity which underlies the Upper Cambrian Lynx dolomites indicates a temporary withdrawal of the shelf sea.

Pre-Kaskaskia unconformity

Following accumulation of the Sauk shelf sequence, the craton margin began to develop a pattern of subbasins. The mid-Paleozoic stratigraphy of the study area reflects the strong influence of the Peace River Arch to the northwest, and a changing distribution of more rapidly subsiding areas to the south and southeast. Major paleogeographic responses were a restricted circulation of seawater during transgressive phases and a susceptibility to erosion of strata accumulated over 'arch' areas during regressive phases.

As a result of these developments, Ordovician-Silurian strata of the Tippecanoe sequence are now confined to the Williston Basin centered on the Saskatchewan-North Dakota border. The western erosional limit underlies southeast Alberta where Ordovician carbonates cap the 250 m high Meadow Lake Escarpment (van Hees 1958; Parsons 1973). The nature of any Tippecanoe sequence initially present across the study area is speculative, but a condensed, more shoreward equivalent of the evaporitic and carbonate depositional systems which dominated the central Williston Basin is probable (Porter et al. 1982). Southward from Lesser Slave Lake, the pre-Kaskaskia unconformity (figure 6) truncates the bevelled tops of successively younger Cambrian formations (figure 7) with a southwestward dip that steepens from 2.8 to 8.2 m/km.

Kaskaskia sequence

Devonian strata which overlie the pre-Kaskaskia unconformity accumulated under a different set of paleogeographical controls. Inundation was initially from the northwest over eroded remnants of the Sauk sequence and reexposed Precambrian basement. Major elements in Lower-Middle Devonian paleogeography were the Peace River and Western Alberta Arches, which acted as sediment-producing ridge areas, and the Meadow Lake Escarpment until its burial beneath Frasnian strata. The more rapidly subsiding area enclosed by these paleotopographic features is termed the Elk Point Basin. Distribution of Upper Devonian strata indicates a simpler paleogeography, involving a restored connection with the Cordilleran basin and burial of the Peace River Precambrian inlier by Famennian time. Major lithological expressions of this diminishing degree of restricted circulation are the evaporites that dominate Lower and Middle Devonian formations (Hamilton 1982) and the subsequent southward migration of reef carbonates (Klovan 1974). By Mississippian time, an open shelf setting had been restored. Total thickness of the Kaskaskia sequence averages 1100 to 1200 m over most of the study area (figure 8).

Within the study area, Lower and Middle Devonian formations show a westward depositional onlap (figure 9) corresponding to an initial expanding phase of the Elk Point Basin. As a result, Eifelian- and Givetian-stage strata form the base of the Kaskaskia sequence east and west of the injection site, respectively. Due to later regional tilting, this initially horizontal succession now dips southwestward at about 6.3 m/km.

The Lower Elk Point Subgroup (Eifelian) is apparently conformable (Grayston et al. 1964). Its Basal Red Beds represent a veneer of coarse, arkosic sediment washed into the basin from the Peace River upland by ephemeral drainage. A comparison of isopachs with structure contours shows that this alluvium infilled local relief on the underlying unconformity. In the onlapping series of formations, this basin-edge redbed facies is overstepped by up to 150 m of halite (Lotsberg Formation) reflecting restricted circulation due to carbonate buildups across the northern outlet (Fuller and Porter 1969; Parsons 1973). The overlying Ernestina Lake Formation mostly consists of dolomitic limestone in the study area (Grayston et al. 1964). This unit forms the middle part of a depositional cycle, with a red shale below and thin anhydrite (Cold Lake Formation) above, that indicates progressive shallowing and increased restriction of basin water inflow. The Lower Elk Point Subgroup is capped by dolomitic shales (Contact Rapids Formation) over the south flank of the Peace River Arch; north of the arch the correlative Chinchaga Formation consists of anhydrite.

A long interval of widespread reef growth, reflecting more open circulation across the craton margin, began with the Upper Elk Point Subgroup (Porter et al. 1982) and subsequently dominated the paleogeography of Upper Devonian reservoir rocks across the central Alberta region. These varied from fringing

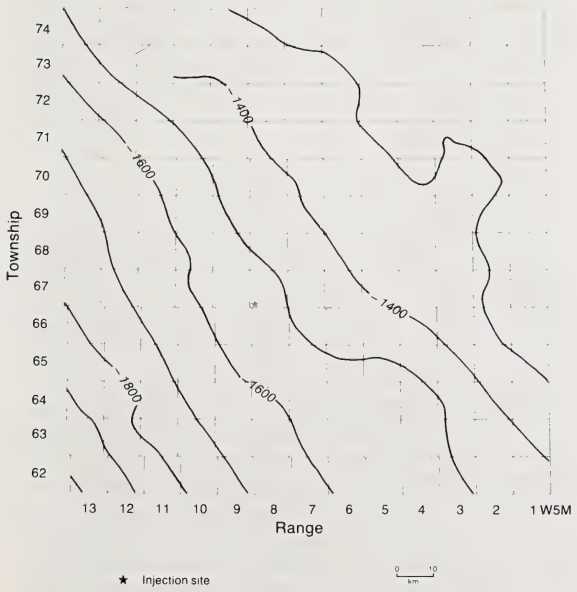

Figure 6. Structure contours (100 m interval) on top of preserved Cambrian strata, i.e. pre-Kaskaskia unconformity.

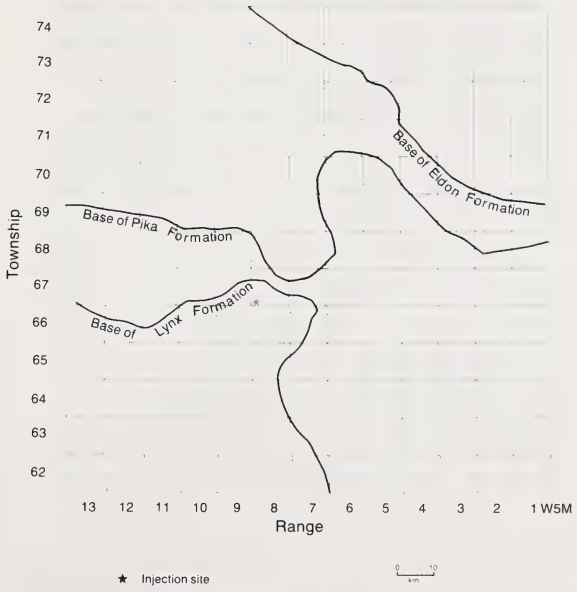

Figure 7. Subcrop distribution, at the pre-Kaskaskia unconformity, of the lower boundaries of the southwestward-dipping Cambrian Eldon, Pika and Lynx Formations.

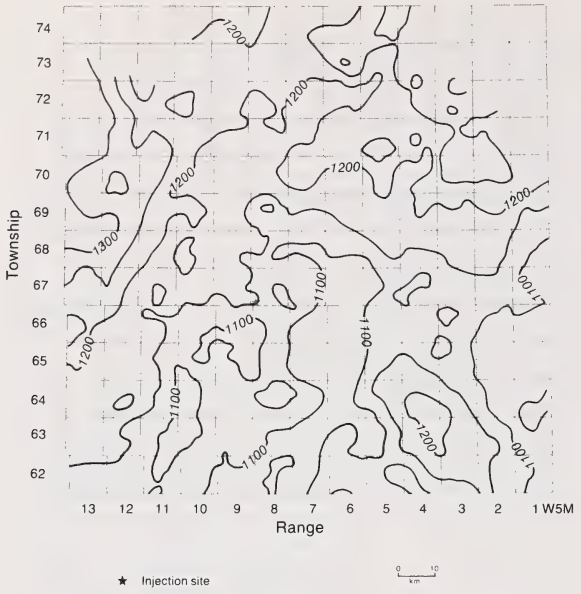

Figure 8. Isopachs (50 m interval) of preserved Devonian to Mississippian strata, corresponding to the Kaskaskia sequence.

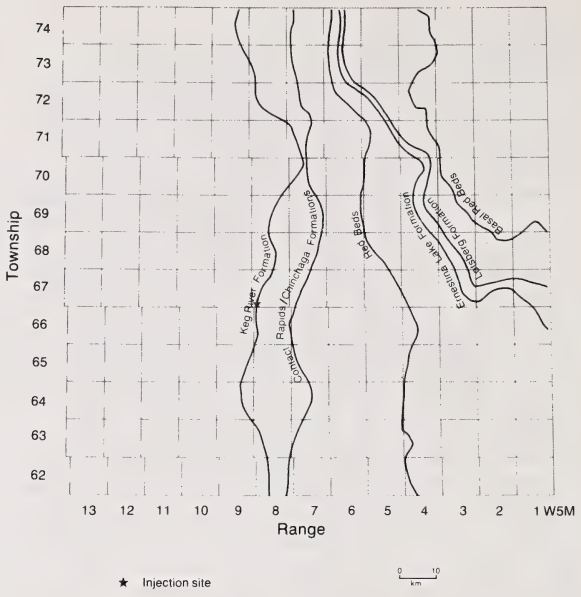

Figure 9. Subcrop distribution of westwardly-onlapping depositional limits for the Lower Devonian Basal Red Beds, Lotsberg, Ernestina Lake and Cold Lake Formations, and Middle Devonian Contact Rapids/Chinchaga and Keg River Formations.

reefs near shorelines, to patch reefs over shallow areas, to pinnacle reefs in deeper offshore areas (Parsons 1973). For this interval it should be noted that formation names commonly relate to depositional systems that coexisted laterally; for example, in the Middle Devonian Beaverhill Lake Group, topographically high carbonate reefs of the Swan Hills Formation pass laterally into nodular off-reef shales of the Waterways Formation (Jansa and Fischbuch 1974).

The Upper Elk Point Subgroup begins with the Keg River Formation. In the Rainbow-Zama area northwest of the Peace River Arch it contains numerous oil- and gas-bearing pinnacle reefs (Klovan 1974) which grew behind the Presqu'ile barrier (Hamilton 1982). Correlative deposits flanking the still emergent Peace River Arch were thin, locally-derived sands (McCamis and Griffith 1967). Overlying the Keg River Formation is the 25 to 125 m thick Muskeg Formation (syn. Prairie Formation) which indicates the onset of restricted circulation behind the Presqu'ile barrier. Muskeg Formation lithology involves alternation of anhydrite and dolomite with minor interbeds of halite and bioturbated shale. Opinions on the type of depositional system vary from stratified brines in relative deep water (Klingspor 1969; Davies and Ludlam 1973) to subtidal lagoons and supratidal flats (Jansa and Fischbuch 1974). Paleogeographic maps by McCamis and Griffith (1967) for Keg River and Muskeg time clarify that the boundary between inshore clastic and offshore carbonate-evaporite depositional systems lay close to the study area. Overlying formations represent a coastal plain and southward delta system (Gilwood Member) produced from drainage off the Peace River landmass that flowed into a shallow basin of prodelta shale (Watt Mountain Formation). In the study area, the Gilwood Member represents a return to Keg River facies due to slight reactivation of the Peace River Arch under a moister climate. Similarly, the Fort Vermilion Formation marks a return to a Muskeg-type depositional system.

According to Jansa and Fischbuch (1974), differential compaction over the Gilwood delta complex influenced the local relief of the disconformity above the Fort Vermilion evaporites and the geometry of the Middle Devonian Swan Hills carbonates that followed. This new eastward transgression flooded the West Alberta Arch and heralded one of the most significant stratigraphic intervals for oil and gas exploration in Alberta (Parsons 1973). The Swan Hills reef complex adjacent to the remaining Peace River landmass, and its partly correlative Waterways shale unit (Sheasby 1971) to the east, have been intensively studied. As noted by Klovan (1974), these platform reefs with their cyclic growth and periodic exposure formed under conditions of oscillatory subsidence. Within the framework of early diagenesis (Havard and Oldershaw 1976), dolomitization was restricted to windward sides of the reef perhaps due to localized action of Mg-fixing algae (Cameron 1968).

The Swan Hills reef-building period was terminated by renewed transgression; the resulting Woodbend Group contains the famous Leduc reef reservoirs. In a similar manner to the Swan Hills-Waterways complex, the upward accumulation of localized reef environments was concomitant with deposition of inter-reef, Ireton shale basins (Oliver and Cowper 1965). From the standpoint of the study area, the Peace River Arch was now surrounded by a fringing reef (Parsons 1973; Stoakes 1980) bounded to the southeast by basinal shales. To the east lay an extensive carbonate platform complex (Grosmont Formation) which, according to Harrison (pers. comm.), prograded westward during Leduc time. The uppermost level in the Woodbend Group is mostly Ireton shale facies which signifies a new transgression that effectively drowned out the Leduc-Grosmont carbonate complexes. The overlying Winterburn Group developed as a new depositional cycle in response to a northwestward regression of the platform sea (Parsons 1973). A carbonate shelf rimmed by Nisku pinnacle reefs now lay through the Pembina-Edmonton line, north of which was the deeper Winterburn basin accumulating shaley carbonates (Exploration Staff, Chevron Standard Limited 1979). A regional cross section in Parsons (1973) implies that the Peace River Arch area was a shallow carbonate bank at this time, and thus would have been a northern margin to the Winterburn basin. The final Late Devonian transgression deposited the thick Wabamun Group; it represents a broad carbonate shelf across the now inactive Peace River Arch that grades into dolomite toward the southeastern corner of the study area (Belyea 1964).

Within the study area, the upper Mississippian part of the Kaskaskia sequence occurs as a deeply bevelled series of west-dipping subcrops (figures 10 and 11). Their preservation here partly reflects proximity to the Peace River Arch area which at this time underwent block subsidence and accumulation of a relatively thick Mississippian succession (Lavoie 1958; Parsons 1973). This period began with a rapid eastward transgression, and because the Alberta shelf now lacked any internal high-relief arches, depositional systems were uniformly developed over wide areas. Macauley et al. (1964) pointed out how three Mississippian map-units can be traced from outcrop in the Cordillera into the subsurface of the plains. With respect to the study area, the Exshaw and Banff Formations are assigned to their lower unit and the Pekisko, Shunda and Debolt Formations to their middle unit. The basal Exshaw Formation is a thin, upward-coarsening bituminous shale (Macqueen and Sandberg 1970) deposited under poorly-oxgenated, probably stillstand conditions. The overlying Banff Formation is an interbedded shale-to-carbonate succession (Ethier 1975) which indicates continued transgression and greater shelf circulation. That this trend was maintained is shown by the mostly limestone succession of the overlying Pekisko, Shunda and Debolt Formations (Macauley 1958).

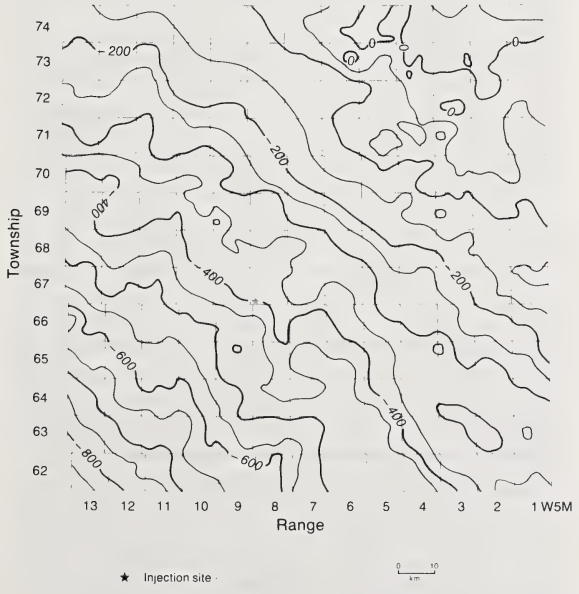

Figure 10. Structure contours (50 m interval) on top of Mississippian strata, i.e. pre-Absaroka unconformity.

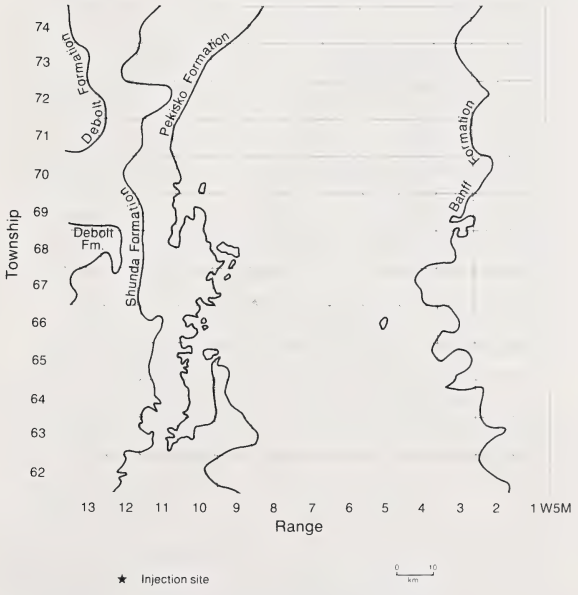

Figure 11. Subcrop distribution, at the pre-Absaroka/Zuni composite unconformity, of tops of the westwardly-dipping Mississippian Banff, Pekisko, Shunda and Debolt Formations.

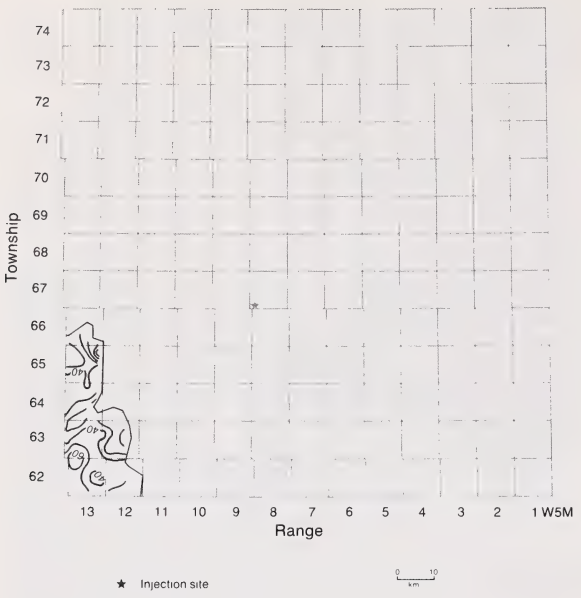

Figure 12. Isopachs (10 m interval) of preserved Lower Jurassic strata between the post-Paleozoic and pre-Cretaceous unconformities, corresponding to the Absaroka sequence.

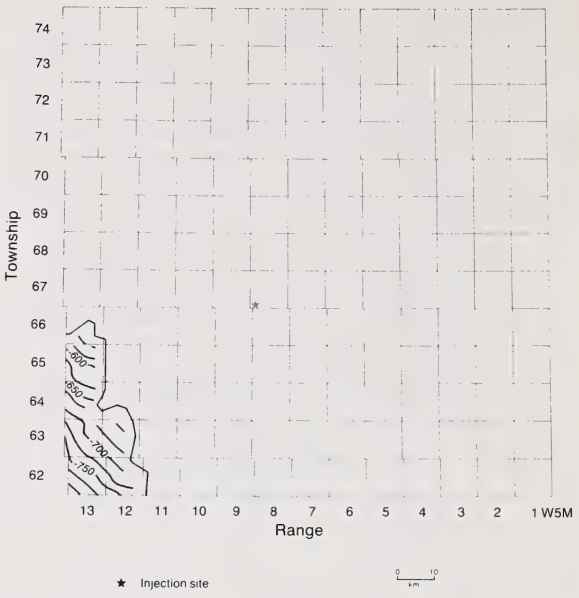

Figure 13. Structure contours (25 m interval) on top of preserved Lower Jurassic strata, i.e. pre-Zuni unconformity.

Pre-Absaroka unconformity

Regression of Mississippian seas back to the narrowing Cordilleran basin was accompanied by a westward tilt of the craton margin (Porter et al. 1982) and continued foundering of the Peace River Arch area (Lavoie 1958). This emergence and mild relief triggered extensive erosion which stripped back the Mississippian rocks effectively to their present subcrop pattern. Procter and Macauley (1968) consider that they may have originally extended as far as the present Canadian Shield area. Paleogeomorphological work by Martin (1966) indicates that early southwest-flowing drainage was rectilinear between a series of northeast-facing limestone escarpments. Structure contours on the top of Paleozoic strata in the study area (figure 10) reveal a steplike topography (locally as steep as 10.9 m/km) with northwest-southeast alignment which is suggestive of this type of landform.

Elsewhere in the continental interior (e.g. Williston Basin), the Absaroka sequence straddles the Paleozoic-Mesozoic boundary with a continuous Late Pennsylvanian to very Early Jurassic series of strata. In the vicinity of the study area, however, the Pennsylvanian was a period of subaerial erosion. The original Permian cover (Belloy Formation) was almost completely removed by further erosion in the Early Triassic. Later Triassic beds were probably not deposited, and the original Lower Jurassic cover (Fernie Group) was almost completely removed by pre-Cretaceous erosion. The net result of these developments was that, except for the southwest corner of the study area (figure 12), the pre-Absaroka and pre-Zuni unconformities were merged into a composite feature.

Absaroka sequence

This sequence represents the final episode in the long history of development of the passive margin. By this time, the main depositional area had shifted to the outer margin of the Paleozoic continental platform against a marginal, back-arc basin (Price 1984). The Permian Belloy Formation in the subsurface of the Peace River region (Halbertsma 1959) comprises three members. As summarized by McGugan et al. (1964), these mainly consist of interbedded sandstones, siltstones, porous dolomites, bedded cherts and occasional limestones. Within the Peace River embayment, the carbonate facies is distributed as northwest-southeast trending banks surrounded by detrital sediment (Naqvi 1972). Following Triassic emergence, the Lower Jurassic calcareous shales and thin cherty sandstones of the Nordegg Member (Fernie Group, figures 12 and 13) accumulated on the outer shelf (Springer et al. 1964). This paleogeographic situation shows minimal supply of sediment from cratonic land areas to the east, and as such heralds the onset of a fundamental change in basin conditions associated with Cordilleran deformation to the west.

Cordilleran evolution

Pre-Zuni unconformity

As noted above, this unconformity within the study area mostly coincides with the pre-Absaroka break and is widely referred to as the pre-Cretaceous unconformity. Northeast of the updip erosional edges of Triassic and Lower Jurassic strata, Lower Cretaceous rocks rest on southwest-dipping Mississippian carbonates and shales, thus creating a gap of about 200 Ma in the local stratigraphic record. In this region, the pre-Zuni unconformity acts as a trap for bitumen in the Upper Devonian Grosmont Formation (Harrison, pers. comm.) and the surface itself is known to be extensively saturated with oil (Masters 1984).

Between Middle Jurassic and Early Cretaceous time, ocean-to-continent collision along the Pacific rim compressed the outer part of the Paleozoic craton-margin sedimentary pile and resulted in its eastward displacement as thrust slices. In turn, this thickened crust became a dividing line in drainage directions and the cause of isostatic downwarp over the adjacent Alberta area. In this new foreland basin, the principal paleogeographic features were vast plains of eroded Cordilleran debris and the shallow epicontinental Western Interior Seaway. During accumulation of the Zuni sequence, general trends were changes from longitudinal to transverse drainage (Miall 1984) and from an Arctic to Arctic-to-Gulfian connection for the Western Interior Seaway. As examples, Cretaceous deposition was preceded by the development of northwest-flowing drainage into an Arctic embayment, whereas Upper Cretaceous Wapiti-equivalent beds show southeastward transport (Nurkowski and Rahmani 1984) into a major continuous epicontinental sea southward (Williams and Stelck 1975).

Zuni sequence

This sequence (figure 14) records a constantly changing balance of continental versus marine depositional systems, due to the varying quantity and transport directions of sediment derived from Cordilleran denudation versus the varying extent and level of the Western Interior Seaway. The resulting transgressions and regressions reflect a combined tectono-eustatic mechanism (viz. Caldwell 1984). Sedimentological studies of coastal successions (Rahmani 1984; Rosenthal and Walker 1984; Koster and Currie 1987) and the results of theoretical modelling of epicontinental seas (Parrish et al. 1984) jointly indicate that circulation in the seaway was influenced by both tides and storm-generated waves. Hence, alluvial deposits on the lower foreland commonly have an estuarine character and shoreline sediments typically show signs of redispersal alongshore or offshore.

Cretaceous strata in the Alberta plains are divided, in upward order, into the Mannville, Colorado and Post-Colorado (with conformable continuation into the lowermost Tertiary) Groups. The Mannville Group corresponds to the Columbian phase of Cordilleran deformation, the Colorado Group to a lull in plate convergence, and the Post-Colorado Group to the final Laramide phase of Cordilleran deformation. Each has been studied intensively from various resource-related and academic standpoints, and good recent summary volumes are available (Masters 1984; Stott and Glass 1984).

In the study area, deposition of Mannville Group strata began during the Aptian stage with southeastward transgression of the boreal seaway. This caused alluviation along the opposing northwest-flowing drainage system developed on Paleozoic terrain with 100 to 200 m of local valley relief; one such valley, termed the 'Edmonton Channel,' underlies the study area. This paleogeographical change is recorded by a continental-marine transition in the early Mannville stratigraphy. The basal Gething Formation consists of valley-fill fluvial sands overlain by laminated sands and shales of tidal flat and shoreline environments (Rottenfusser 1982), and then in Albian time by shallow marine, glauconitic sands of the Bluesky Formation (Smith et al. 1984). Rudkin (1964) considered that the Bluesky depositional system was simply a reworked top of the Gething onshore sands. The richest heavy oil concentrations within the Gething Formation are associated with tidal channel, shoreline and shallow marine strata (Rottenfusser 1982). With farther south-

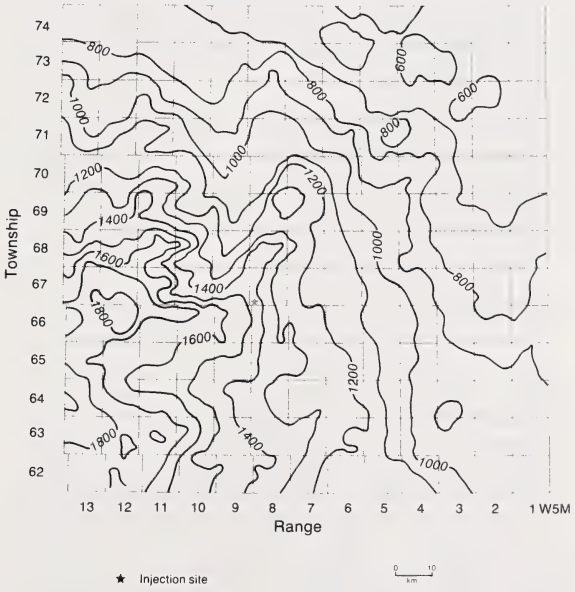

Figure 14. Isopachs (100 m interval) of preserved Cretaceous and Paleocene strata, corresponding to the Zuni sequence. This distribution partly reflects the modern topography of the Swan Hills Upland and Lesser Slave Lowland (figure 15), and includes minor surficial deposits of later Tertiary age.

ward advance of the transgression, Bluesky Formation sands were onlapped by marine shales (Clearwater and Wilrich Formations) representing more offshore environments. This later marine phase, however, was brief due to an increased rate of Cordilleran tectonism that triggered northward progradation of clastic wedges (Spirit River Formation; Cant 1983; Smith et al. 1984). Beach and barrier-island successions of the Glauconitic sandstone were coeval with offshore shales of the Clearwater Formation to the north (Jackson 1984). The overlying Grand Rapids Formation is mostly sandstone, and according to Rudkin (1964) Lesser Slave Lake approximately divides fully marine successions to the north from predominantly nonmarine deposits to the southeast. Jackson (1984) shows that within this transition zone progradational shore-related sands shifted back and forth about an east-west line.

Deposition of the Mannville Group was terminated by a late Albian eustatic sea level rise. This led to complete inundation of the Western Interior (Rudkin 1964) and marine conditions were maintained throughout accumulation of the Colorado Group. The offshore setting of the study area is recorded by dark gray shales of the Joli Fou Formation and higher up-section by the speckled shales, containing prominent fish-scale marker horizons, of the Upper Colorado Group. Deposition of argillaceous sediments was interrupted by the offshore-bar sand complex of the Viking Formation in late Albian time (Boethling 1976); this unit is gas-bearing at its updip eastern margin. A similar depositional system was responsible, in Coniacian time, for the Badheart sandstone near the top of the Colorado Group.

Laramide deformation triggered the deposition of a series of eastward-thinning, nonmarine clastic wedges that were intercalated with continuing deposition of argillaceous sediments in the Western Interior Seaway. This cyclicity of Post-Colorado Group strata is best developed in the southern Alberta plains because of more frequent incursions by the seaway. There, the Milk River, Judith River and Edmonton-Paskapoo refer to the clastic wedges and Pakowki and Bearpaw to the intervening marine intervals (Lerand 1982; Walker 1982); north of Edmonton, Milk River and Bearpaw environments were not developed. The result of these regional stratigraphic trends is that the Post-Colorado Group of the study area comprises a single marine (Lea Park Formation) to continental (Wapiti and Paskapoo Formations) succession. The Lea Park Formation represents a continuation of deposition of argillaceous sediments from the preceding Joli Fou and upper Colorado intervals, the boundary being placed at the 'first white specks' marker. The overlying Wapiti Formation is a coal-bearing alluvial succession of lenticular sandstones enclosed by mudstones (Kramers and Mellon 1972). These are conformably overlain by a mostly sandstone succession of the alluvial Paskapoo Formation which, according to Carrigy (1971), represents paleodrainage from northern Montana.

Post-Zuni erosion

Following the terminal stage of Laramide deformation in the Paleocene, the modern drainage system of Alberta began to evolve. Apart from a braidplain gravel sheet of Oligocene age (Vonhof 1965; Kramers and Mellon 1972) now confined to plateau-capping outliers, the geomorphic role of the developing northeast-ward drainage has been erosional. Thus, as noted in the introduction to this section of the bulletin, the modern physiography of the study area involves the Swan Hills Upland capped by Paskapoo-Oligocene sandstones and gravels, and the Lesser Slave Lowland along its eastern and northern borders underlain by earlier Post-Colorado Group rocks. This bedrock geology (figure 15) is veneered by a variety of glacial and postglacial surficial deposits of Quaternary age (St. Onge and Richard 1975).

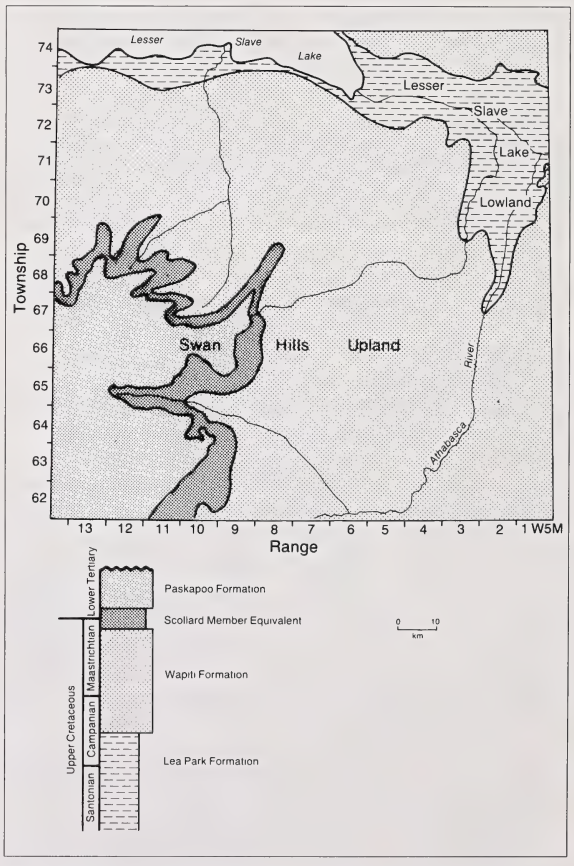

Figure 15. Bedrock geology of the study area (based on Green 1982).

Hydrogeology

Introduction

The term 'hydrostratigraphic unit' refers either to a single stratigraphic unit or to a group of stratigraphic units that are contiguous in the stratigraphic succession and have similar flow parameters. Characterization of individual hydrostratigraphic units is based on information on the properties of the fluids and porous matrix obtained from formation water analyses, drill-stem tests and core analyses, combined with knowledge of the stratigraphic geometry and lithology; see Bachu et al. (1987) for data processing and synthesis techniques. In addition to the processing of standard formation water analyses using the techniques described by Bachu et al. (1987), 33 detailed analyses of formation waters (appendix B) were studied using the computer code SOLMNEQF (Aggarwal et al. 1986) and the results reported in terms of mineral saturations.

For a fully saturated succession of sedimentary rocks, gravity-driven flow is given by Darcy's law (momentum equation):

$$\bar{q} = -(\bar{\bar{k}}/\mu)[\mathrm{grad}(p) + \rho\bar{g}\,] \qquad (1)$$

where $\bar{q}$ is the specific discharge, $\bar{\bar{k}}$ is the permeability tensor, μ is dynamic viscosity, and $\bar{g}$ is the gravity vector in a system of coordinates oriented upward. For a homogeneous fluid of constant density, ρ_o, a flow potential can be defined, and equation (1) can be written in terms of the hydraulic head H:

$$H = p/(\rho_o g) + z \qquad (2)$$

where z is the elevation above a reference datum. For a variable density fluid, equation (1) can be written as:

$$\bar{q} = -(\bar{\bar{k}}\rho_o g/\mu)[\mathrm{grad}(H) + (\Delta\rho/\rho_o)\mathrm{grad}(z)] \qquad (3)$$

where $\Delta\rho$ is the density variation with respect to the reference density, ρ_o. The most common value used for the reference density is $\rho_o = 1000\ kg/m^3$ (freshwater density). However, it must be pointed out that any other constant value can be used (e.g. the minimum, the maximum or the average water density in an aquifer).

Equation 3 shows that the lateral component of flow of formation waters can be described by the magnitude and direction at each point of the horizontal component of the specific discharge vector and is a function of the hydraulic conductivity and of the freshwater hydraulic head gradient (Lusczynsky 1961; De Wiest 1965; Bear 1972; Frind 1980). The vertical component of equation 3 shows that vertical flow in a hydrostratigraphic unit is driven both by piezometric differences and variations of fluid density. The geometry of an aquifer can also induce a vertical component to the fluid flow. In a system of coordinates oriented downward, the vertical component of equation 1 is:

$$q_z = -\frac{k}{\mu}\left[\frac{\partial p}{\partial z} - \rho g\right] \qquad (4)$$

This relation allows the analysis of vertical fluid movement using pressure vs depth plots. At any location, there is no vertical flow if the slope of the curve of pressure as a function of depth is equal to the product, ρg, at that location. A slope either less than or greater than ρg shows that the flow has a downward or an upward vertical component, respectively. If the fluid density is constant, it is often convenient to represent the variation with depth of the pressure-head, $p/\rho g$, which has length dimensions. In this case, the slope of the curve, $p/\rho g = f(z)$, is dimensionless and easier to compare with hydrostatic conditions. A slope less than or greater than unity shows downward or upward flow, respectively. In many cases, the pressure (or pressure-head) variation with depth is represented by a straight line, particularly when there are few data points (measurements) at the respective location.

In practice, if the fluid density is variable, the assumption commonly made is that the fluid flow is nearly horizontal and that buoyancy effects are very small and, therefore, negligible. As a result, equivalent freshwater heads effectively characterize the system. Davies (1987) has shown that it is not the absolute magnitude of the density-related error term, but rather the relative magnitude of this term versus the magnitude of the equivalent freshwater head term that determines whether density-related gravity effects will be significant in a given situation. Davies (1987) calls this relative strength of the two driving forces DFR (Driving-Force Ratio), as defined by:

$$DFR = (\Delta\rho|\mathrm{grad}(E)|)/(\rho_o|\mathrm{grad}(H_o)|) \qquad (5)$$

where $|\mathrm{grad}(E)|$ is the magnitude of the elevation gradient, and $|\mathrm{grad}(H_o)|$ is the magnitude of the freshwater hydraulic gradient. Assuming an isotropic medium, Davies (1987) has shown through numerical experiments that the value DFR = 0.5 is the approximate threshold at which buoyancy-related gravity effects may become significant. This threshold may vary slightly, depending on actual flow conditions and on the scale and accuracy required for a particular study. The errors introduced by the use of equivalent freshwater hydraulic heads are associated with both

Table 5. Hydraulic parameters from drillstem tests.

Hydrostratigraphic unit	Number of determinations	Intrinsic permeability (m^2)			Hydraulic conductivity (m/d)			Specific storage (m^{-1})
		Minimum	Average	Maximum	Minimum	Average	Maximum	Average
Badheart aquifer	2	-	$6.3x10^{-14}$	-	-	$5.2x10^{-2}$	-	-
Second White Speckled aquifer	2	-	$1.8x10^{-16}$	-	-	$1.5x10^{-4}$	-	-
Base of Fish Scales Zone aquifer	8	$1.4x10^{-18}$	$4.1x10^{-17}$	$1.7x10^{-16}$	$1.2x10^{-6}$	$3.5x10^{-5}$	$1.4x10^{-4}$	-
Viking aquifer	26	$3.6x10^{-16}$	$3.5x10^{-15}$	$4.1x10^{-14}$	$3.0x10^{-4}$	$2.9x10^{-3}$	$3.5x10^{-2}$	-
Joli Fou aquitard	7	$1.8x10^{-18}$	$1.5x10^{-17}$	$4.6x10^{-17}$	$1.5x10^{-6}$	$1.2x10^{-5}$	$3.9x10^{-5}$	0.000330
Upper Mannville aquifer system	65	$2.0x10^{-16}$	$1.1x10^{-14}$	$1.4x10^{-12}$	$1.7x10^{-4}$	$9.2x10^{-3}$	1.2	0.000380
Clearwater-Wilrich aquitard	17	$9.9x10^{-19}$	$1.8x10^{-17}$	$1.1x10^{-16}$	$8.2x10^{-7}$	$1.5x10^{-5}$	$9.4x10^{-5}$	-
Lower Mannville aquifer system	141	$6.4x10^{-17}$	$7.0x10^{-15}$	$6.2x10^{-12}$	$5.3x10^{-5}$	$5.8x10^{-3}$	5.2	0.000280
Fernie aquitard	1	-	$7.7x10^{-19}$	-	-	$6.4x10^{-7}$	-	-
Belloy aquifer	2	-	$2.3x10^{-15}$	-	-	$1.9x10^{-3}$	-	-
Shunda aquifer	1	-	$4.6x10^{-15}$	-	-	$3.8x10^{-3}$	-	-
Pekisko aquifer	9	$5.6x10^{-17}$	$6.0x10^{-16}$	$5.9x10^{-15}$	$4.7x10^{-5}$	$5.0x10^{-4}$	$4.9x10^{-3}$	-
Banff carbonate aquifer	7	$1.3x10^{-16}$	$1.2x10^{-15}$	$3.9x10^{-13}$	$1.1x10^{-4}$	$9.8x10^{-4}$	$3.3x10^{-1}$	-
Banff shale aquitard	2	-	$4.2x10^{-18}$	-	-	$3.0x10^{-6}$	-	-
Wabamun aquifer	11	$1.4x10^{-16}$	$8.0x10^{-15}$	$1.3x10^{-13}$	$1.2x10^{-4}$	$6.5x10^{-3}$	$1.1x10^{-1}$	0.000350
Upper Winterburn aquifer	6	$4.5x10^{-18}$	$1.8x10^{-15}$	$5.9x10^{-14}$	$3.5x10^{-6}$	$1.4x10^{-3}$	$4.8x10^{-2}$	0.000087
Nisku aquifer	8	$1.6x10^{-17}$	$1.2x10^{-14}$	$2.5x10^{-13}$	$1.2x10^{-5}$	$9.4x10^{-1}$	$1.9x10^{-1}$	0.001000
Grosmont aquifer	1	-	$2.5x10^{-14}$	-	-	$2.0x10^{-2}$	-	-
Ireton aquitard	1	-	$1.3x10^{-15}$	-	-	$1.1x10^{-3}$	-	-
Swan Hills-Slave Point aquifer	22	$1.6x10^{-18}$	$7.0x10^{-16}$	$8.3x10^{-13}$	$1.2x10^{-6}$	$5.4x10^{-4}$	$6.5x10^{-1}$	0.000079
Upper Watt Mountain aquitard	4	$1.2x10^{-19}$	$3.1x10^{-18}$	$1.3x10^{-16}$	$9.2x10^{-8}$	$2.4x10^{-6}$	$9.7x10^{-5}$	0.000040
Gilwood aquifer	48	$5.8x10^{-17}$	$4.4x10^{-15}$	$7.5x10^{-13}$	$4.3x10^{-5}$	$3.3x10^{-3}$	$5.6x10^{-1}$	0.000210
Muskeg aquitard	1	-	$9.4x10^{-20}$	-	-	$6.9x10^{-8}$	-	-
Keg River aquifer	7	$1.6x10^{-16}$	$3.5x10^{-15}$	$6.1x10^{-14}$	$1.1x10^{-4}$	$2.5x10^{-3}$	$4.4x10^{-2}$	0.000480
Contact Rapids aquifer	1	-	$2.8x10^{-14}$	-	-	$2.0x10^{-2}$	-	0.000120
Granite Wash aquifer	3	$4.1x10^{-15}$	$8.4x10^{-14}$	$7.2x10^{-13}$	$3.0x10^{-3}$	$6.2x10^{-2}$	$5.3x10^{-1}$	0.000110
Lynx aquifer	3	$3.3x10^{-17}$	$1.3x10^{-16}$	$3.0x10^{-16}$	$2.4x10^{-5}$	$9.2x10^{-5}$	$2.2x10^{-4}$	-
Pika aquifer	4	$9.5x10^{-16}$	$1.6x10^{-14}$	$3.9x10^{-13}$	$6.9x10^{-4}$	$1.2x10^{-2}$	$2.9x10^{-1}$	-
Eldon aquifer	2	-	$2.4x10^{-14}$	-	-	$1.8x10^{-2}$	-	0.000360
Basal Cambrian aquifer	3	$1.9x10^{-16}$	$6.0x10^{-16}$	$2.3x10^{-15}$	$1.4x10^{-4}$	$4.4x10^{-4}$	$1.7x10^{-3}$	-
Precambrian aquiclude	1	-	$1.6x10^{-17}$	-	-	$1.2x10^{-5}$	-	0.000110

magnitude and the direction of the specific discharge vector.

The aquifer systems in the Phanerozoic section of the Swan Hills study area are not horizontal. The general dip is from northeast to southwest, with Paleozoic strata having more pronounced dips than do Cretaceous strata. The density of formation waters is variable, both within as well as between hydrostratigraphic units, as it will be shown subsequently. Therefore, some buoyancy-related effects must be present in the flow. In order to assess the importance of these effects, the DFR was computed on a regional scale for the aquifers in the study area, considering the average fluid density in each aquifer as the reference density ρ_o for that aquifer. The results show that the DFR values for the Cretaceous aquifer systems are significantly below the threshold as defined by Davies (1987), while for the Paleozoic aquifer systems the DFR values are around this threshold. However, the anisotropy of the aquifers (vertical permeability less than the horizontal permeability) practically has the effect of diminishing the vertical flow, such that the value of DFR = 0.5 is most probably an underestimate of the true threshold of significance for buoyancy-related effects. Therefore, taking the aquifer anisotropy into account, it is considered that the buoyancy effects are negligible in the Paleozoic aquifers as well.

Based on the above theoretical and practical considerations, the lateral flow of formation waters is analysed in the following section using freshwater potentiometric surfaces which indicate the flow directions if the aquifers are assumed to be isotropic in the horizontal plane. For easier representation and analysis, the vertical flow between aquifer units is described on a local scale by pressure-head vs depth plots based on data points. On a regional scale, the analysis is performed using hydraulic head profiles along cross sections. The hydraulic head profiles were produced as cross sections through surfaces of static hydraulic head computed with actual values of formation water density. Assuming that buoyancy effects are

Table 6. Hydraulic parameters from core analyses.

Hydrostratigraphic unit	Number of determinations	Intrinsic permeability (m^2)			Hydraulic conductivity (m/d)			Anisotropy	Porosity (%)		
		Minimum	Average	Maximum	Minimum	Average	Maximum	K_h/K_v	Min.	Avg.	Max.
Base of Fish Scales Zone aquifer	7	$2.8x10^{-15}$	$1.0x10^{-13}$	$1.4x10^{-12}$	$2.6x10^{-3}$	$2.6x10^{-3}$	6.81	0.9	8.5	15.4	22.0
Viking aquifer	37	$13.x10^{-16}$	$1.2x10^{-14}$	$5.1x10^{-13}$	$1.1x10^{-4}$	$1.0x10^{-2}$	0.47	4.2	9.3	14.4	24.7
Upper Mannville aquifer system	7	$2.1x10^{-15}$	$8.5x10^{-15}$	$3.6x10^{-14}$	$1.8x10^{-3}$	$7.0x10^{-3}$	0.03	3.4	10.1	15.1	19.6
Lower Mannville aquifer system	33	$1.4x10^{-16}$	$1.0x10^{-14}$	$8.8x10^{-13}$	$1.2x10^{-4}$	$8.7x10^{-3}$	0.74	8.3	7.6	16.5	28.3
Belloy aquifer	9	$4.1x10^{-14}$	$1.3x10^{-13}$	$4.2x10^{-13}$	$3.6x10^{-2}$	0.11	0.35	3.5	1.6	13.7	19.0
Shunda aquifer	10	$4.0x10^{-16}$	$7.4x10^{-15}$	$1.9x10^{-13}$	$3.2x10^{-4}$	$6.1x10^{-3}$	0.16	1.8	0.7	9.4	15.6
Pekisko aquifer	13	$3.5x10^{-16}$	$2.6x10^{-15}$	$2.2x10^{-14}$	$2.9x10^{-4}$	$2.2x10^{-3}$	0.02	4.0	4.3	7.3	10.3
Banff carbonate aquifer	14	$7.4x10^{-17}$	$7.5x10^{-16}$	$4.1x10^{-14}$	$6.2x10^{-5}$	$6.3x10^{-4}$	0.04	13.8	1.8	6.2	16.7
Wabamun aquifer	4	-	$1.9x10^{-14}$	-	-	$1.6x10^{-2}$	-	14.6	5.4	18.9	24.5
Upper Winterburn aquifer	2	-	$6.9x10^{-14}$	-	-	$5.0x10^{-2}$	-	-	-	10.0	-
Nisku aquifer	15	$5.1x10^{-17}$	$5.8x10^{-15}$	$2.1x10^{-13}$	$3.8x10^{-5}$	$4.4x10^{-3}$	0.20	11.8	1.3	6.3	15.9
Grosmont aquifer	4	$3.8x10^{-15}$	$9.9x10^{-14}$	$8.7x10^{-13}$	$3.1x10^{-3}$	$8.0x10^{-2}$	0.71	9.1	4.0	6.6	10.3
Ireton aquitard	2	-	$3.5x10^{-16}$	-	-	$2.6x10^{-4}$	-	10.0	-	4.0	-
Beaverhill Lake-Cooking Lake aquifer	153	$3.7x10^{-17}$	$1.1x10^{-14}$	$9.1x10^{-13}$	$2.8x10^{-5}$	$8.4x10^{-3}$	0.72	1.2	0.4	6.8	18.4
Swan Hills-Slave Point aquifer	2456	$1.2x10^{-17}$	$2.9x10^{-15}$	$2.4x10^{-12}$	$9.6x10^{-6}$	$2.2x10^{-3}$	1.84	4.9	0.4	5.2	19.2
Upper Watt Mountain aquitard	74	$1.2x10^{-17}$	$3.8x10^{-16}$	$1.4x10^{-14}$	$9.0x10^{-6}$	$2.8x10^{-4}$	0.01	10.0	1.0	5.5	12.1
Gilwood aquifer	334	$2.1x10^{-17}$	$4.8x10^{-14}$	$8.5x10^{-13}$	$1.5x10^{-5}$	$3.5x10^{-2}$	0.64	6.4	1.8	10.8	19.9
Muskeg aquitard	20	$2.2x10^{-17}$	$4.9x10^{-16}$	$6.8x10^{-14}$	$1.6x10^{-5}$	$3.7x10^{-4}$	0.05	1.2	1.8	6.4	14.0
Keg River aquifer	9	$2.8x10^{-16}$	$9.1x10^{-15}$	$3.6x10^{-13}$	$2.0x10^{-4}$	$6.4x10^{-3}$	0.26	12.9	2.9	9.1	16.6
Contact Rapids aquifer	4	$3.9x10^{-17}$	$2.7x10^{-15}$	$1.7x10^{-13}$	$2.8x10^{-5}$	$2.0x10^{-3}$	0.12	5.1	2.2	5.5	9.1
Ernestina Lake aquifer	1	-	$6.9x10^{-15}$	-	-	$4.5x10^{-3}$	-	3.1	-	10.4	-
Granite Wash aquifer	1	-	$1.7x10^{-13}$	-	-	0.12	-	3.5	-	16.4	-
Lynx aquifer	3	-	$5.2x10^{-15}$	-	-	$3.8x10^{-3}$	-	2.4	8.1	10.0	13.6
Lower Cambrian aquifer	1	-	$7.8x10^{-17}$	-	-	$5.7x10^{-5}$	-	-	-	4.0	-
Basal Cambrian aquifer	4	$2.7x10^{-16}$	$2.3x10^{-14}$	$1.8x10^{-13}$	$2.0x10^{-4}$	$1.7x10^{-2}$	0.13	8.4	8.6	10.0	13.3

K_h = horizontal hydraulic conductivity, K_v = vertical hydraulic conductivity

negligible, the relative position of the hydraulic head profiles of two adjacent aquifer systems separated by an aquitard shows the direction of possible vertical flow. The hydraulic head values in potentiometric surfaces and in corresponding vertical profiles do not match because of the different scaling of the pressure term, one with respect to freshwater density and one with respect to the real density of formation waters. It should be pointed out here that the evaluation for possible vertical flow using pressure-head and actual hydraulic head profiles should be done only for adjacent aquifer systems with "relatively close" values of formation water density, although more than two aquifer systems are represented usually in the same figure. As was mentioned earlier, only in this case can the buoyancy effects be neglected for the specific conditions in the Swan Hills study area.

Along the same vertical, aquifers of different hydraulic properties are in continuity if they exhibit a linear hydrostatic slope on a pressure head versus depth plot; on a more regional scale, the point water hydraulic head profiles should be coincident. These conditions of hydraulic continuity may be present even when aquifers are separated by thin and weak aquitards. The aquifers can then be grouped into a single aquifer system for the purpose of this analysis. Marked deflections on pressure-head versus depth plots reflect weak vertical leakage between aquifers

Table 7. Regional hydraulic parameters.

Hydrostratigraphic unit	Ratio K_{core}/K_{dst}	(#core/#dst)	Bulk hydraulic conductivity (m/d)	[Source]	Specific storage (m^{-1}) $[(Ss)_{core}+(Ss)_{dst}]/2$	Diffusivity (m^2/d)
Badheart aquifer	-	[0/2]	$5.2x10^{-2}$	[DST]	-	-
Second White Speckled aquifer	-	[0/2]	$1.5x10^{-4}$	[DST]	-	-
Base of Fish Scales Zone aquifer	2430.0?	[7/8]	$4.0x10^{-2}$	[Weighted]	$2.1x10^{-4}$	190.9
Viking aquifer	3.4	[37/26]	$7.1x10^{-3}$	[Weighted]	$2.0x10^{-4}$	36.2
Joli Fou aquitard	-	[0/7]	$1.2x10^{-5}$	[DST]	$3.3x10^{-4}$	0.04
Upper Mannville aquifer system	0.8	[7/65]	$9.0x10^{-3}$	[Weighted]	$3.6x10^{-4}$	24.8
Clearwater-Wilrich aquitard	-	[0/17]	$1.5x10^{-5}$	[DST]	-	-
Lower Mannville aquifer system	1.5	[33/141]	$6.4x10^{-3}$	[Weighted]	$3.3x10^{-4}$	19.4
Fernie aquitard	-	[0/1]	$6.4x10^{-7}$	[DST]	-	-
Belloy aquifer	57.9	[9/2]	$9.0x10^{-2}$	[Weighted]	$6.7x10^{-5}$	1347.0
Shunda aquifer	1.6	[10/1]	$5.9x10^{-3}$	[Weighted]	$4.6x10^{-5}$	128.7
Pekisko aquifer	4.4	[13/9]	$1.5x10^{-3}$	[Weighted]	$3.6x10^{-5}$	41.7
Banff carbonate aquifer	0.6	[14/7]	$7.5x10^{-4}$	[Weighted]	$3.0x10^{-5}$	24.9
Banff shale aquitard	-	[0/2]	$3.0x10^{-6}$	[DST]	-	-
Wabamun aquifer	2.5	[4/11]	$9.0x10^{-3}$	[Weighted]	$3.2x10^{-4}$	28.2
Upper Winterburn aquifer	35.7	[2/6]	$1.4x10^{-2}$	[Weighted]	$1.2x10^{-4}$	113.3
Nisku aquifer	0.5	[15/8]	$6.1x10^{-3}$	[Weighted]	$5.5x10^{-4}$	11.1
Grosmont aquifer	4.0	[4/1]	$6.8x10^{-2}$	[Weighted]	$3.4x10^{-5}$	2000.0
Ireton aquitard	0.2	[2/1]	$1.5x10^{-8}$	[Literature]	$1.5x10^{-5}$	0.001
Beaverhill Lake-Cooking Lake aquifer	-	[153/0]	$8.4x10^{-3}$	[Core]	$2.5x10^{-5}$	336.0
Swan Hills-Slave Point aquifer	4.1	[2456/22]	$2.2x10^{-3}$	[Core]	$2.0x10^{-5}$	110.0
Upper Watt Mountain aquitard	116.7	[74/4]	$2.7x10^{-4}$	[Core]	$2.8x10^{-5}$	9.6
Gilwood aquifer	10.6	[334/48]	$3.1x10^{-2}$	[Weighted]	$2.1x10^{-4}$	147.6
Muskeg aquitard	-	[10/1]	$6.9x10^{-8}$	[DST]	$7.3x10^{-5}$	0.001
Keg River aquifer	2.6	[9/7]	$4.7x10^{-3}$	[Weighted]	$1.1x10^{-4}$	118.0
Contact Rapids aquifer	0.1	[4/1]	$7.0x10^{-3}$	[Weighted]	$9.3x10^{-5}$	75.3
Ernestina Lake aquifer	-	[1/0]	$4.5x10^{-3}$	[Core]	$1.8x10^{-4}$	25.0
Granite Wash aquifer	1.9	[1/3]	$7.6x10^{-2}$	[Weighted]	$1.9x10^{-4}$	400.0
Lynx aquifer	41.3	[3/3]	$3.8x10^{-3}$	[Core]	$1.1x10^{-4}$	34.6
Pika aquifer	-	[4/0]	$1.2x10^{-2}$	[DST]	-	-
Eldon aquifer	-	[2/0]	$1.8x10^{-2}$	[DST]	$3.6x10^{-4}$	50.0
Basal Cambrian aquifer	38.6	[4/3]	$4.4x10^{-4}$	[DST]	$1.1x10^{-4}$	4.0

through the intervening (strong) aquitards that cannot be neglected. The same can be said of well separated point water hydraulic head profiles along cross sections.

An aquifer system, as previously defined, can be regionally characterized by composite values of the aquifer parameters, depending on whether the continuity is vertical (most frequent case) or lateral (in the case of depositional boundaries). Based on these principles, the objective of the analysis of the natural fluid flow regime is to simplify the flow system into groups of units. Consequently, for a given block of sediments, one may consider two levels of definition for the hydrostratigraphy: an initial level based on the geometry and lithology of the individual stratigraphic units, and a second (synthesis) level based on the regional analysis of the fluid flow. Besides its intrinsic interest, this synthesis has obvious applications for any further modelling effort. At the same time, it explains why regional values of the hydraulic parameters used in modelling cannot be defined prior to the regional analysis of the flow regime itself.

Based on the examination of 635 drillstem tests, hydraulic parameters were determined on 416 tests, and the results reported in table 5. Hydraulic parameters from 3217 core analyses are shown in table 6. The regional hydraulic parameters subsequently used in the numerical modelling are listed in table 7. While recognizing that the regional values are, to an extent, subjectively selected, on a regional scale they best represent the in situ hydraulic properties based on available information. The difficulty in selecting a representative bulk hydraulic conductivity is exemplified by the data in table 8 which show the minimum and maximum values of horizontal and vertical hydraulic conductivities for 23 hydrostratigraphic units.

Hydrostratigraphic geometry

In hydrogeological studies it is important to determine the geometry of the major lithological units, particularly that of the aquitards and aquicludes, because the absence of these water-retarding hydrostratigraphic units allows juxtaposition of the aquifers. Often of equal im-

Table 8. Range of hydraulic conductivities from core analyses.

Hydrostratigraphic unit	Horizontal hydraulic conductivity (m/d)			Vertical hydraulic conductivity (m/d)		
	Minimum	Representative	Maximum	Minimum	Representative	Maximum
Base of Fish Scales Zone aquifer	$1.4x10^{-3}$	$8.0x10^{-2}$	2.11	$4.7x10^{-3}$	$9.0x10^{-2}$	0.62
Viking aquifer	$2.9x10^{-4}$	$1.3x10^{-2}$	0.85	$4.0x10^{-5}$	$3.2x10^{-3}$	0.22
Upper Mannville aquifer system	$4.6x10^{-3}$	$1.7x10^{-2}$	0.031	$6.8x10^{-4}$	$4.9x10^{-3}$	$3.0x10^{-2}$
Lower Mannville aquifer system	$2.8x10^{-4}$	$1.8x10^{-2}$	2.10	$5.0x10^{-5}$	$2.1x10^{-3}$	0.26
Belloy aquifer	$3.6x10^{-2}$	0.13	1.22	$3.2x10^{-2}$	$4.0x10^{-2}$	0.10
Shunda aquifer	$4.8x10^{-4}$	$7.8x10^{-3}$	0.27	$2.2x10^{-4}$	$4.2x10^{-3}$	$9.2x10^{-2}$
Pekisko aquifer	$6.8x10^{-4}$	$2.8x10^{-3}$	0.067	$1.2x10^{-4}$	$7.0x10^{-4}$	$5.2x10^{-3}$
Banff carbonate aquifer	$2.4x10^{-4}$	$2.8x10^{-3}$	0.092	$1.6x10^{-5}$	$2.0x10^{-4}$	$1.3x10^{-2}$
Wabamun aquifer	$3.1x10^{-3}$	$3.0x10^{-2}$	0.52	-	$2.0x10^{-3}$	-
Upper Winterburn aquifer	-	$8.2x10^{-3}$	-	-	$9.9x10^{-3}$	-
Nisku aquifer	$1.6x10^{-4}$	$2.2x10^{-2}$	1.60	$9.0x10^{-6}$	$1.9x10^{-3}$	$2.5x10^{-2}$
Grosmont aquifer	$5.9x10^{-4}$	0.20	12.13	$1.6x10^{-2}$	$2.2x10^{-2}$	$4.2x10^{-2}$
Beaverhill Lake -Cooking Lake aquifer	$6.4x10^{-5}$	$9.2x10^{-3}$	1.72	$1.2x10^{-5}$	$7.7x10^{-3}$	0.30
Swan Hills-Slave Point aquifer	$1.1x10^{-5}$	$4.9x10^{-3}$	3.35	$8.4x10^{-6}$	$9.9x10^{-4}$	1.01
Upper Watt Mountain aquitard	$1.0x10^{-5}$	$8.5x10^{-5}$	0.034	$8.2x10^{-5}$	$8.5x10^{-5}$	$3.3x10^{-3}$
Gilwood aquifer	$3.2x10^{-5}$	$7.9x10^{-2}$	1.13	$7.4x10^{-6}$	$1.2x10^{-2}$	0.36
Muskeg aquitard	-	$1.4x10^{-7}$	-	-	$1.1x10^{-7}$	-
Keg River aquifer	$6.1x10^{-4}$	$1.7x10^{-2}$	1.16	$6.8x10^{-5}$	$1.3x10^{-3}$	$5.7x10^{-2}$
Contact Rapids aquifer	$6.4x10^{-5}$	$1.3x10^{-2}$	0.17	$1.2x10^{-5}$	$2.5x10^{-3}$	$8.4x10^{-2}$
Ernestina Lake aquifer	-	$9.0x10^{-3}$	-	-	$2.9x10^{-3}$	-
Granite Wash aquifer	-	0.17	-	-	$4.9x10^{-2}$	-
Lynx aquifer	$2.5x10^{-3}$	$8.4x10^{-3}$	0.011	-	$1.3x10^{-3}$	$2.5x10^{-3}$
Basal Cambrian aquifer	$1.4x10^{-3}$	$2.6x10^{-2}$	0.30	$2.8x10^{-5}$	$3.0x10^{-3}$	$5.8x10^{-2}$

portance is the distribution of aquifers with limited extent, because if they have a high permeability they may act as 'drains' to the flow system. Unconformities are particularly important also, because, in addition to allowing the possibility of juxtaposition of hydrostratigraphic units of contrasting hydraulic properties, they may be associated with regoliths or karst development, both of which may short-circuit flow systems. It is clear from the review of the regional geology that the Swan Hills study area includes some complex geometric relations, three of which are regarded as critical hydrogeological situations.

The first is the relation of hydrostratigraphic units associated with the pre-Devonian unconformity. Figure 16a shows the subcrop distribution of the Lynx, Pika, Eldon and Basal Cambrian aquifers beneath Lower and Middle Devonian strata; the blank regions of the map are the subcrop areas of the intervening aquitards (Sullivan, Upper Eldon, and Stephen-Cathedral-Mount Whyte). Immediately overlying the Cambrian throughout the central part of the study area and oriented in a northwest-southeast direction is a blanket of Granite Wash, ranging up to 70 m thick (figure 5). This unit, shown stippled in figure 16a where it contacts the underlying Cambrian aquifers, is a major short circuit at the base of the Lower and Middle Devonian. The overlapping nature of the Elk Point Group allows the subcropping Cambrian aquifers to be overlain by a succession (from east to west) of an aquiclude (Basal Red Beds-Lotsberg), an aquifer (Ernestina Lake), an aquitard (Cold Lake), an aquifer (Keg River-Contact Rapids), and covering the entire study area, the Muskeg aquitard. Thus, although the Cambrian aquifers within the study area may be short-circuited through the overlying Granite Wash and through both the Ernestina Lake and Keg River-Contact Rapids aquifers, with respect to the Lower and Middle Devonian the entire study area is covered by the Muskeg aquitard which effectively separates the pre-Muskeg hydrostratigraphic units from the overlying regional Beaverhill Lake aquifer system.

The second critical area is that associated with the Grosmont Formation (figure 16b). This unit ranges up to more than 200 m thick, but is overlain by only a thin succession (maximum 20 m) of Upper Ireton Formation shales. By contrast, the Ireton Formation is about 300 m thick over most of the study area. Studies elsewhere in Alberta (Hitchon 1969b, 1984a) have shown that the Grosmont Formation acts as a major drain to the regional flow system and its presence in the eastern third of the study area may result in significant cross-formational flow through the thin, overlying Upper Ireton Formation shales. Of unknown relevance at this stage is the presence of the thin (approximately 10 m) Fort Vermilion aquiclude in the same part of the study area.

The pre-Cretaceous unconformity presents the third potentially critical hydrostratigraphic situation. Along the eastern margin of the study area, Lower Mannville strata lie directly on the carbonates of the Upper Devonian Wabamun Group (figure 16b). Immediately to the west of the Wabamun Group subcrop is a narrow band, about two townships wide, in which the combined Lower Mannville-Upper Banff porous unit is separated from the Wabamun Group carbonates by less than 10 m of Exshaw Formation shale. As a re-

Table 9. Chemical composition (mg/L), physical properties and production data for formation waters from the Basal Cambrian aquifer.

Location	6-36-63-12-W5M	7-6-65-4-W5M	16-12-66-13-W5M	10-5-68-2-W5M	8-11-68-10-W5M
Depth (m)	3235.5–3258.3	2368.3–2411.0	3180.9–3194.6	2048.3–2079.3	2713.3–1725.5
Source	DST 30	DST 3	DST 11	DST 5	DST 17
Recovery	823.0 m sw	1127.8 m sw 91.4 m mud	1207.0 m sw	493.8 m sw	54.9 m sw 54.9 m mud
Na (diff.)	52385	109735	57794	116885	71292
Ca	24120	17217	22496	17061	19739
Mg	2335	2430	4928	3541	2526
Cl	130200	206600	143000	190000	152000
HCO_3	60	92	290	61	340
SO_4	23	135	152	714	23
TDS (110°C)	–	–	308900	326390	274715
TDS (ignition)	208450	320380	221120	295330	244360
TDS (calc.)	209123	336209	228660	311201	245920
pH (laboratory)	6.2	5.5	6.2	5.5	6.2
Density (25°C)	1.146	–	1.155	1.202	1.165
Refractive index (25°C)	–	1.3865	–	–	–
Resistivity (ohm m)	0.05 (22.2°C)	0.048 (20°C)	0.0655 (20°C)	0.047 (20°C)	0.0524 (20°C)

– = not determined, sw = salt water

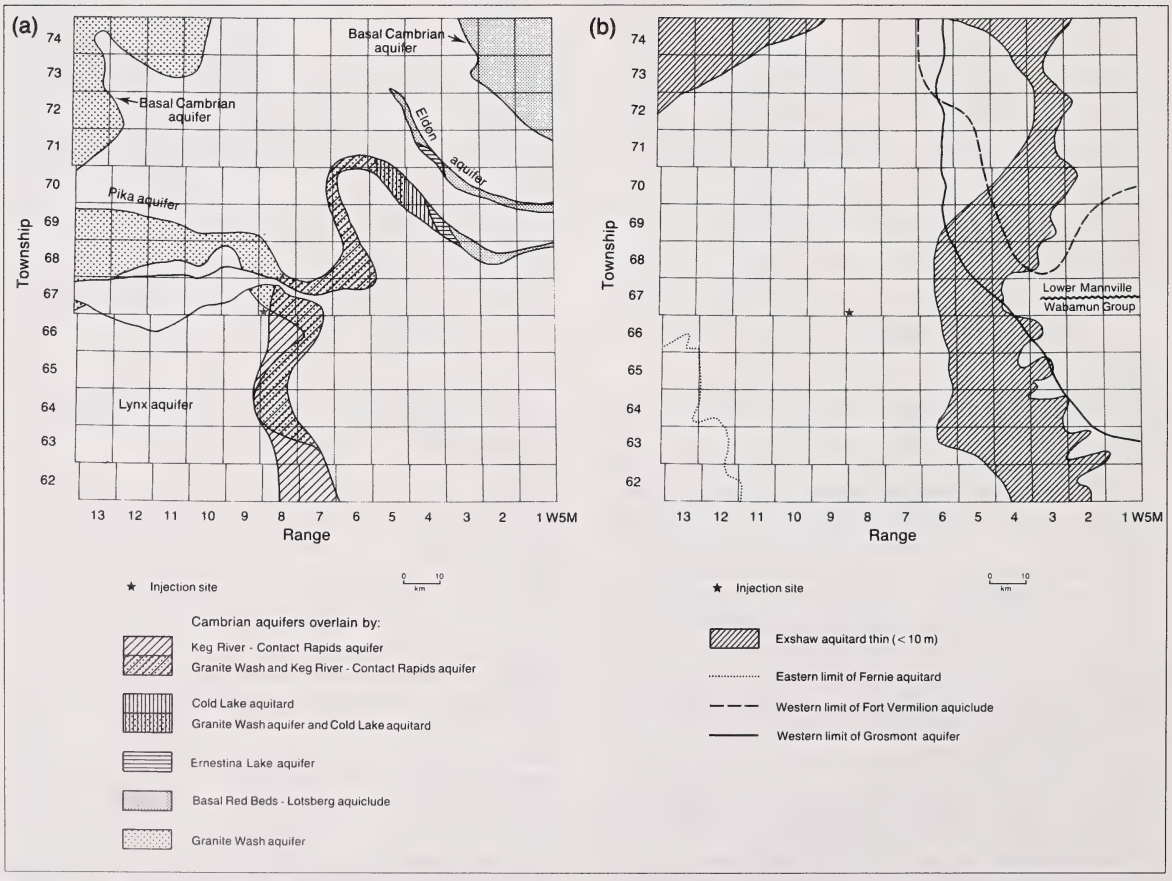

Figure 16. Diagrammatic sketches of critical hydrostratigraphic situations, a) hydrostratigraphic units overlying Cambrian aquifers at the pre-Devonian unconformity, b) hydrostratigraphic units associated with the pre-Cretaceous unconformity.

sult, in the entire eastern third of the study area, there may be hydraulic continuity between the Lower Mannville aquifer system and the underlying carbonates of the Upper Devonian Wabamun and Winterburn Groups. These latter units are then separated from the underlying Grosmont Formation, in the same part of the study area, by only the thin Upper Ireton Formation shales.

The extreme northwest corner of the study area also has but a thin succession of Exshaw Formation shales; however, its position far from the injection site makes its presence less critical. Similarly, the thin (approximately 20 m) Fernie Group shales in the extreme southwest of the study area (figure 16b) are not likely to be critical with respect to the injection site.

Analysis of the natural flow regime

Precambrian aquiclude

For the purpose of this study, and as a general observation, the Precambrian basement is assumed to be an aquiclude, and therefore a zero-flow boundary. Although recent studies (Fritz and Frape 1987) have demonstrated the presence of saline formation waters (some exceeding 250 000 mg/L at depths greater than 1 km in the exposed Canadian Shield), no work has been done in western Canada which would indicate similar saline formation waters, even at shallower depths, in the covered Precambrian.

Basal Cambrian aquifer

The Basal Cambrian sandstone and associated detritus derived from the crystalline basement (Granite Wash) range in thickness from less than 20 to about 55 m in the study area (figure 17a). In the northern half the aquifer is mainly Granite Wash, whereas in the southern half it includes both the Basal Cambrian sandstone and underlying Granite Wash.

Only five reliable analyses of formation waters are available from this aquifer, all of which are from the Basal Cambrian sandstone (table 9). As a broad generalization, salinity increases from a range of 209 000 to 246 000 mg/L in the southwest part of the study area to a maximum of 336 000 mg/L in the southeast corner of the study area (figure 17b). There are corresponding increases in Cl (130 000 to 207 000 mg/L), but Ca and Mg exhibit a fairly narrow concentration range throughout the study area (17 000 to 24 000 mg/L, and 2300 to 4900 mg/L, respectively). Sulfate is generally less than 150 mg/L except for the well at 10-5-68-2-W5M which is within the area overlain by the Lower Devonian Lotsberg Formation.

As illustrated in figure 17d, flow in this aquifer is mainly to the northeast in the Swan Hills study area, a direction which corresponds generally with the basin-wide regional flow and with increasing salinity. The southeastward component in the northwest corner of the study area may be a local feature related to the depositional limit of the Cambrian which runs to the north of Lesser Slave Lake (see Bachu et al. 1986). Figure 17c shows that at about 16 km to the northwest of the injection site, the 50 m of Cambrian (mostly shale) that separate the basal sandstone from the Pika Formation is not a 'strong aquitard' (the slope of the pressure-head versus depth line is close to unity). It is not possible to generalize this observation for the entire Middle Cambrian aquitard system; however, this observation is supported to some extent by examination of formation waters from the Basal Cambrian sandstone (table 9), and the Eldon and Pika Formations (table 10) from the well at 16-12-66-13-W5M. Over a depth range of nearly 190 m, salinity only increases from 202 000 mg/L in the Pika Formation to 229 000 mg/L in the basal sandstone; corresponding changes are 124 000 to 143 000 mg/L for Cl, 15 900 to 22 500 mg/L for Ca, and 1600 to 4900 mg/L for Mg. Sulfate decreases from 320 to 150 mg/L.

As a broad generalization and at any location, salinity and Cl increase with depth in Cambrian aquifers and also increase in the direction of flow and toward the northeast where Cambrian rocks are overlain by Lower Devonian Lower Elk Point Group halite (Lower Devonian aquiclude). There are corresponding inverse changes in SO_4 which tentatively suggest hydraulic connection between Cambrian aquifers and both the overlying Muskeg Formation anhydrites and the various evaporitic phases of the Lower Elk Point Subgroup in the northeastern portion of the study area.

The variable spacing of the hydraulic head contours in the Basal Cambrian aquifer may be a consequence of data distribution and the contouring software utilized for plotting, but it could also be a reflection of permeability contrasts in the aquifer. Unless there is more proof of hydraulic continuity with the overlying Cambrian carbonates, this aquifer should only be considered as a backup position for injection. It is thin (20 m average) and has a relatively low diffusivity (4 m^2/d).

Middle Cambrian aquitard system and Lower Devonian aquiclude

The Basal Cambrian aquifer is overlain by a series of aquitards and aquifers of Middle Cambrian age. In ascending order they comprise the Mount Whyte-Cathedral-Stephen aquitard, the Lower Eldon aquifer, the Upper Eldon aquitard, the Pika aquifer, and the Sullivan aquitard. None are continuous throughout the study area. Overlying the Cambrian in the eastern third of the region is a westwardly-onlapping succession of Lower Devonian rocks of which the four lowermost units comprise the Basal Red Beds-Lotsberg aquiclude, the Ernestina Lake aquifer, and the Cold Lake aquitard, in ascending order (figure 16a). Within these Middle Cambrian and Lower Devonian rocks the aquifers are thin (generally less than 25 m) and the in-

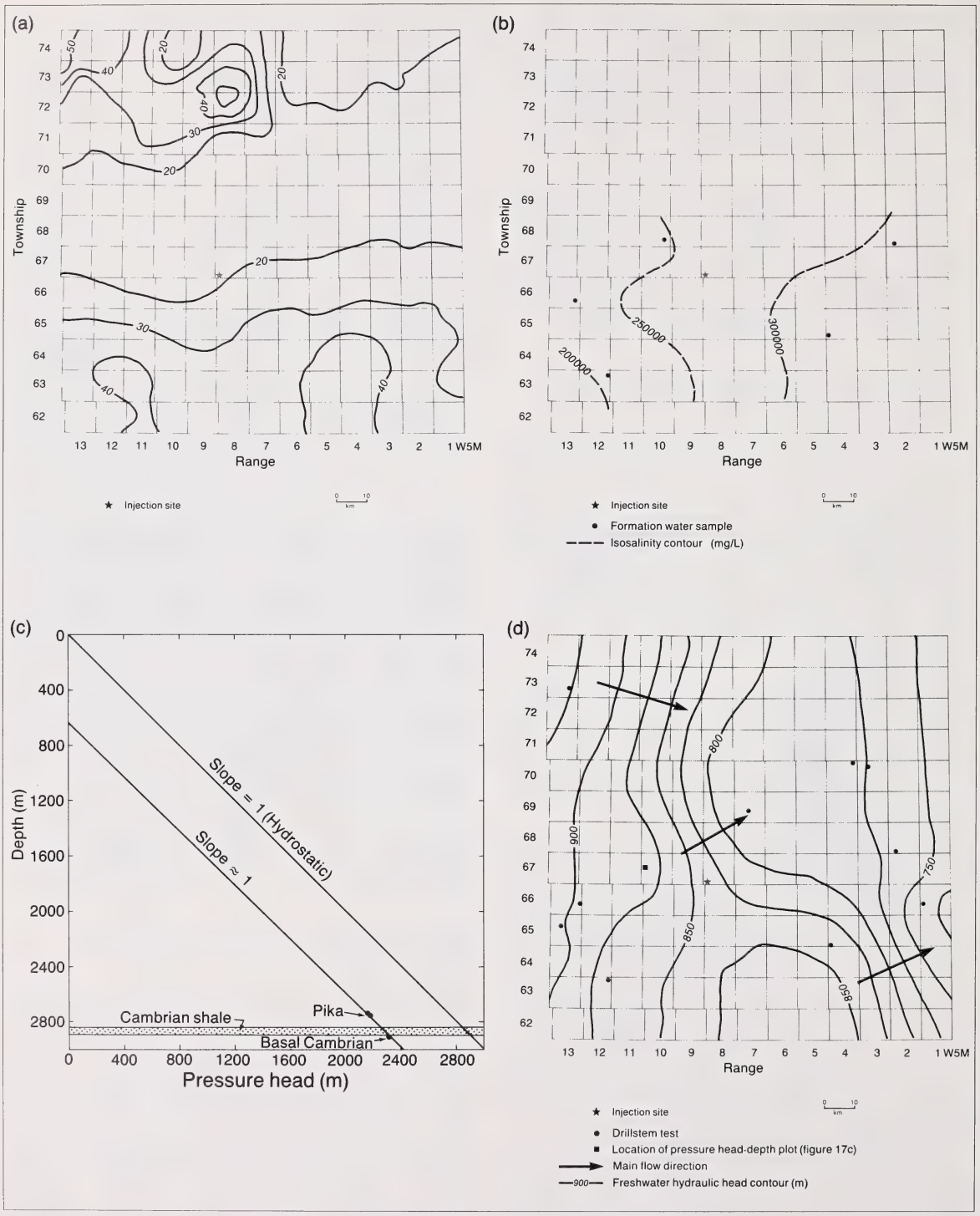

Figure 17. Characteristics of the flow regime in the Basal Cambrian aquifer, a) isopachs (10 m interval), b) salinity distribution, c) pressure head-depth plot at Tp 67 R 10, showing hydraulic continuity of the Basal Cambrian and Pika aquifers, d) potentiometric surface.

Table 10. Chemical composition (mg/L), physical properties and production data for formation waters from the Cambrian Eldon and Pika Formations.

Stratigraphic unit	Eldon Fm.	Eldon Fm.	Pika Fm.	Pika Fm.	Pika Fm.
Location	16-12-66-13-W5M	8-26-71-6-W5M	9-20-65-13-W5M	16-12-66-13-W5M	4-4-67-11-W5M
Depth (m)	3122.7–3134.9	2208.0–2216.8	3024.8–3029.1	3005.3–3020.6	2961.1–2969.4
Source	DST 10	DST 6	DST 18	DST 12	DST 6
Recovery	757.4 m sw	1804.4 m sw	1253.9 m sw	1642.9 m sw	164.6 m mc sw 54.9 m swc mud
Na (diff.)	60787	96114	96914	59488	57109
Ca	21261	25890	17644	15880	12000
Mg	2907	3049	1996	1602	1680
Cl	139500	202500	155000	124000	114000
HCO_3	230	245	195	440	295
SO_4	251	343	202	321	23
TDS (110°C)	272230	371200	265490	226603	228080
TDS (ignition)	211090	308850	230130	200070	175900
TDS (calc.)	224936	328141	254307	201731	185107
pH (laboratory)	6.0	5.75	7.0	6.6	7.5
Density (25°C)	1.150	1.206	1.158	1.137	1.118
Refractive index (25°C)	–	–	–	–	1.3580
Resistivity (ohm m, 20°C)	0.055	0.065	0.049	0.0615	0.065

– = not determined, sw = salt water, mc = mud cut, swc = salt water cut

dividual aquitards and aquicludes range up to more than 100 m in places. This entire succession, which ranges up to 295 m in thickness, has been divided into the Middle Cambrian aquitard system (figure 18a) and the Lower Devonian aquiclude (figure 18b).

There is a paucity of hydraulic data from the intervening aquifers and only five reliable formation water analyses, all from the Eldon and Pika Formations (table 10). As a result, it was not possible to determine the regional flow patterns within the aquifers. Formation waters are generally similar to those in the underlying Basal Cambrian aquifer.

Cambro-Devonian aquifer system

The Middle Cambrian aquitard system and Lower Devonian aquiclude are overlain by four contiguous aquifers of different ages which are almost continuous across the study area (figure 19). In order of decreasing age, these are the Lynx aquifer (Upper Cambrian), the Granite Wash overlying the Cambrian (pre-Lower-

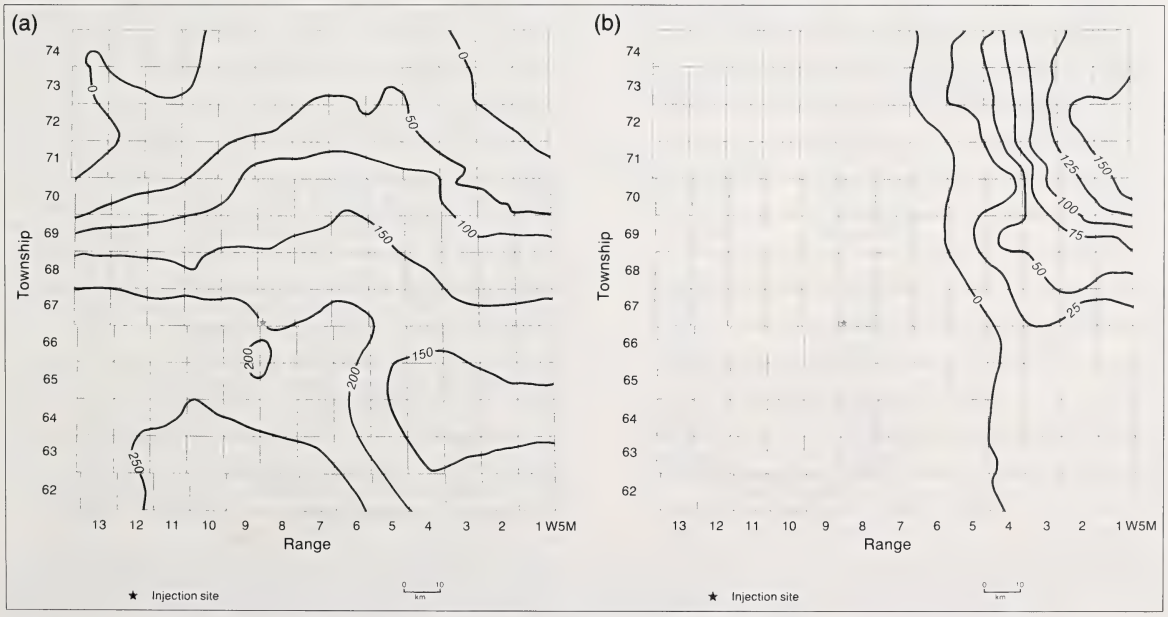

Figure 18. Isopachs, a) of the Middle Cambrian aquitard system (50 m interval), b) Lower Devonian aquiclude (25 m interval).

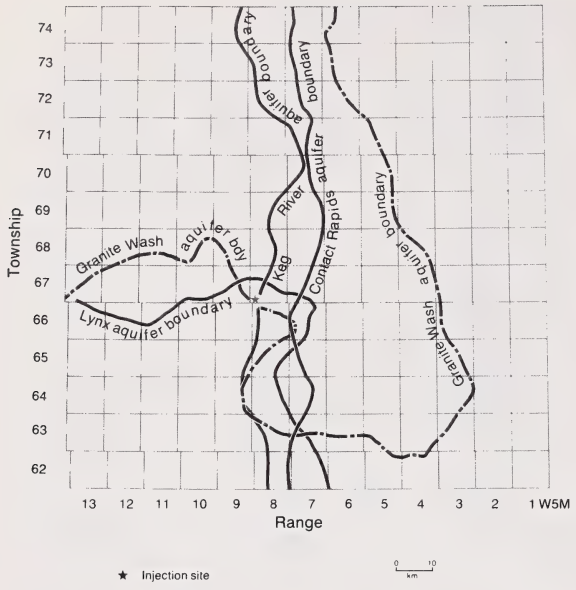

Figure 19. Boundaries of aquifers overlying the Middle Cambrian aquitard system and the Lower Devonian aquiclude.

Middle Devonian) and the Middle Devonian Contact Rapids and Keg River aquifers. These aquifers have been designated the Cambro-Devonian aquifer system, which ranges in thickness from zero up to 140 m (figure 20a).

Formation water analyses are available from the Lynx (table 11), the Granite Wash overlying the Cambrian (table 12), the Middle Devonian Contact Rapids (table 13), and the Keg River (table 14) aquifers. Although this is a very diverse set of samples with respect to age of the aquifers, plotting them as a group reveals some interesting features. The range in salinity is 231 000 to 380 000 mg/L, but all formation waters with salinities greater than 300 000 mg/L occur in the extreme northeast and southeast portions of the study area, with the least saline occurring along the east-central margin of the study area (figure 20b). This pattern broadly coincides with the flow pattern in this aquifer system (figure 20d).

Table 11. Chemical composition (mg/L), physical properties and production data for formation waters from the Cambrian Lynx Formation.

Location	10-20-62-8-W5M	8-11-68-10-W5M
Depth (m)	2450.6–2463.4	2545.7–2558.2
Source	DST 4	DST 15
Recovery	1445.1 m sw	1645.9 m sw
Na (diff.)	60067	80558
Ca	36810	26025
Mg	6448	4805
Cl	176220	184000
HCO_3	75	290
SO_4	372	134
TDS (110°C)	318260	329370
TDS (ignition)	279720	292370
TDS (calc.)	279992	292555
pH (laboratory)	5.2	6.4
Density (25°C)	1.198	1.201
Refractive index (25°C)	–	–
Resistivity (ohm m) (20°C)	0.051	0.0495

– = not determined, sw = salt water

Similar compositional patterns can be demonstrated for Cl (140 000 to 246 000 mg/L), Ca (14 000 to 99 000 mg/L), and Mg (1800 to 11 800 mg/L). With respect to the latter two constituents, it must be noted that formation waters from the Contact Rapids Formation at 10-35-62-2-W5M and 4-16-64-2-W5M, and from the Keg River Formation at 2-28-72-2-W5M and 4-30-73-2-W5M exceed the minimum detailed exploration limit of 60 000 mg/L for Ca, and the formation waters from three of these same wells exceed the minimum detailed exploration limit of 9000 mg/L for Mg (table 1). It is important to ensure that injection of fluids at the Special Waste Injection Site does not contaminate these potential sources of industrial minerals. Although the pattern for SO_4 is not so clear, some of the highest contents (up to 1840 mg/L) occur in the area with the lowest salinity, and contents generally less than 275 mg/L are associated with the most saline formation waters.

The hydraulic continuity between the Contact Rapids aquifer and the Granite Wash aquifer overlying the Cambrian is clear at Tp 71 R 6-7 (figure 20c) where there is also a vertical downward connection from the overlying Gilwood aquifer (slope=0.48) in spite of the intervening thin Muskeg aquitard. Formation waters from the well at 16-12-66-13-W5M show increasing salinity, Cl, Ca and Mg, and decreasing SO_4 with depth in the pre-Lynx Cambrian succession. In contrast, formation waters from the well at 8-11-68-10-W5M to the northeast show the reverse trends between the Lynx aquifer and the Basal Cambrian aquifer with the same order of magnitude difference, but also with decreasing SO_4 content. This suggests that the lower part of the Lynx Formation may well act as an important aquitard in the western part of the study area, but in the northeastern half, where it is absent, there is some hydraulic connection across the Cambrian-Middle Devonian boundary.

In addition to the presence of potentially commercial brines, the Cambro-Devonian aquifer system should not be considered for injection regardless of a relatively high (composite) diffusivity (approximately 160 m^2/d), because of the weakness of the overlying Muskeg aquitard, and therefore a potential for contamination of the Swan Hills oilfield. Also, in the area of the injection site the host zone would have to be the Lynx aquifer, which has a diffusivity 4.5 times lower than the regional value for this aquifer system.

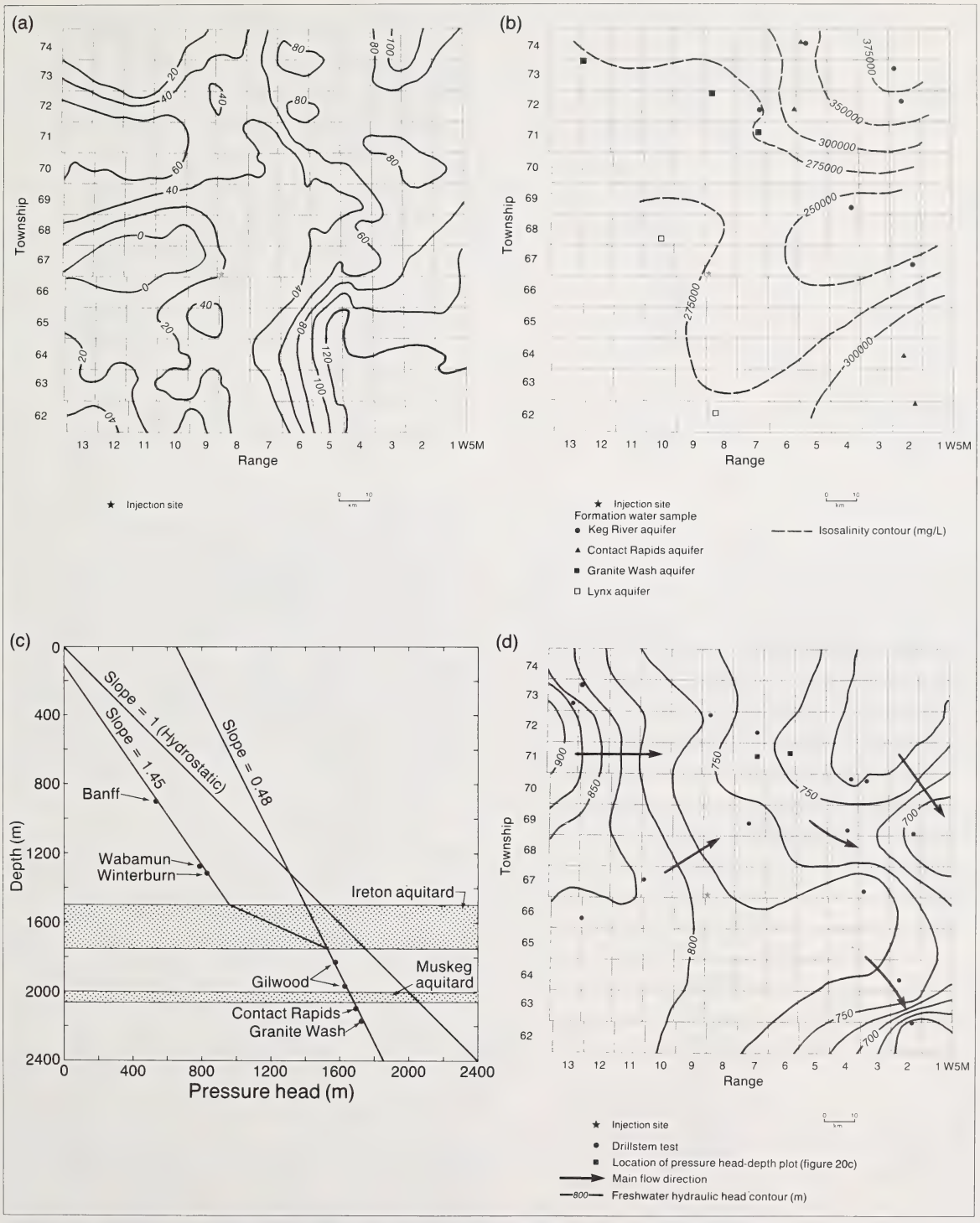

Figure 20. Characteristics of the flow regime in the Cambro-Devonian aquifer system, a) isopachs (20 m interval), b) salinity distribution, c) pressure head-depth plot at Tp 71 R 6-7, showing cross-formational flow and hydraulic continuity, d) potentiometric surface.

Table 12. Chemical composition (mg/L), physical properties and production data for formation waters from the Granite Wash overlying Cambrian.

Location	10-23-71-7-W5M	10-32-72-8-W5M	16-31-73-12-W5M
Depth (m)	2154.9–2167.7	2057.1–2064.7	2048.3–2061.7
Source	DST 3	DST 3	DST 3
Recovery	1280.2 m sw	1676.4 m sw 104.9 m mc sw	1828.8 m sw
Na (diff.)	75963	67085	74182
Ca	25120	26994	26160
Mg	3288	3968	2385
Cl	170800	162514	167409
HCO_3	66	37	64
SO_4	432	311	232
TDS (110°C)	308900	307600	324280
TDS (ignition)	271980	259540	261390
TDS (calc.)	275669	260909	270432
pH (laboratory)	5.7	6.4	6.2
Density (15.56°C)	1.202	1.180	1.181
Refractive index	1.3805 (25°C)	–	–
Resistivity (ohm m)	0.049 (25°C)	0.053 (20°C)	0.052 (20°C)

– = not determined, sw = salt water, mc = mud cut

Muskeg aquitard

In the study area the oldest stratigraphic unit that is continuous across the region and acts as an aquitard is the Muskeg Formation. It ranges in thickness from less than 25 m along the western margin to more than 125 m in the northeast corner as the center of the Elk Point Basin is approached (figure 21). As shown by the pressure-head-depth plot in figure 20c, it is not an efficient aquitard.

Beaverhill Lake aquifer system

The Beaverhill Lake aquifer system lies above the Muskeg aquitard and beneath the Ireton aquitard. The aquifer system comprises, in ascending order, the Watt Mountain aquitard (Middle Devonian) and the Middle/Upper Devonian Beaverhill Lake and Cooking Lake aquifers. The Beaverhill Lake Group contains within it the important reef complexes of the Swan Hills Formation. The Watt Mountain Formation includes the Gilwood aquifer, from which hydrocarbons have been produced at several fields in the study area. Lying within the Beaverhill Lake aquifer in the northeast corner of the study area (figure 16b) is the thin (about 10 m) Fort Vermilion aquiclude. The aquifer system increases gradually in thickness from about 160 m along the western margin of the study area to about 240 m

Table 13. Chemical composition (mg/L), physical properties and production data for formation waters from the Middle Devonian Contact Rapids Formation.

Location	10-35-62-2-W5M	4-16-64-2-W5M	16-13-72-6-W5M	12-19-74-5-W5M
Depth (m)	1955.6–1972.1	1915.7–1978.2	1879.1–1905.0	1825.0–1857.0
Source	DST 2	DST 2	DST 1	DST 1
Recovery	530.0 m sw 60.0 m mud	815.3 m sw 137.2 m mc sw	1411.2 m sw 168.0 m wc mud	1412.0 m sw
Na	40462 (diff.)	45957 (diff.)	73359 (diff.)	83050
K	–	–	–	1550
Ca	65906	68083	41046	39020
Mg	9428	6584	3979	3509
Cl	206200	210238	197238	208518
HCO_3	130	91	63	56
SO_4	255	276	73	195
TDS (110RC)	397640	–	–	–
TDS (ignition)	321680	–	–	–
TDS (calc.)	322381	331229	315758	335241
pH (laboratory)	5.3	5.58	5.6	5.6
Density	1.217 (15.56°C)	1.2433 (15.56°C)	1.2208 (15.56°C)	1.2245 (15.4°C)
Refractive index	1.3985 (25°C)	–	1.3919 (22.2°C)	1.3885 (24°C)
Resistivity (ohm m)	0.061 (20°C)	0.048 (25°C)	0.046 (21.1°C)	0.035 (25°C)

– = not determined, sw = salt water, mc = mud cut, wc = water cut

Table 14. Chemical composition (mg/L), physical properties and production data for formation waters from the Middle Devonian Keg River Formation.

Location	12-14-67-2-W5M	6-11-69-4-W5M	2-28-72-2-W5M	7-14-72-7-W5M	4-30-73-2-W5M	12-19-74-5-W5M
Depth (m)	1780.0–1800.8	1938.0–1953.0	1652.0–1676.4	2052.0–2063.0	1734.0–2750.0	1825.0–1833.0
Source	DST 3	DST 2	DST 1	DST 1	DST 1	DST 2
Recovery	182.9 m mc sw	1694.0 m mc sw 164.6 m swc mud	364.2 m sw	530.0 m sw 60.0 m mud	230.4 m sw 18.3 m wc mud	1000.0 m sw 50.0 m wc mud
Na	54998 (diff.)	71705	26025 (diff.)	62842	23128 (diff.)	81494
K	–	1620	–	1440	–	1043
Ca	35284	13810	95200	24500	99324	41432
Mg	5214	1786	10449	5127	11865	4958
Cl	161600	140300	238915	156000	245740	214252
HCO_3	240	110	100	69	165	34
SO_4	927	1841	85	681	159	72
TDS (110°C)	279980	248000	–	293900	–	–
TDS (ignition)	243830	221200	–	241900	–	–
TDS (calc.)	258263	230536	370799	250659	380381	342835
pH (laboratory)	7.4	6.7	5.2	6.2	5.5	5.4
Density (25°C)	1.171 (23.3°C)	1.156	1.2898 (15.56°C)	1.166	1.281 (15.56°C)	1.2285 (15.4°C)
Refractive index (25°C)	–	1.3724	–	1.3750	–	1.3895
Resistivity (ohm m, 25°C)	0.051 (20°C)	0.056	0.048 (23.9°C)	0.053	0.063 (15.56°C)	0.035

– = not determined, sw = salt water, mc = mud cut, swc = salt water cut, wc = water cut

on the eastern boundary (figure 22a). Major crude oil reserves are found in two stratigraphic units (Gilwood sandstone and Swan Hills Formation) and injection of liquid waste into this aquifer system is not recommended.

Formation waters in the Gilwood aquifer of the Watt Mountain Formation show salinities increasing in a broad band across the study area from about 220 000 mg/L on the west side to more than 300 000 mg/L along the eastern boundary (figure 22b). There are similar trends for Cl (140 000 to 180 000 mg/L) and density, but the distribution pattern for Ca, Mg and SO_4 is irregular and without obvious explanation.

Analyses of formation waters from the Beaverhill Lake Group are limited mainly to the region of producing oilfields. Salinities are of the order of 50 000 mg/L lower than those in the underlying Gilwood aquifer, with commensurately lower contents of other components. Six detailed analyses of formation waters from the Beaverhill Lake aquifer are given in table B1 (appendix B). Adjusted pH values are 0.3 to 0.75 pH units lower than the value determined in the laboratory; for reservoir temperatures ranging from 79.5° to 96°C the adjusted pH values are in the range 5.91 to 6.77. Formation waters are generally saturated with respect to calcite and dolomite, as expected; they are undersaturated with respect to halite, and close to saturation (slightly oversaturated or slightly undersaturated) for anhydrite. The sample (D-41) for which silica was preserved in the field is saturated with respect to quartz (SI=0.18); the other samples show slight undersaturation, almost certainly because of loss of silica during transport of the sample to the laboratory. For most samples, barite and fluorite are close to saturation. The quartz geothermometer temperature (84.8°C) shows excellent correlation with reservoir temperature (87.8°C) for sample D-41, for which silica was properly preserved in the field. Contents of Pb and Zn range up to 63 mg/L and 3.5 mg/L, respectively, with Pb>Zn; amounts of Fe and Mn are very variable; Cu ranges up to 0.6 mg/L.

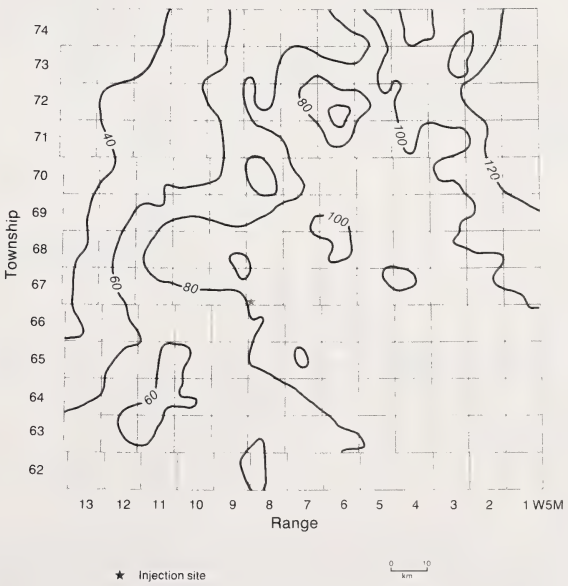

Figure 21. Isopachs (20 m interval) of the Muskeg aquitard.

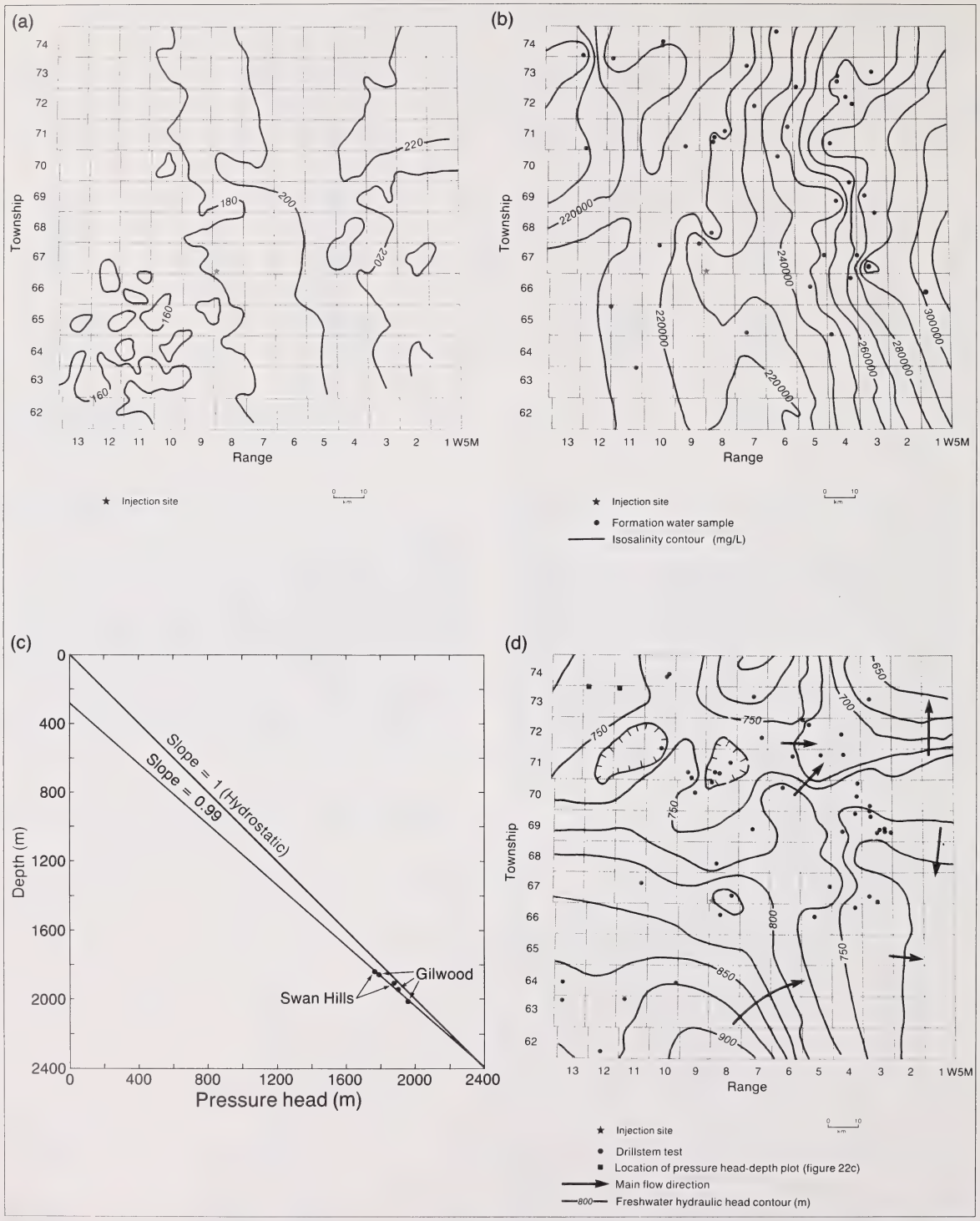

Figure 22. Characteristics of the flow regime in the Beaverhill Lake aquifer system, a) isopachs (50 m interval), b) salinity distribution in the Gillwood aquifer of the Watt Mountain aquitard, c) pressure head-depth plot at Tp 73-74 R 11-12, showing hydraulic continuity, d) potentiometric surface.

The potentiometric surface (figure 22d) shows general regional flow to the northeast, with northern and eastern flow components in the eastern margin of the study area. There are few similarities in the trends and pattern between the salinity distribution in the Gilwood aquifer (figure 22b) and the potentiometric surface for the entire Beaverhill Lake aquifer system (figure 22d). In part, this may be due to inclusion of some data from wells subject to water flooding. Only sorting of the drillstem test information into preinjection and postinjection groups will resolve this matter, which was a task beyond the scope of the present study.

Hydraulic continuity within this aquifer system is demonstrated by the pressure-head-depth plot in figure 22c. The major characteristic of the flow in the Beaverhill Lake aquifer system is the hydraulic-head high in the southwestern quarter of the study area (figure 22d). One can consider as a possible cause for this hydraulic head high, relict higher pressures in the reef complex of the Swan Hills Formation that have survived through geological time without becoming adjusted to the present hydrogeological environment. This would imply that the Swan Hills aquifer is well sealed laterally by a strong contrast of hydraulic diffusivity (three to four orders of magnitude higher in the reef aquifer than around it).

Beyond the hydraulic-head high, flow in the Beaverhill Lake aquifer system shows some general similarities to flow in the Cambro-Devonian aquifer system. The range of freshwater hydraulic-head values is similar to the range in the Cambro-Devonian aquifer system. However, the hydraulic head cross sections in figure 23, which are constructed on the basis of formation water densities, show that flow is generally potentially downward from the Beaverhill Lake aquifer system into the Cambro-Devonian aquifer system. The Beaverhill Lake aquifer system has one of the highest regional diffusivities in the Swan Hills area and could be considered as a potential injection aquifer except that it contains important hydrocarbon deposits.

Ireton aquitard and Grosmont aquifer

Probably the most important aquitard in the regional flow regime of the Swan Hills study area is that formed by the shales of the Ireton Formation. As will be shown later in the section on numerical simulation, they effectively isolate the hydrogeological environment of the major hydrocarbon reserves in the Beaverhill Lake aquifer system from overlying aquifer systems. Over much of the region the Ireton aquitard is about 300 m thick (figure 24a). Where the Grosmont Formation carbonates occur, in the northeast part of the region, about 150 m of Ireton shale are overlain by 200 m of Grosmont Formation carbonates (figure 24b), which in turn are covered by a thin veneer (10 to 20 m) of Upper Ireton Formation shales (figure 24c). This latter sequence of shales represents one of the critical hydrogeological boundaries cited in the previous section of this bulletin.

Wabamun-Winterburn aquifer system

The carbonates of the Winterburn and Wabamun Groups average about 375 m thick over most of the study area, but thin to less than 250 m along the eastern boundary where the Wabamun Group subcrops beneath the Lower Cretaceous (figure 25a).

Formation waters from the Winterburn aquifer range in salinity from about 200 000 mg/L in the southwest

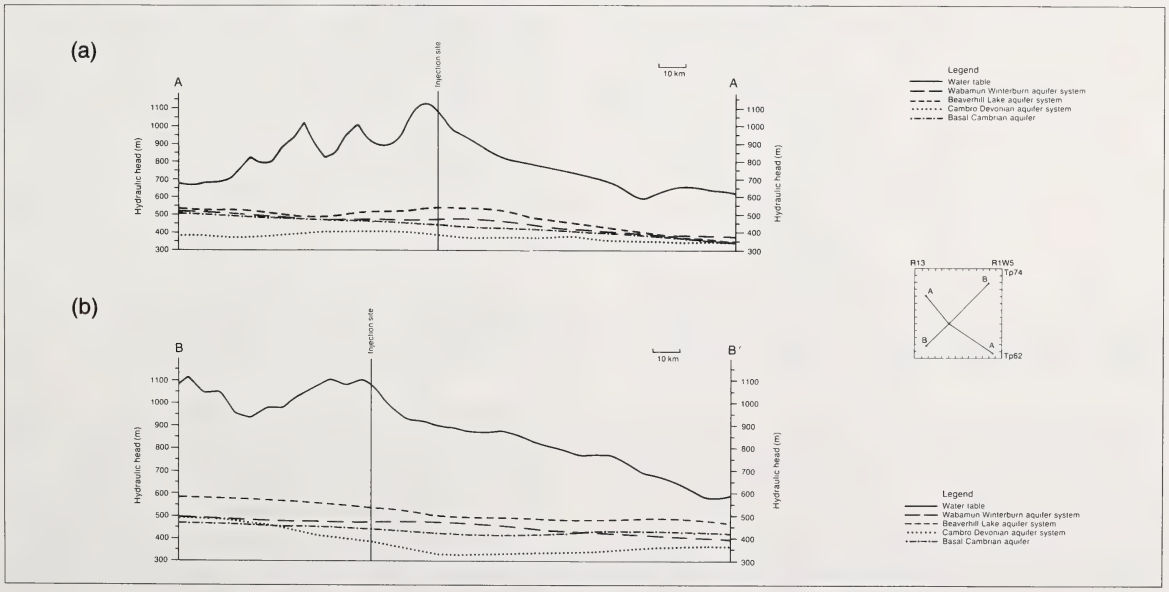

Figure 23. Hydraulic-head profiles for the pre-Ireton aquifers, a) strike cross section, b) dip cross section.

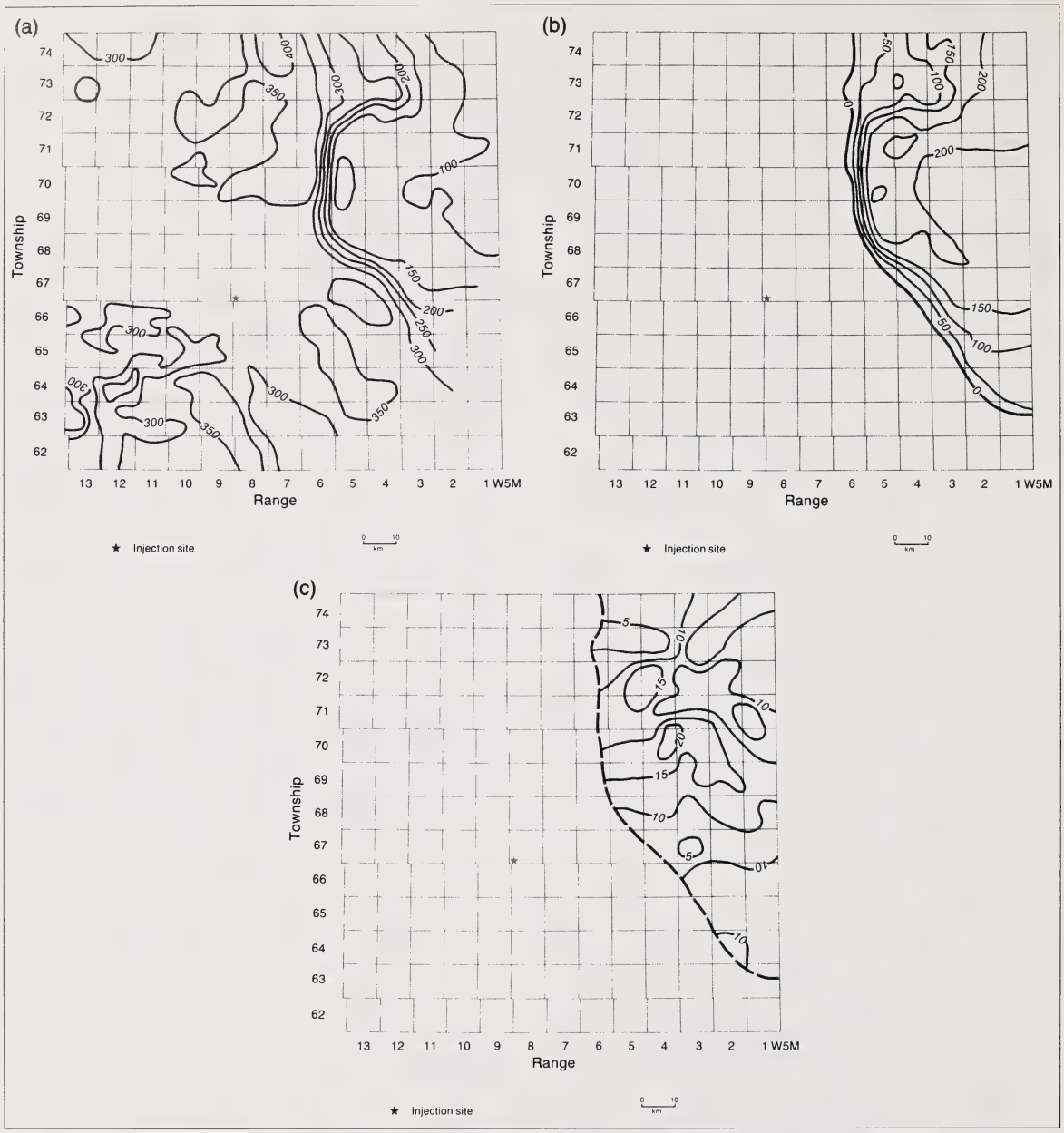

Figure 24. Isopachs of formations in the Woodbend Group, a) Ireton Formation (50 m interval), b) Grosmont Formation (50 m interval), c) Upper Ireton Formation shales (5 m interval).

corner of the study area to less than 50 000 mg/L along the northeast boundary and in the region underlain by the Grosmont Formation (figure 25b); the pattern generally resembles that of the potentiometric surface (figure 25d). Analyses of formation waters from the Wabamun aquifer are available only for the southeast half of the study area and have compositional trends also generally similar to that of the potentiometric surface with salinities ranging from about 140 000 mg/L in the southwest to less than 30 000 mg/L in the subcrop region beneath the Lower Cretaceous Mannville Group (figure 25c). The effect of the drain resulting from the presence of the underlying Grosmont aquifer is best confirmed by maps of HCO_3 distribution: in the Winterburn aquifer HCO_3 contents greater than 500 mg/L and in the Wabamun aquifer

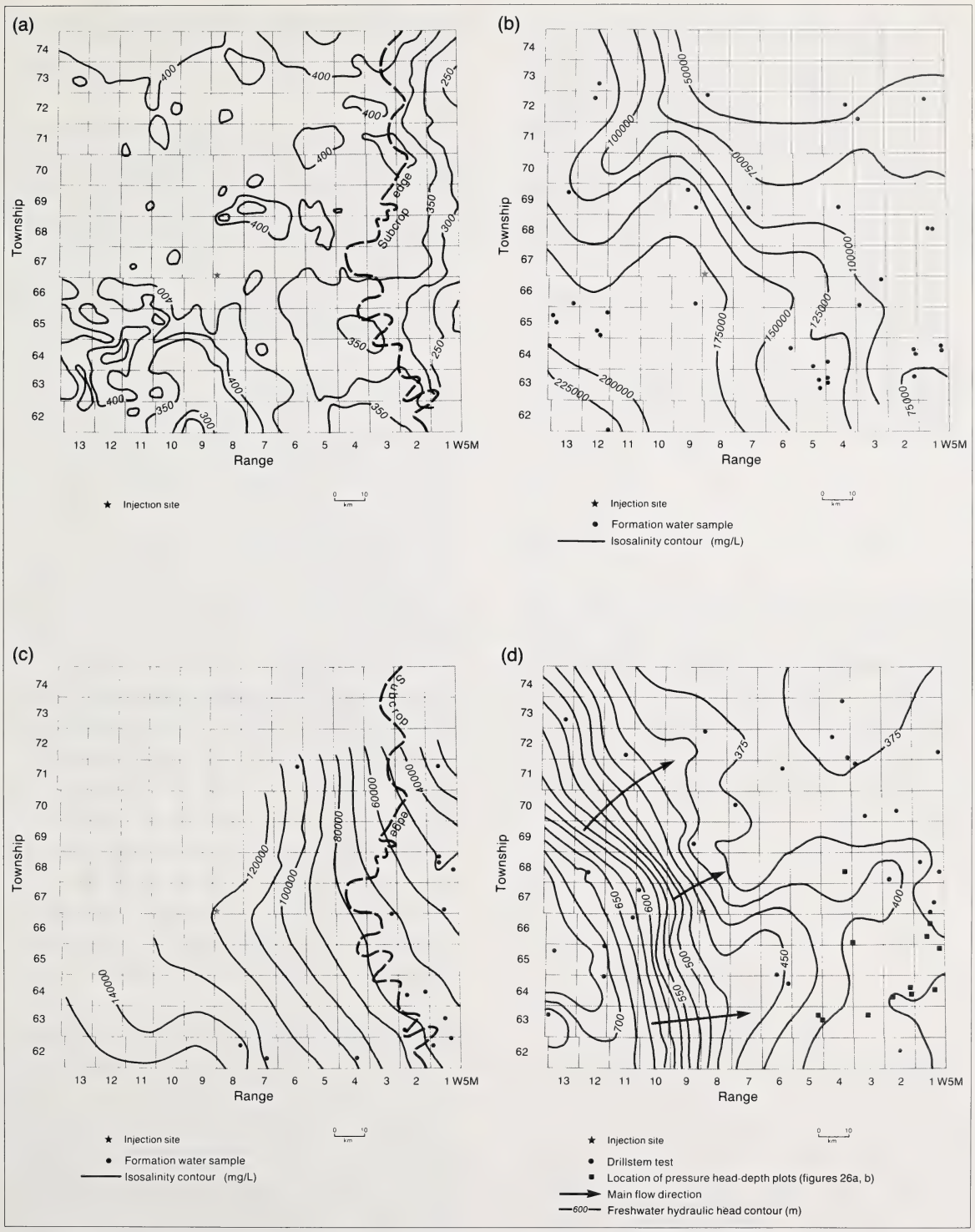

Figure 25. Characteristics of the flow regime in the Wabamun-Winterburn aquifer system, a) isopachs (50 m interval), b) salinity distribution in the Winterburn aquifer, c) salinity distribution in the Wabamun aquifer, d) potentiometric surface.

HCO_3 contents greater than 800 mg/L effectively outline the position of the Grosmont aquifer. Detailed analyses are available for two formation waters from the Wabamun-Winterburn aquifer system (appendix B, table B2). Adjusted pH values are lower by about 0.1 to 0.2 pH units. Both formation waters are saturated with respect to calcite, dolomite and quartz, but undersaturated with respect to halite and anhydrite. Bearing in mind the difficulty of obtaining a reliable determination for Al, the sample from the Wabamun aquifer is undersaturated with respect to feldspars (albite, anorthite, microcline) and clay minerals (illite, kaolinite, montmorillonite).

The flow in this aquifer system is generally eastward in the western half of the study area with steep hydraulic gradients, but in the east the potentiometric surface tends to be rather flat (figure 25d). The general flatness may be related to the drain effect induced by the Grosmont aquifer, which has a very high diffusivity (table 7). In the area around Tp 64-66 R 1-2, the hydraulic continuity between the Wabamun-Winterburn aquifer system and the Grosmont aquifer is well evidenced by the pressure-head depth plot in figure 26a. The downward flow component that results from the Grosmont drain is confirmed by a slope of 0.88 of the regression line. It follows, then, that the thin Upper Ireton aquitard that separates the Winterburn aquifer from the Grosmont aquifer is not an efficient hydraulic barrier. The scatter of the control points around the regression line in figure 26a can be explained by the diversity of the geographic locations of the points.

Immediately west of the area illustrated by the data in figure 26a the flow conditions are hydrostatic, as shown by the pressure-head-depth plot in figure 26b. Cross-formational flow, although theoretically upward from the Beaverhill Lake aquifer system to the Wabamun-Winterburn aquifer system (figure 23), is probably minimal.

Only some zones of the Wabamun-Winterburn aquifer system have good diffusivities (lower part of the Wabamun aquifer and probably lower Nisku aquifer) and the range of regional diffusivity is low (11 and 28 m^2/d for the Nisku aquifer and the Wabamun aquifer, respectively). Injection into this aquifer system is recommended if such high diffusivity zones can be found at the injection site and if the lower half of the aquifer system is considered. Its significant thickness (380 m at the injection site) essentially explains why it should be considered first.

Exshaw-Lower Banff aquitard

With the exception of the two easternmost townships of the study area, the Wabamun-Winterburn aquifer system is overlain by an aquitard comprising the Exshaw Formation and shaley lower portion of the overlying Banff Formation, both of Mississippian age. The combined thickness ranges up to about 40 m, but averages about 15 m (figure 27).

Hydraulic continuity between the Wabamun-Winterburn aquifer system and the overlying Lower Mannville-Rundle aquifer system is clear in the southeast quarter of the study area (figure 28a); in the northeast quarter of the study area, the continuity is present only in the first four ranges (figures 28b). The potential for downward cross-formational flow from the overlying Lower Mannville and Rundle aquifers through the Exshaw-Lower Banff aquitard to the Wabamun-Winter-

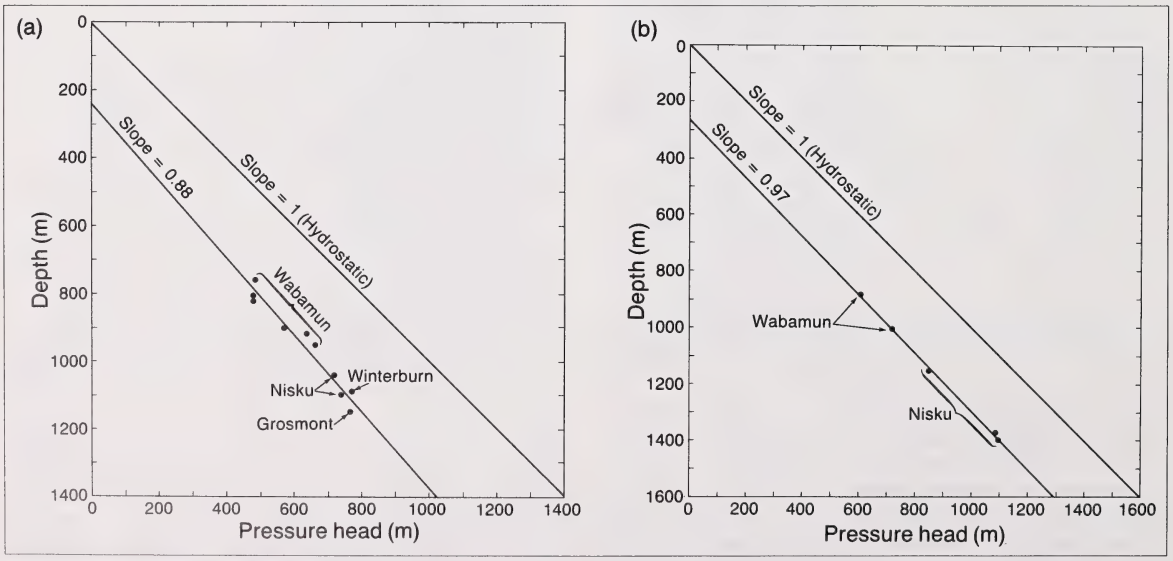

Figure 26. Hydraulic continuity, a) between the Wabamun-Winterburn aquifer system and the Grosmont aquifer (Tp 64-66 R 1-2), b) within the Wabamun-Winterburn aquifer system (Tp 63-68 R 3-5).

burn aquifer system is much more pronounced in the western part of the study area (figure 28c). Thus, the Exshaw-Banff aquitard has very weak sealing properties.

Lower Mannville-Rundle aquifer system

A continuous succession of eroded Mississippian carbonates (in ascending order: Upper Banff, Pekisko, Shunda and Debolt aquifers) are in direct contact with the lower part of the Lower Cretaceous Mannville Group throughout the study area except where the Jurassic Fernie Group is present in the extreme southwest corner (figures 12 and 13), where the Permian Belloy Formation has been preserved from erosion, and along the two easternmost townships where Mississippian rocks are absent and the Mannville Group rests directly on the Wabamun Group. Figure 29 includes a diagrammatic dip cross section (figure 29a) and subcrop boundary map (figure 29b) to illustrate the relations of these aquifers and aquitards, as well as isopachs of the Upper Banff-Rundle (figure 29c) and Lower Mannville (figure 29d) aquifers. Because the Jurassic hydrostratigraphic units are thin (figure 12) and the Belloy aquifer is of negligible areal extent and thickness (see figure 29b), the Lower Mannville, Rundle and Upper Banff strata have been grouped together as the Lower Mannville-Rundle aquifer system. This aquifer system ranges in thickness from less than 50 m to more than 400 m, with an average thickness of 220 m (figure 30a).

The grouping of the Lower Mannville with the Rundle and the Upper Banff carbonate aquifers is justified by the pressure-head-depth profiles in figure 31. In figure 31b, the strong downward flow already noted in figure 28c is confirmed. The two plots (figure 31) are for areas located about 36 km apart. The potentiometric surface of the Lower Mannville-Rundle aquifer system in the southwestern part of the study area (figure 30d) is almost identical to the potentiometric surface of the Wabamun-Winterburn aquifer system (figure 25d). This can also be verified on the hydraulic-head cross sections in figures 28a,b. In the eastern part of the study area a similar situation as for the Wabamun-Winterburn aquifer system prevails (figure 30d). The regional diffusivity is less than 50 m^2/d.

Formation water composition in the Upper Banff aquifer generally reflects the potentiometric surface pattern (figure 30b). The comparison is less clear for formation waters in the Lower Mannville aquifer (figure 30c). In the southwestern part of the study area, where freshwater hydraulic heads are greater than 550 m, formation waters in the Lower Mannville aquifer have salinities around 50 000 mg/L (figure 30c), with those in the underlying Rundle aquifer being about 60 000 mg/L, and in the Upper Banff aquifer about 100 000 mg/L (figure 30b). The steep southeast-northwest trending hydraulic gradient in the

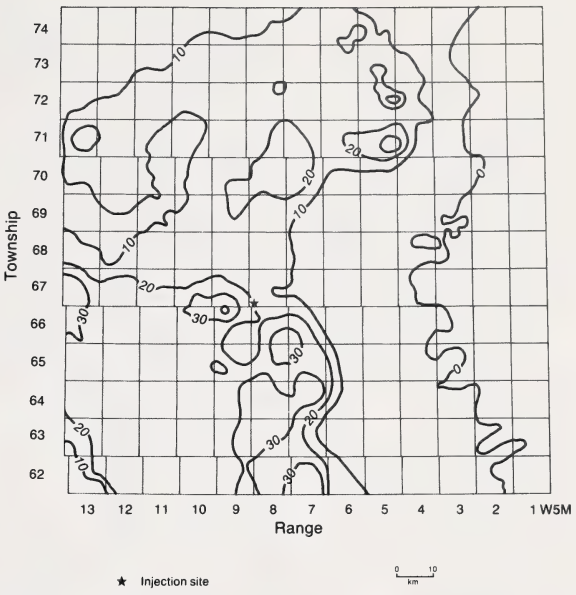

Figure 27. Isopachs (10 m interval) of the Exshaw-Lower Banff aquitard.

vicinity of the injection site does not show up in the salinity patterns. In the northwest part of the study area, the region with freshwater hydraulic heads greater than 500 m coincides with salinities generally about 40 000 mg/L in the Lower Mannville, Rundle and Banff aquifers. The eastern half of the study area, where the Wabamun Group carbonates and Exshaw-Lower Banff aquitard subcrop against the overlying Lower Cretaceous, shows a more complex pattern on the potentiometric surface which is reflected in a similar complex salinity pattern of formation waters from the Lower Mannville aquifer, although individual 'high' salinity (greater than 60 000 mg/L) and 'low' salinity (less than 30 000 mg/L) areas cannot be matched directly with the hydraulic-head pattern. In part, this reflects the early statement of Hitchon (1963, p. 63) that "there is free fluid connection across the unconformity and that formation-fluid movement in proximity to the unconformity is...in whichever set of strata offers the least resistance to movement, i.e. those having the highest permeability."

Detailed analyses of formation waters are available from the Upper Banff and Pekisko aquifers (appendix B, table B3) and the Lower Mannville aquifer (appendix B, table B4). For the two samples from carbonate reservoirs (table B3), adjusted pH values are about 0.3 pH units lower than laboratory-determined values. Trace metals are generally less than 1 mg/L. Both waters are saturated with respect to calcite, dolomite and barite, and undersaturated with respect to halite, anhydrite and fluorite; both are effectively saturated with respect to quartz. Eleven detailed analyses from

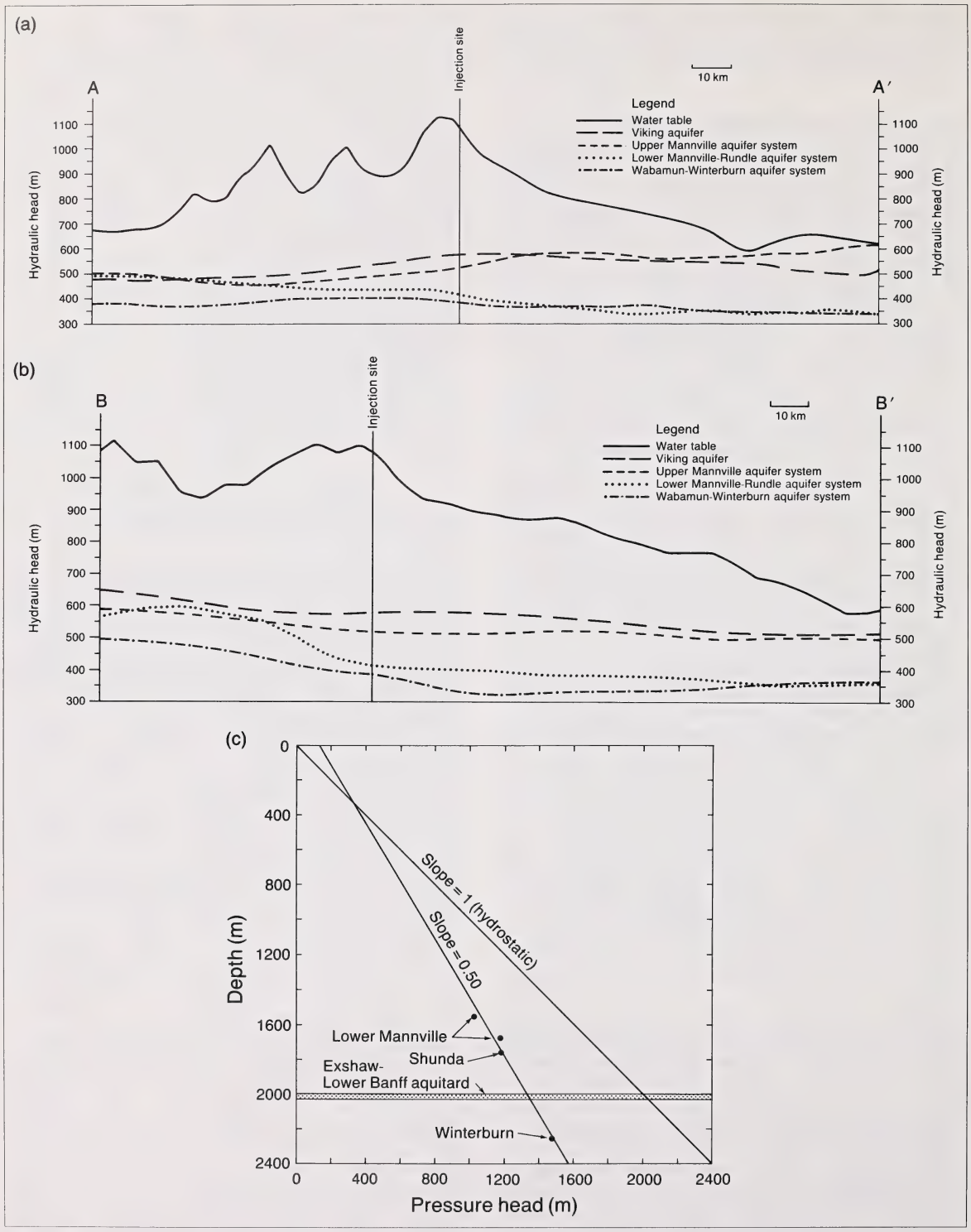

Figure 28. Hydraulic-head profiles for the post-Ireton aquifers, a) strike cross section, b) dip cross section, c) pressure head-depth plot showing hydraulic continuity across the Exshaw-Lower Banff aquitard (Tp 66 R11-13).

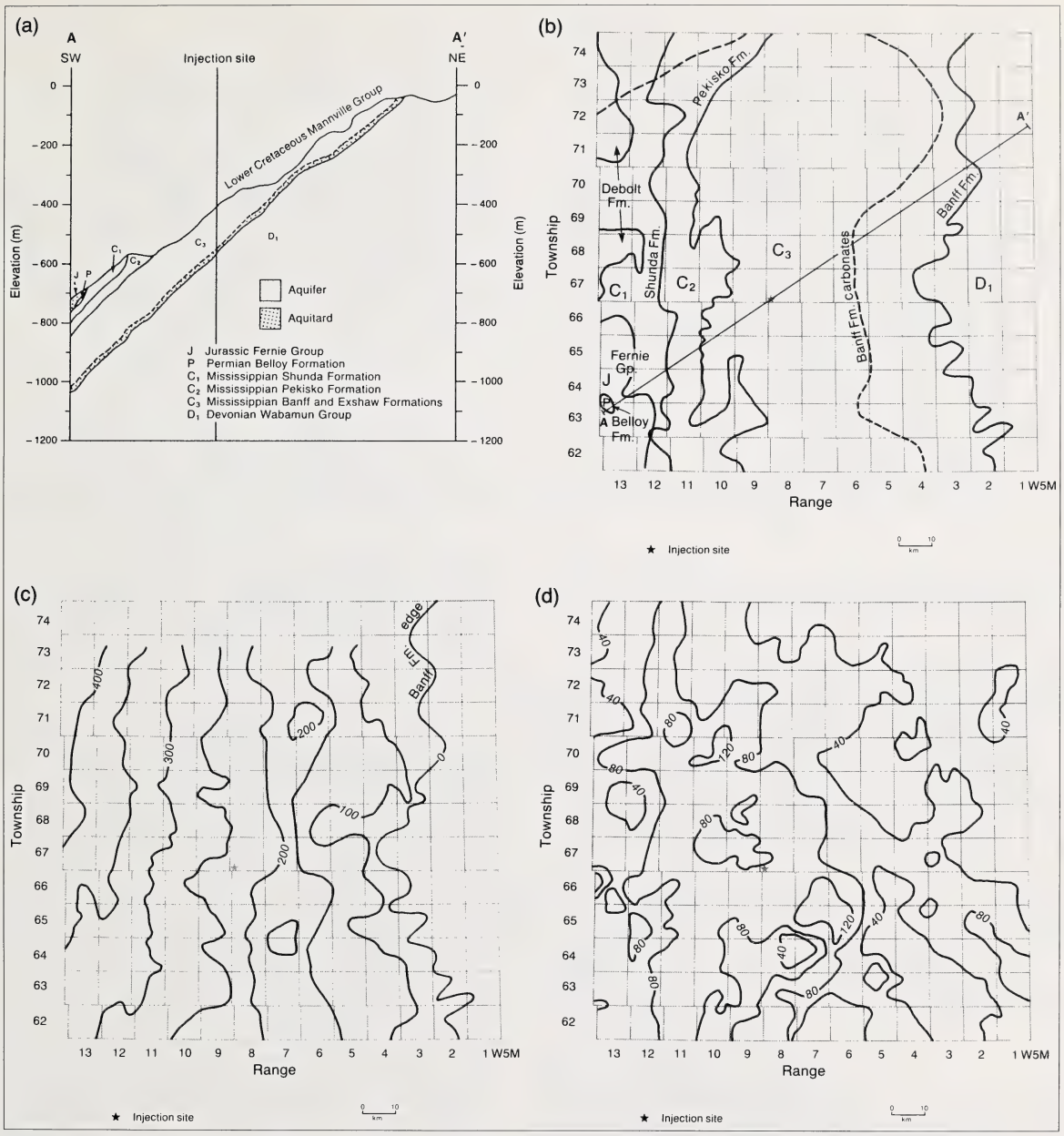

Figure 29. Lower Mannville-Rundle aquifer system, a) diagrammatic cross section showing aquifer and aquitard relations, b) subcrop boundary map, c) isopachs (50 m interval) Upper Banff-Rundle aquifer, d) isopachs (40 m interval) Lower Mannville aquifer.

the clastic Lower Mannville aquifer (table B4) are saturated with respect to calcite, dolomite, quartz, feldspars (albite, anorthite, microcline), clay minerals (montmorillonite, illite, kaolinite) and a variety of accessory minerals commonly found in these rocks. They are undersaturated with respect to halite, anhydrite and fluorite. Barite may be either undersaturated or oversaturated; the content of Ba is generally less than 10 mg/L, but two samples showing considerable oversaturation with respect to barite have 78 and 169 mg/L Ba reported. Although the trace metals Cu, Zn, Pb, Fe and Mn generally occur at levels less than 1 mg/L, up to 4.7 mg/L Zn, 1.8 mg/L Pb and 3.2 mg/L Mn have been reported. The quartz geothermometer

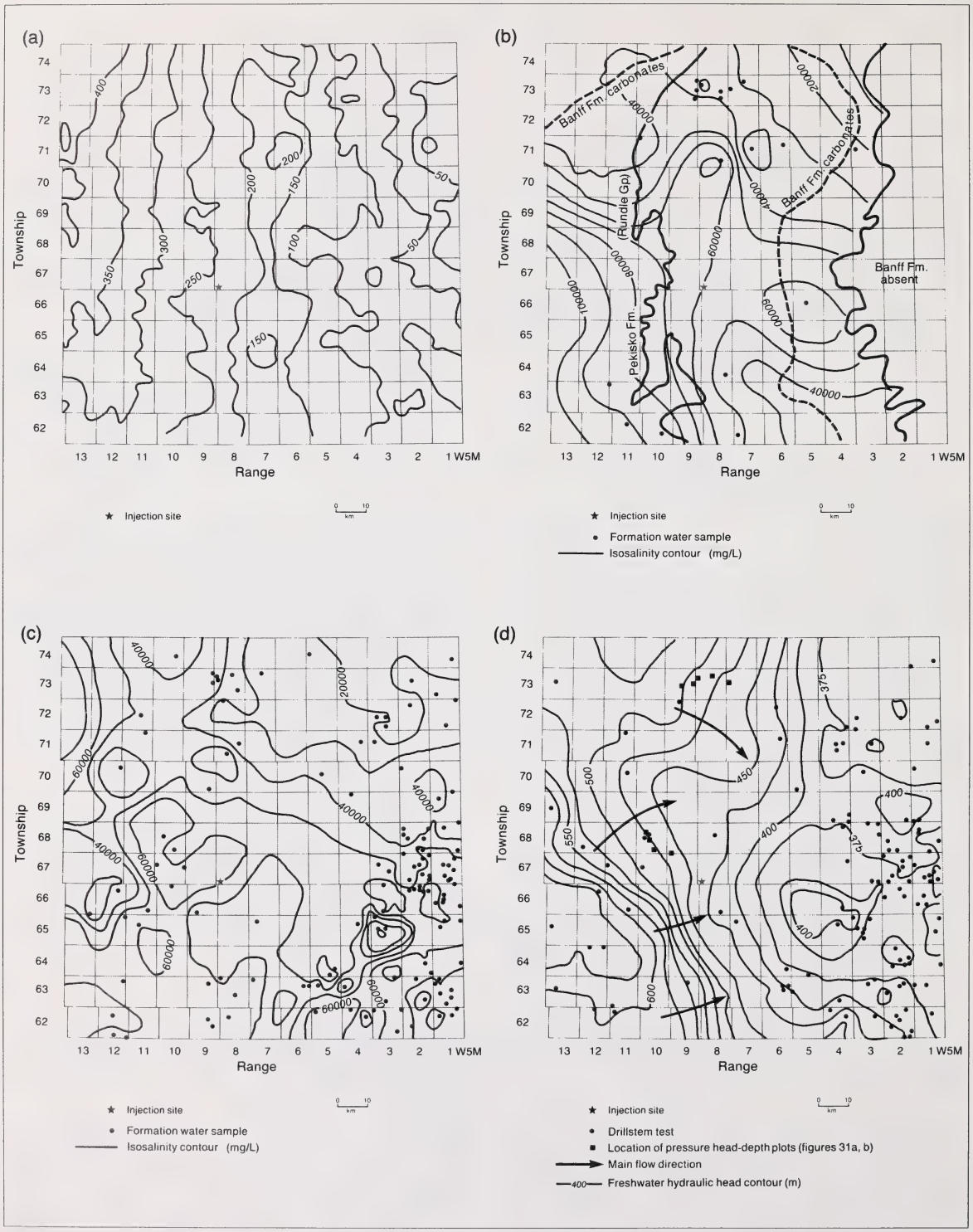

Figure 30. Characteristics of the flow regime in the Lower Mannville-Rundle aquifer system, a) isopachs (50 m interval), b) salinity distribution in the Upper Banff aquifer, c) salinity distribution in the Lower Mannville aquifer, d) potentiometric surface.

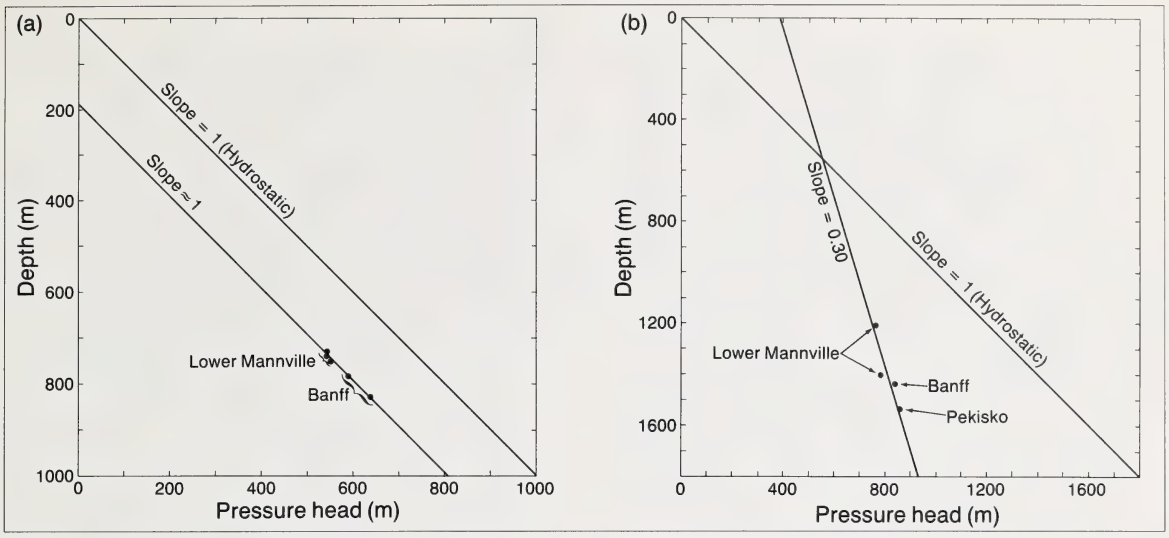

Figure 31. Pressure head-depth plots showing hydraulic continuity of the Lower Mannville, Rundle and Upper Banff aquifers, a) Tp 73 R 8-9, b) Tp 68 R 9-10.

temperature and reservoir temperature are generally in good agreement, except for those samples showing undersaturation with respect to quartz; as noted previously, this reflects the lack of preservation of silica in the field during sampling and not of actual quartz undersaturation.

Clearwater-Wilrich aquitard

The Lower Cretaceous Mannville Group comprises three hydrostratigraphic units. The Lower Mannville aquifer is part of the Lower Mannville-Rundle aquifer system. Above this aquifer system, and extending across the entire study area, is the thin (12 to 61 m, average 35 m) Clearwater-Wilrich aquitard (figure 32a). The remainder of the Mannville Group above this aquitard comprises the Upper Mannville aquifer system. The pressure-head-depth plots in figure 32b, c, d clearly demonstrate that, despite being relatively thin, the Clearwater-Wilrich aquitard is an important hydraulic barrier. Further, the potentiometric surface maps for the aquifers above (Upper Mannville aquifer system, figure 33c) and below (Lower Mannville-Rundle aquifer system, figure 30d) have distinctly different flow patterns, confirming its efficiency as an aquitard.

Upper Mannville aquifer system

This aquifer system lies between the Clearwater-Wilrich and Joli Fou aquitards, and varies in thickness from about 80 to 240 m (figure 33a). The potentiometric surface map (figure 33c) shows dominantly northward flow, a direction unlike that in any of the deeper aquifers, and still not demonstrating a clear reflection of the effect of recharge at the Swan Hills. The pattern of formation water salinity is similar to that of the potentiometric surface, with values greater than 60 000 mg/L in the south and decreasing to less than 20 000 mg/L along the northern boundary of the study area (figure 33b).

Four detailed analyses of formation waters are available from the Upper Mannville aquifer system (appendix B, table B5), all from the extreme northeast corner of the study area. The waters have salinities in the range 20 000 to 27 000 mg/L, very low trace metals, are close to saturation with respect to calcite, dolomite, quartz and barite, and are undersaturated with respect to halite and anhydrite.

Joli Fou aquitard

The shales of the Lower Cretaceous Joli Fou Formation are thin (average 10 m, figure 34) and act as a rather ineffective aquitard between the Upper Mannville aquifer system and the Viking aquifer (figures 32b, c and compare the potentiometric surface maps in figures 33c and 35c).

Viking aquifer

The Viking sandstone varies from 2.5 m to just over 65 m in the study area (figure 35a) with no clearly discernible trends. Like the Upper Mannville aquifer system, flow is dominantly northward (figure 35c), although there is a southeastward component in the southeast corner of the study area which is probably a reflection of the very northern part of the closed potentiometric surface low shown by Hitchon (1969b, figure 4). Again, there is no clear reflection of the effect of recharge at the Swan Hills.

The region with freshwater hydraulic heads greater than 600 m has formation waters with salinities generally less than 20 000 mg/L (figure 35b). The

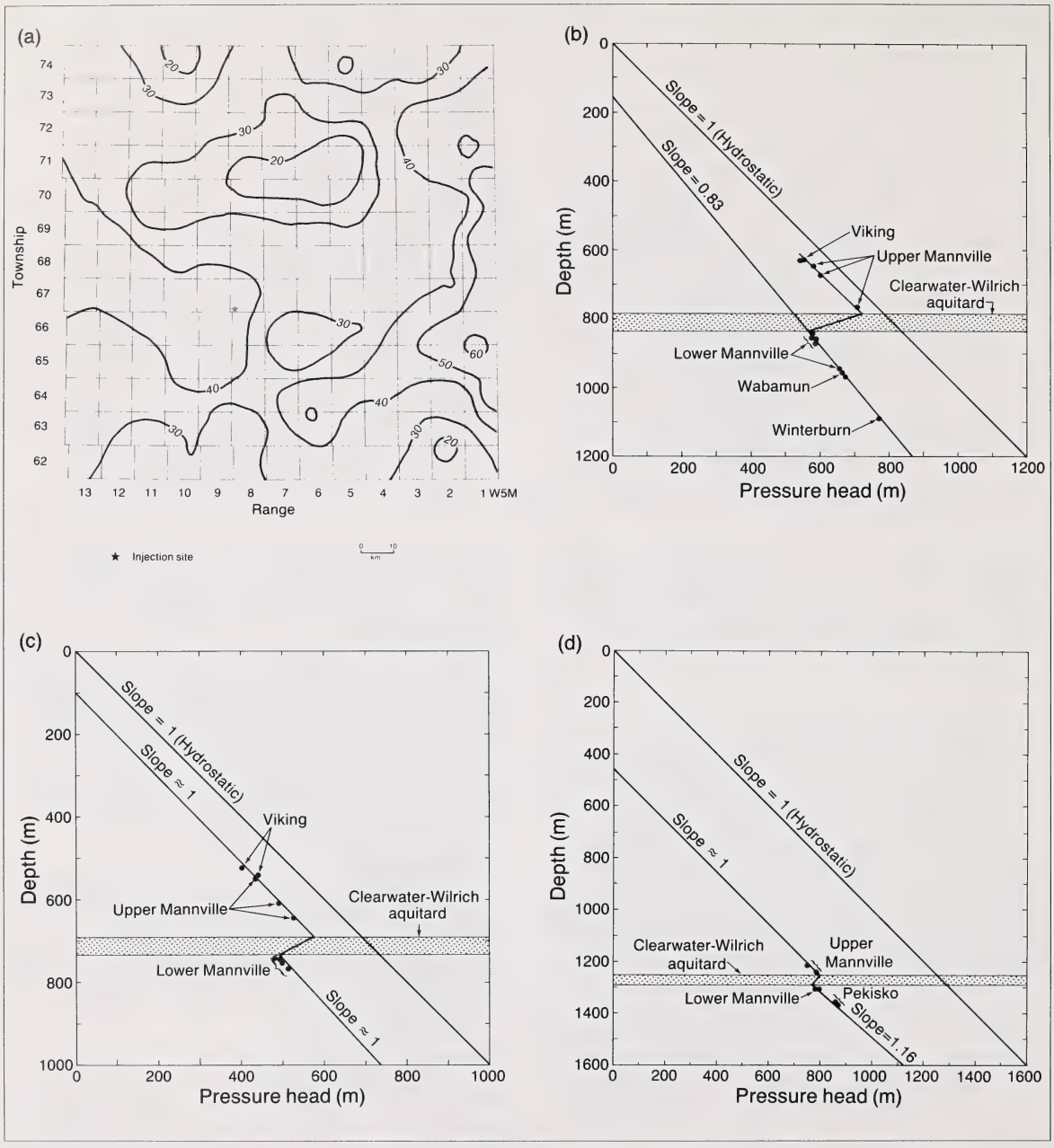

Figure 32. Characteristics of the Clearwater-Wilrich aquitard, a) isopachs (10 m interval), b) pressure head-depth plot (Tp 64 R 1-2), c) pressure head-depth plot (Tp 67 R 2), d) pressure head-depth plot (Tp 68 R 10).

broad central region with freshwater hydraulic heads about 550 m corresponds to a region with salinities in the range 30 000 to 40 000 mg/L; salinities decrease to less than 10 000 mg/L to the north. The southeasterly flow component, however, coincides generally with increasing salinities, some of which exceed 50 000 mg/L. Eight detailed analyses of formation waters from the Viking aquifer are given in appendix B (table B6). Adjusted pH values are generally less than 0.2 pH units below the laboratory determined value. All are saturated with respect to calcite, dolomite, quartz, barite and fluorapatite, and the one sample reporting Al is saturated with respect to feldspars (albite, anorthite, microcline) and clay minerals (illite,

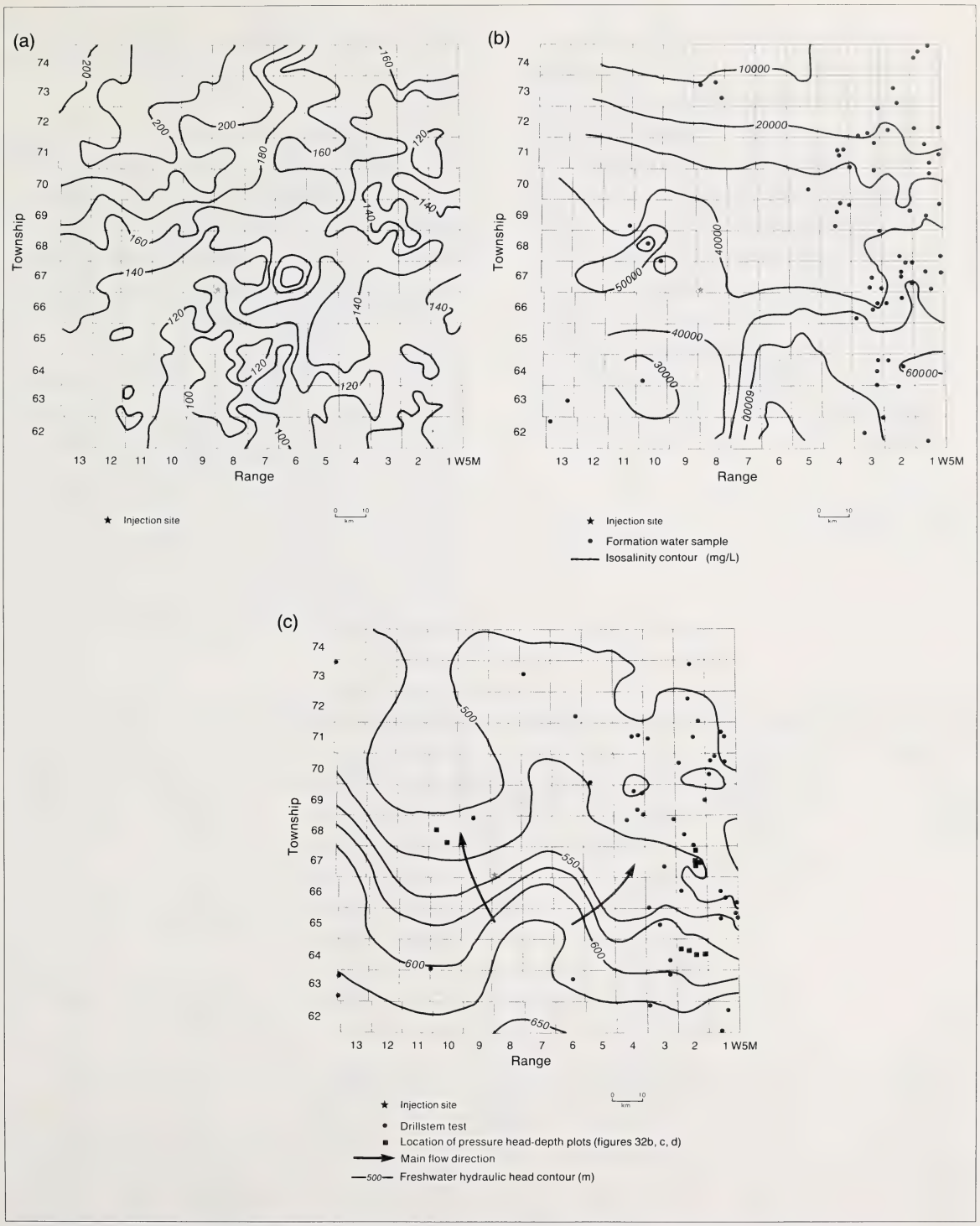

Figure 33. Characteristics of the flow regime in the Upper Mannville aquifer system, a) isopachs (20 m interval), b) salinity distribution, c) potentiometric surface.

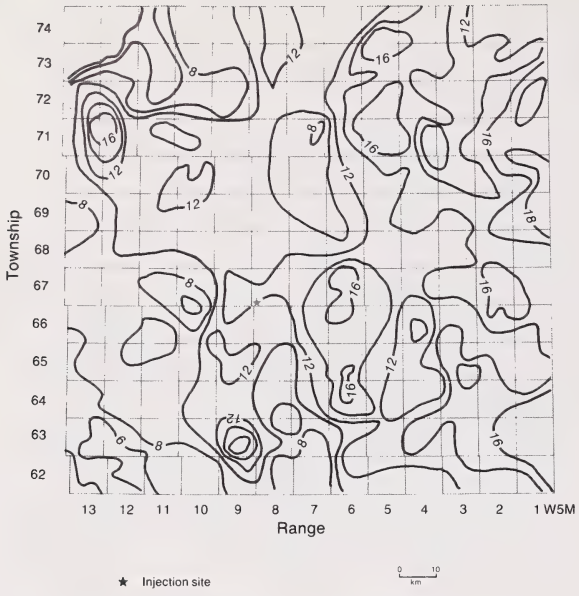

Figure 34. Isopachs (2 m interval) of the Joli Fou aquitard.

kaolinite, montmorillonite). All are undersaturated with respect to halite, anhydrite and fluorite. The trace metals Cu, Zn, Pb, Mn and Fe are generally less than 1 mg/L; up to 135 mg/L Ba is reported.

Post-Viking aquifers and aquitards

The entire post-Viking succession has been termed the Post-Viking aquitard system, and although it is dominantly shale there are several discontinuous aquifers. Thickness of this succession ranges from 300 to 1615 m (figure 36). Paucity of interpretable drillstem tests precludes analysis of post-Viking aquifers; table 15 shows the composition of formation waters recovered from the Second White Speckled Shale, Belly River Group and Edmonton Group.

Quaternary hydrostratigraphic units

Work carried out in the Cold Lake area of Alberta (Basin Analysis Group 1985) has demonstrated that where Quaternary hydrostratigraphic units are underlain by a thick aquitard, the Phanerozoic and Quaternary flow regimes may be decoupled. Accordingly, the Quaternary hydrostratigraphy was not investigated and, for the record, we report here two near-surface groundwater investigations which cover the Swan Hills study area (Tokarsky 1977; Vogwill 1978) and the summary of Hackbarth (1985) on the groundwater and surface water monitoring program at the Alberta Special Waste Management Corporation site.

Table 15. Chemical composition (mg/L), physical properties and production data for formation waters from the Upper Cretaceous.

Stratigraphic unit	Second White Speckled Shale	Belly River Gp.	Belly River Gp.	Belly River Gp.	Belly River Gp.	Edmonton Gp.
Location	6-2-70-9-W5M	10-3-62-6-W5M	11-5-62-7-W5M	11-10-62-10-W5M	6-27-63-8-W5M	12-6-65-10-W5M
Depth(m)	599.0–605.0	290.8–303.0	3388.0–396.0	694.6–734.3	441.4–467.0	152.4–224.0
Source	DST 6	DST 1	DST 6	DST 1	DST 3	Swabbing
Recovery	198.0 m sl. muddy water	44.2 m fw	312.0 m fw	531.9 m fw 27.4 m mud	61.0 m mc fw 221.0 m fw	–
Na	5456	1469 (diff.)	614	2221 (diff.)	600 (diff.)	235 (diff.)
K	26	–	10	–	–	–
Ca	178	25	24	47	7	15
Mg	74	11	5	9	2	4
Cl	8690	2136	809	3120	378	14
HCO_3	417	347	323	585	522	555
CO_3	*	*	2	59	39	*
SO_4	51	8	19	16	290	87
TDS (110°C)	15270	–	1880	–	–	630
TDS (ignition)	14290	–	1345	5500	–	334
TDS (calc.)	14892	3997	1806	6057	1839	910
pH (laboratory)	7.5 (20°C)	8.4	8.6 (20°C)	9.0	8.4	7.7
Density (25°C)	1.010	1.0038 (15.6°C)	1.002	1.007	1.0016	1.002
Refractive index (25°C)	1.3360	1.3330 (23°C)	1.3333	–	1.3322 (22°C)	–
Resistivity (ohm m, 25°C)	0.384	1.30	3.7	–	3.80	12.35 (20°C)

– = not determined, * = below detection, fw = fresh water, mc = mud cut

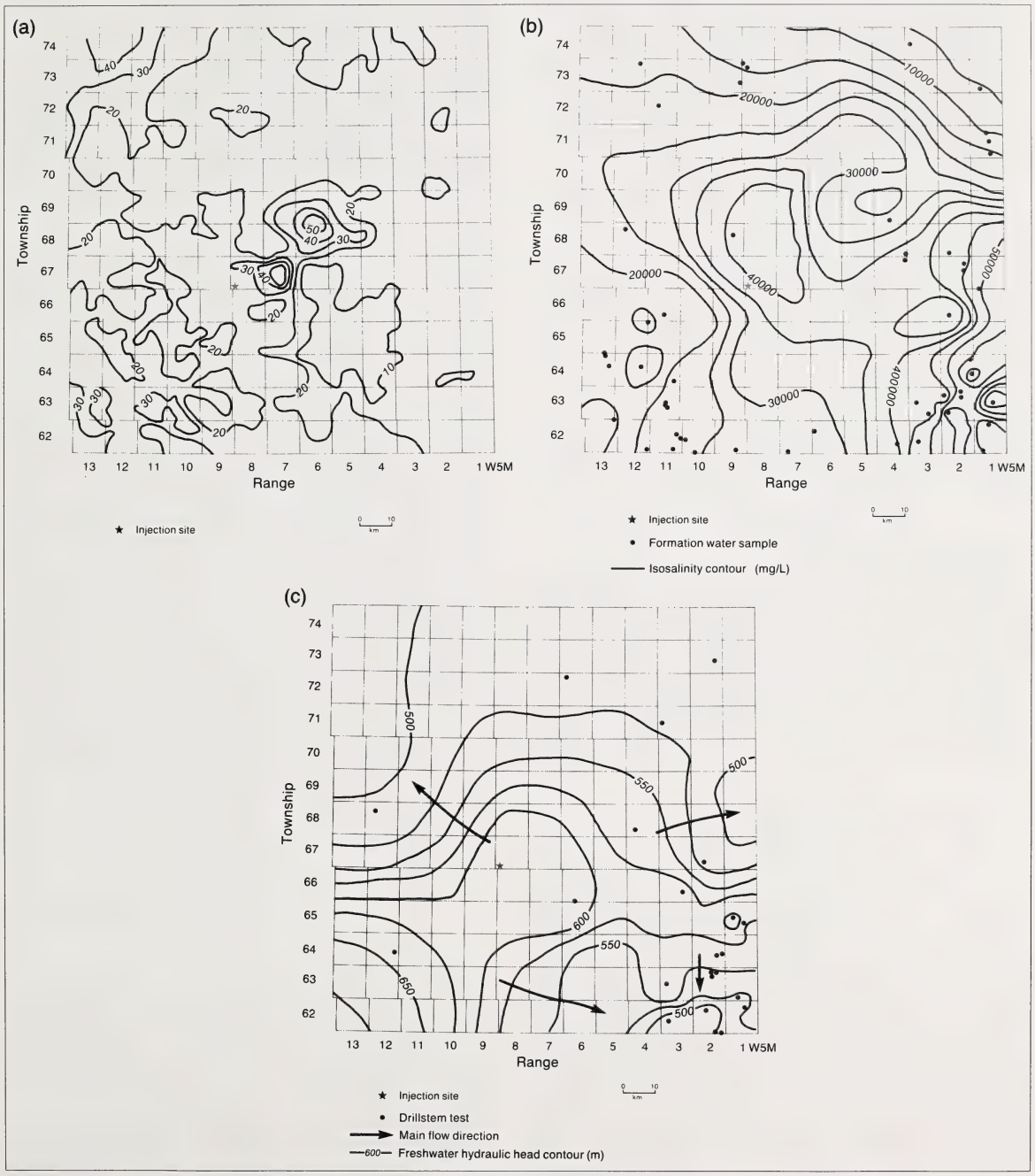

Figure 35. Characteristics of the flow regime in the Viking aquifer, a) isopachs (10 m interval), b) salinity distribution, c) potentiometric surface.

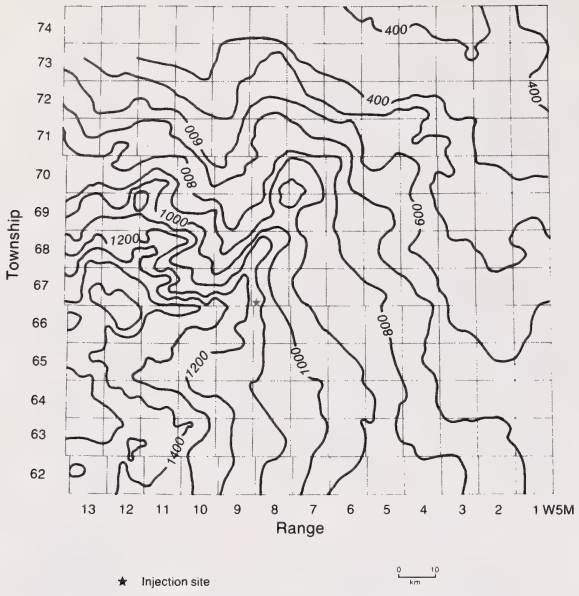

Figure 36. Isopachs (100 m interval) of the Colorado aquitard system.

Numerical simulation

Mathematical and numerical models

The use of aquifers is increasing, both as a source of water and as media for storing various aqueous wastes. Due to the complexity of stratigraphic geometry and the variability of properties of the fluids and solid matrix in the subsurface environment, there are few analytical solutions to problems of flow in porous media. Numerical modelling of fluid flow in aquifers is a tool that can aid in studying and understanding subsurface flow systems.

The objective of mathematical modelling and numerical simulation of formation water flow and fluid injection in the Swan Hills study area was to provide a predictive tool for determining the effects, in terms of hydraulic head buildup, of deep waste injection on the natural hydrogeological regime in the region. The modelling process was carried out in two stages. The first stage was to model the natural conditions that exist prior to any injection. The second stage was to examine how the hydrogeological system would react to, and be modified by, the waste injection processes. Therefore, the first step of the present investigation was to calibrate a numerical model for simulation of steady-state natural flow of formation waters within the complex hydrogeological system in the Swan Hills study area. Following model calibration, the system was perturbed by simulating the injection of the fluids at specified rates. For a given hydrostratigraphic configuration, the sensitivity analysis of the system response for different values of hydraulic properties indicated the effects of injection in the various aquifers in the stratigraphic succession.

The mathematical model for flow in porous media consists of a partial differential equation together with appropriate boundary and initial conditions that express conservation of mass and that describe the variation of hydraulic heads over the region of interest. The unsteady saturated flow in nonhomogeneous porous media of a slightly compressible and homogeneous fluid is described by the following partial differential equation (Bear 1972):

$$\nabla.(\bar{\bar{K}}\nabla H) - Q = S_s \partial H/\partial t \qquad (6)$$

where $\bar{\bar{K}}$ is the hydraulic conductivity tensor, S_s is the specific storage, Q is the strength of the sources and sinks, and t is time. Equation (6) represents the most general case of flow in nonhomogeneous and anisotropic porous media. It is a diffusion-type equation and is derived by combining the fluid state, mass conservation (mass balance) and momentum conservation (Darcy's law) equations.

In order to obtain a solution to equation (6), additional information about the boundary and initial conditions is required. Mathematically, the boundary conditions include the geometry of the boundary and values of prescribed heads and prescribed fluxes. In the case of steady-state natural flow, there are no flow sources or sinks in the model area, and equation (6) becomes an elliptic partial differential equation:

$$\nabla.(\bar{\bar{K}}\nabla H) = 0 \qquad (7)$$

whose solution requires definition of the lateral boundary conditions. The hydraulic heads were imposed along the lateral boundary of the model area for each aquifer in the hydrostratigraphic succession.

The initial conditions are simply the values of the dependent variable (heads) specified everywhere inside the boundary at the time when the processes start.

In the case of the Swan Hills study area it is not possible to obtain an analytical solution due to the complexity of the three-dimensional hydrostratigraphic structure, and to the variability of hydraulic parameters between various hydrostratigraphic units. In order to solve equation (7), it is necessary to obtain a numerical solution, provided by a numerical model.

For the purpose of this study, the model FE3DGW (Finite Element 3-Dimensional GroundWater) was selected for the numerical simulation of the flow. This model was developed by Pacific Northwest Laboratory (U.S.A.), and the complete description of the numerical formulation and of the pertinent software is given in Gupta et al. (1979, 1984). This software package was received by the Basin Analysis Group, from Battelle Memorial Institute, Ohio, and was implemented on the Research Council's computer system (VAX/VMS).

In order to apply the numerical model FE3DGW to this study, it was necessary to prepare the input data as required by the model. At the same time, the results of the modelling process had to be represented in the same manner as all synthesized data from the Swan Hills study area. To achieve this, pre- and post-processor software packages were developed to link the representation and storage of synthesized data for the Swan Hills study area with the FE3DGW model, such that human intervention was minimized. The distribution of freshwater hydraulic heads at all nodes in the finite element grid was transformed into a distribution of values at nodes in a regular grid, which were graphically represented as potentiometric surface maps. Using the final grids and maps, the results of the numerical simulation were compared with other synthesized data stored in the same form.

The results of the numerical simulation have to be compared with the results of the flow analysis

presented previously. This comparison is made in two ways: observed versus computed potentiometric surfaces of aquifers; and computed hydraulic heads at the nodes in the finite element model versus hydraulic heads at the same locations in the regular grids describing the potentiometric surfaces. In assessing these comparisons, one has to take into account the approximations and assumptions made at each step in each of the data processing procedures and in the numerical simulation.

A first approximation is made when values at nodes in a regular grid are obtained from an irregular distribution of real (measured) values. The regular grid distribution depends, among many factors, on its resolution, on the initial data size and sample distribution, on the gridding method, on the parameters and constraints of the method itself, and on the interpolation and extrapolation procedures. In the graphical representation of the regular grids as contour maps there are approximations and differences depending on the grid resolution and on the interpolation method. In the mathematical modelling there are basic assumptions about the flow (e.g. homogeneous single phase or single component fluid and isothermal flow), the porous matrix (e.g. isotropic) and the boundary conditions. In the numerical simulation there are assumptions (e.g. in this study, assigning a constant hydraulic conductivity to each layer) and approximations inherent to the discretization process, as well as to the numerical method (finite element or finite difference). In addition, there are approximations in the gridding and contouring of the computed values at the nodes in the finite element grid, for comparison with the initial potentiometric surface maps. As a result, a complete match between observed and computed data is not to be expected.

Mass balance and estimation of hydraulic parameters

One of the most difficult tasks in modelling subsurface flow is the estimation of the aquifer parameters to be used in the predictive stage of the numerical simulations based on field measurements of these parameters. Usually, hydraulic-head data are available, together with field and laboratory estimates of the aquifer parameters. These data are usually sparse and may be of varying quality. For deep aquifers, the only hydraulic data generally available are measured pressures, permeabilities and porosities, which for practical reasons are measured only for aquifers and not for aquitards. Real fluxes (recharge and discharge) are not measured. Estimation of the aquifer parameters from hydraulic-head data is recognized to be difficult and may be unstable or nonunique (Yakowitz and Duckstein 1980).

Initial estimates of aquifer parameters for the Swan Hills study area (tables 7 and 8) were provided based on drillstem test interpretation and core analyses; these represent the input data for the numerical model. The traditional approach for calibration of a subsurface flow model has been to modify the estimates of aquifer parameters by a trial and error procedure until the simulated and the measured hydraulic-head data are reasonably close, given known boundary conditions, sources and sinks, and a conceptual model of the fluid flow. The trial and error method for refining the input data is very costly in terms of time and computer resources and becomes prohibitive for large models with complex structures, as is the case for the Swan Hills study area. In order to overcome this difficulty a parameter estimation method is used, based on the general principle of mass conservation in any system. A consistent set of hydraulic parameters is obtained by applying the mass balance to the entire hydrostratigraphic succession. It must be stressed here, however, that the estimates of the aquifer parameters are not unique and their associated uncertainty cannot be determined. In the absence of controlling measured fluxes, any consistent set of hydraulic parameters may provide a reasonable representation of the observed hydraulic-head data.

The sedimentary succession in the Swan Hills study area is not a closed hydrogeological system. The only impervious boundary is assumed to be the Precambrian basement; there are no known hydraulic boundaries in the area (impervious, imposed hydraulic head or prescribed flux) other than those in the succession. In steady state conditions, the mass balance must close for any sedimentary block defined by an arbitrary closed contour. At the top of the block there is natural replenishment into the system. Fluid flow in the aquitards is essentially vertical (Bear 1972), so that within them there is no mass exchange along any lateral boundary between the sedimentary block and the surroundings. In contrast, the fluid flow in the aquifers is mainly horizontal, and the fluid moves in and out of the system. The lateral inflow or outflow across the boundary of each aquifer can be computed according to:

$$Q = \Sigma q_i A_i \qquad (8)$$

where Q is the total flux crossing the lateral boundary, A_i is the area of an element of the lateral surface bounding the aquifer, and q_i is the specific discharge normal to the respective surface element. The specific discharge is computed according to Darcy's law. A computer program automatically handles this procedure, starting from regular grids defining the top and the bottom of the respective aquifer, and the corresponding potentiometric surface and hydraulic conductivity. A single regional value of the hydraulic conductivity was used for each aquifer, dictated partly by the fact that the numerical model FE3DGW considers each hydrostratigraphic unit as homogeneous.

A closed contour was chosen arbitrarily to cover an area of 7384 km^2 between Tp 63-73 R 2-12 W5M. Not all of the Swan Hills study area was covered because there was need for a band of about one township around the closed contour for computation of the hydraulic gradient normal to the boundary. The lateral fluxes across this boundary are presented in table 16 for the aquifers in the hydrostratigraphic succession. The lateral fluxes are computed using the representative values of horizontal hydraulic conductivity in table 8.

For any modelling process, it is necessary to know the hydraulic conductivity of the aquitards. A value of $1x10^{-13}$ m/s is indicated by Bredehoeft and Hanshaw (1968) for shales, but more precise values for the average effective hydraulic conductivity can be obtained by calculating the flow mass balance for the entire hydrostratigraphic succession.

There is a difference of several orders of magnitude between the hydraulic conductivities of aquifers and aquitards. It follows, then, that the entire drop of hydraulic head between two aquifers separated by an aquitard takes place effectively over the thickness of the aquitard. Given the potentiometric surfaces in each aquifer and the thickness of the aquitard, it is possible to compute the vertical hydraulic gradients in the aquitard. Assuming values for the hydraulic conductivity of the aquitard, the total crossflow between aquifers can then be computed. This procedure was automated using a program which reads as input the grids defining the isopach of the respective aquitard, the potentiometric surfaces for the aquifers above and below it, the contour of a closed area, and a value of the average hydraulic conductivity assigned to that aquitard. The closed area has to be divided into elements defined by their nodes, which in any case is a necessary procedure in finite-element modelling. The output contains information about the area, specific discharge and flux for each element as well as for the entire model area. The only unknown data for computing the vertical flow through the aquitards are their hydraulic conductivities. These values can be found by a trial and error procedure until the flow mass balance of the entire system is closed.

Table 16. Lateral fluxes for aquifers along a closed contour covering 7384 km^2.

Aquifer	Hydraulic conductivity (m/d)	Lateral area (km^2)	Inflow (m^3/d)	Outflow (m^3/d)	Net lateral flow (m^3/d)
Viking	0.0130	6.18	26.2	84.2	-58.0
Upper Mannville	0.0170	54.97	733.2	331.5	401.7
Lower Mannville	0.0180	28.65	844.0	224.5	619.5
Shunda	0.0078	0.51	7.0	0.5	6.5
Pekisko	0.0028	5.13	27.6	2.9	24.7
Banff carbonate	0.0028	37.75	167.8	42.1	125.7
Wabamun	0.0300	88.40	1826.0	1292.3	533.7
Upper Winterburn	0.0082	18.93	112.8	79.8	33.0
Nisku	0.0220	26.60	423.7	300.0	123.7
Beaverhill Lake-Cooking Lake	0.0092	49.79	299.2	250.5	48.7
Swan Hills-Slave Point	0.0049	10.57	37.9	16.4	21.5
Watt Mountain	0.0008	3.98	2.3	1.6	0.7
Gilwood	0.0790	3.68	196.0	144.2	51.8
Keg River	0.0170	4.10	11.3	59.9	-48.6
Contact Rapids	0.0130	10.05	23.7	124.0	-100.3
Granite Wash	0.1700	4.36	639.2	422.3	216.9
Lynx	0.0084	0.93	2.2	1.5	0.7
Basal Cambrian	0.0260	9.15	85.3	89.6	-4.3

The hydraulic heads in both the Basal Cambrian aquifer and the Beaverhill Lake aquifer system are higher on average than the hydraulic heads in the Cambro-Devonian aquifer system. It follows, therefore, that there is upward flow through the Middle Cambrian aquitard system from the Basal Cambrian aquifer, and downward flow through the Muskeg aquitard from the Beaverhill Lake aquifer system. There is also upward flow from the Beaverhill Lake aquifer system to the Wabamun-Winterburn aquifer system through the Ireton aquitard due to higher hydraulic heads in the former system than in the latter. On the other hand, there is successive downward flow from the Viking aquifer to the Upper Mannville aquifer system through the Joli Fou aquitard; downward flow from the Upper Mannville aquifer system to the Lower Mannville aquifer system through the Clearwater-Wilrich aquitard; and continued downward flow from the Lower Mannville aquifer system to the Wabamun-Winterburn aquifer system through the Exshaw-Lower Banff aquitard. The cross-formational flow related to the Grosmont aquifer was not determined due to the lack of data for this aquifer.

The lateral and cross-formational flow in the hydrostratigraphic succession in the Swan Hills study area is represented schematically in figure 37.

In the Swan Hills study area there are 22 aquifers, 12 aquitards and 2 aquicludes between the Second White Speckled shales and the Precambrian basement, not including the Jurassic (Nordegg and Fernie), present only in the southwest corner. In terms of numerical simulation, it is impossible to take into account every single aquifer, aquitard or aquiclude, due to limitations of the model (number of nodes and elements) and of computer resources (virtual memory, disk space and CPU time). In order to overcome this problem the hydrostratigraphic units were grouped into eight aquifer systems and eight aquitards. Except for the Grosmont aquifer and the Upper Ireton aquitard overlying it, all the aquifer systems extend over the entire Swan Hills study area and are separated by aquitards. Although the Ernestina Lake, Pika and Eldon Formations are actually aquifers, they are not in contact with each other or with other aquifers to form a continuous conductive layer over the area, and not enough information is available to determine a potentiometric surface for any of them. To

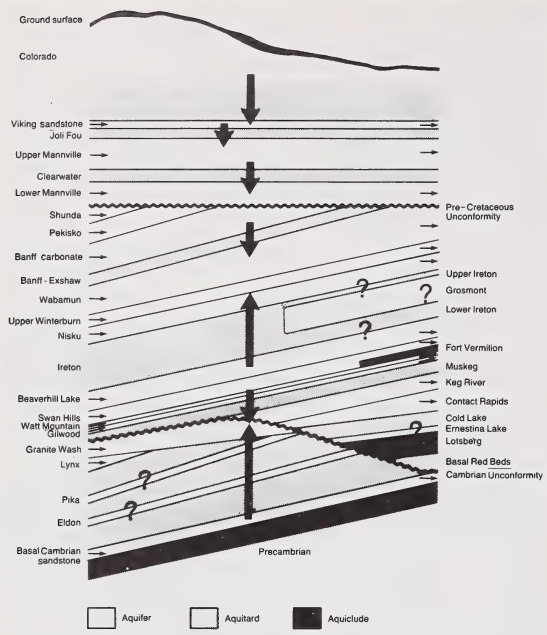

Figure 37. Diagrammatic representation of the lateral and cross-formational flow in the Swan Hills study area (arrows represent flow directions, question marks denote insufficient information).

take them into account individually also increases significantly the computer resources needed for numerical simulation. For these reasons they were incorporated into the Middle Cambrian aquitard system. Also, at the beginning of the numerical simulations it was necessary to combine the Rundle and Lower Mannville aquifers in order to reduce further the number of nodes and elements. The equivalent horizontal and vertical hydraulic conductivities of the aquifer systems were computed (Bear 1972; Bachu et al. 1987) taking into account the direction of the fluid flow with respect to the layering of each system, the average thickness, position and areal distribution of each layer within a system, and the individual hydraulic conductivities of each layer.

Table 17. Equivalent hydraulic conductivities and lateral fluxes for aquifers and aquifer systems.

Aquifer or aquifer system	Hydraulic conductivity horizontal (m/d)	Hydraulic conductivity vertical (m/d)	Lateral inflow (m^3/d)	Lateral outflow (m^3/d)	Net lateral flow (m^3/d)
Viking aquifer	0.0130	0.0032	26.2	84.2	-58.0
Upper Mannville aquifer system	0.0170	0.0049	733.2	331.5	401.7
Lower Mannville-Rundle aquifer system	0.0097	0.0006	1137.0	275.7	861.3
Lower Mannville aquifer system	0.0180	0.0021	–	–	–
Rundle aquifer	0.0028	0.0002	–	–	–
Wabamun-Winterburn aquifer system	0.0250	0.0023	2347.0	1661.0	686.0
Beaverhill Lake aquifer system	0.0080	0.0015	370.8	283.0	87.8
Cambro-Devonian aquifer system	0.0237	0.0125	166.2	360.4	-194.2
Basal Cambrian aquifer	0.0260	0.0030	85.3	89.6	-4.3

The mass balance of the lateral flow in each aquifer system was computed with the new equivalent hydraulic conductivity and thickness for the same closed contour as previously. The results are presented in table 17.

Examination of the lateral and cross-formational flow in the multilayered system of the hydrostratigraphic succession in the Swan Hills study area (figure 37 and table 17) shows that the mass balance for the entire system does not close within reasonable limits and that the hydraulic parameters for some aquifers or aquifer systems have to be modified from the previous regional values in order to achieve closure.

The Basal Cambrian aquifer is isolated from the overlying aquifer system by a tight and thick (152 m) aquitard. The lateral mass balance closes within 5%. It is concluded that this aquifer is independent of all others.

The succession between the Middle Cambrian and Ireton aquitards is also almost independent. There is very little inflow from the Basal Cambrian aquifer upward through the Middle Cambrian aquitard system and very little outflow from the Beaverhill Lake aquifer system to the Wabamun-Winterburn aquifer system through the Ireton aquitard. The main cross-formational flow is from the Beaverhill Lake aquifer system to the Cambro-Devonian aquifer system, through the Muskeg aquitard. Comparing the number and distribution of data used to estimate the hydraulic parameters in each aquifer system (tables 5 and 6), it follows that the hydraulic conductivity for the Beaverhill Lake aquifer system is more reliable than that for the Cambro-Devonian aquifer system. The equivalent hydraulic conductivity of the Cambro-Devonian aquifer system is overestimated due to a very high value for the Granite Wash, based on only four measurements.

In the succession between the Second White Speckled shale and the Clearwater-Wilrich shales there are two aquifers, Viking and Upper Mannville, separated by the Joli Fou aquitard. For a hydraulic conductivity, K, of 5×10^{-9} m/d for the Joli Fou shales, the downward flow from the Viking aquifer to the Upper Mannville aquifer system is about 79 m^3/d over an area of 7384 km^2. The Clearwater-Wilrich aquitard contains sandstone lenses and is therefore not homogeneous. As a result, its hydraulic conductivity should be higher than that for Joli Fou shales. Assuming a hydraulic conductivity of 1×10^{-8} m/d, the

downward flow from the Upper Mannville aquifer system to the Lower Mannville aquifer is about 206 m^3/d. The total mass balance of the Upper Mannville aquifer system will then close, if a value of $5.4x10^{-3}$ m/d is assumed for the horizontal hydraulic conductivity.

The Exshaw-Lower Banff aquitard separating the Rundle aquifer from the Wabamun-Winterburn aquifer system is not homogeneous because the Banff shales are interbedded with carbonates. Assuming a hydraulic conductivity of $1.5x10^{-8}$ m/d, the downward flow from the Lower Mannville-Rundle aquifer system to the Wabamun-Winterburn aquifer system is about 325 m^3/d for the area under consideration. The Ireton Formation shales are more homogeneous, tighter, and 400 to 500 m deeper than the Exshaw-Lower Banff shales, and therefore probably have a lower hydraulic conductivity. The Muskeg Formation is less homogeneous, and even if it is deeper than the Ireton Formation, its hydraulic conductivity is assumed to be higher due to the presence of interbedded dolomites. In order to close the mass balance for the Viking aquifer, the thick aquitard between the water table and the Viking aquifer must accommodate a downward flow of 137 m^3/d over 7384 km^2 ($6.7x10^{-3}$ mm/a). Considering, as a first approximation, the drop in hydraulic head between the water table and the potentiometric surface of the Viking aquifer, it follows that the hydraulic conductivity of the Colorado aquitard system is $3.4x10^{-8}$ m/d, the highest in the whole succession of aquitards. This is consistent with the fact that this aquitard is the least compacted, being the closest to the ground surface, and includes interbedded sandstones.

With respect to the estimation of the hydraulic conductivity characterizing the aquitards, literature values were used as an indication, but the final values were obtained through mass-balance computations, based also on the geology and lithology of the strata. Given all the errors, approximations and assumptions inherent in data measurements and processing, mathematical modelling and numerical simulation, it is only proper that average values of hydraulic conductivity were used in mass balance computations in order to obtain values for the parameters characterizing the aquitards. If measured fluxes had been available, the mass balance could have been used for calibrating the hydraulic parameters such that the computed fluxes matched the measured ones. With respect to measured hydraulic parameters in the aquitards, the system must close, again allowing for calibration of the hydraulic parameters. In the absence of measured fluxes or hydraulic parameters in the aquitards, a combination of hydraulic conductivities for the aquifers will produce a corresponding set of values for the aquitards by closing the system.

The final mass balance for the entire sequence of aquifer and aquitard systems in the Swan Hills study area is presented in table 18, for an area covering 7384 km^2. Examination of table 18 points out a few important aspects. The Basal Cambrian aquifer is relatively independent of the rest of the hydrostratigraphic system. No matter what value of hydraulic

Table 18. Hydraulic conductivities and mass balance for the aquifer and aquitard systems in an area of 7384 km^2 between Tp 2-12 and R 63-73 W5M.

Hydrostratigraphic unit	Horizontal hydraulic conductivity (m/d)	Vertical hydraulic conductivity (m/d)	Total influx (m^3/d)	Total outflux (m^3/d)	Net Mass balance (m^3/d)	Net mass balance Total influx (%)
Post-Viking aquitard		3.4×10^{-8}	137.0	137.0	0	0
Viking aquifer	0.013	0.0032	163.2	163.2	0	0
Joli Fou aquitard		0.5×10^{-8}	79.0	79.0	0	0
Upper Mannville aquifer system	0.006	0.0017	337.8	323.1	14.7	4.35
Clearwater-Wilrich aquitard		1.0×10^{-8}	206.1	206.1	0	0
Lower-Mannville-Rundle aquifer system	0.008	0.0005	1143.8	552.0	591.8	51.74
Exshaw-Lower Banff aquitard		1.5×10^{-8}	324.6	324.6	0	0
Wabamun-Winterburn aquifer system	0.015	0.0014	1743.3	996.2	747.1	42.85
Ireton aquitard		0.3×10^{-8}	10.5	10.5	0	0
Beaverhill Lake aquifer system	0.010	0.0019	463.5	462.7	0.8	0.17
Muskeg aquitard		2.0×10^{-8}	98.5	98.5	0	0
Cambro-Devonian aquifer	0.012	0.0063	184.8	182.5	2.3	1.24
Cambro-Devonian aquitard		1.5×10^{-8}	2.2	2.2	0	0
Basal Cambrian aquifer	0.026	0.0030	85.2	91.8	-6.5	-7.62

conductivity is assigned to this aquifer, the lateral mass balance will close within 5%. The total mass balance also depends on the upward flow, and therefore on the hydraulic conductivity assigned to the Middle Cambrian aquitard system. The mass balances of the pre-Ireton and the post-Clearwater successions also close within 5%. The mass balance of the succession between the Ireton and Clearwater aquitards has a surplus of about 50%, even if the values used for hydraulic conductivity are lower than the regional ones by a factor of two to three. For higher values of hydraulic conductivity for the intervening aquifers the imbalance is even greater. It could be reduced by lowering the values of hydraulic conductivity further, but that would mean a greater discrepancy between the regional values for this hydraulic parameter and those actually used. This large mass imbalance in these two aquifer systems, in fact, can be explained by their geometry and potentiometric surfaces. The flow in both the Lower Mannville-Rundle and the Wabamun-Winterburn aquifer systems generally trends from southwest to northeast, with high gradients in the southwest third of the study area, and low gradients (almost flat) in the eastern third (figures 25d and 30d). For constant hydraulic conductivity in an aquifer, this hydraulic-head distribution means higher velocities in the western part of the study area than in the eastern part. On the other hand, the Wabamun-Winterburn aquifer system is about 100 m thicker in the west than in the east, while the Rundle aquifer, with a total thickness of a few hundred metres in the west, disappears completely in the east. In both cases the difference in thickness is due to erosion along the pre-Cretaceous unconformity (figure 37). This combination of higher input velocity with larger input area, and lower output velocity with smaller output area will always produce a significant lateral imbalance. For a given regional single value of hydraulic conductivity, the ratio between the lateral influx and outflux will be the same. To this must be added the downward flow through the post-Ireton succession, and the upward flow (although almost negligible) from the Beaverhill Lake aquifer system to the Wabamun-Winterburn aquifer system.

In this mass balance computation there are three main elements: the geometry of the layers, the potentiometric surfaces, and the hydraulic parameters. The mass balance can be closed for a given layer by modifying either its geometry or its potentiometric surface (hydraulic gradients), or by using different values for hydraulic conductivity in different parts of the layer. The geometry of the layers is the most reliable; it is based on hundreds of data points and generally fits the depositional and erosional trends in the sedimentary basin. The hydraulic conductivity data are obtained from laboratory measurements of cores and from drillstem test interpretations. The data distributions vary from layer to layer, but for each layer they are statistically homogeneous, that is, the variability of the data is random. No consistent pattern in the areal distribution of hydraulic conductivity data could be detected for the Lower Mannville-Rundle or Wabamun-Winterburn aquifer systems. Even if the hydraulic conductivity varied regionally in a systematic manner, this fact could not be incorporated into the numerical simulation because the FE3DGW model specifies the use of a single value for the hydraulic parameters characterizing each layer.

In the computation of hydraulic heads from drillstem test interpretations all pertinent factors were taken into account, and the data were rechecked after the mass balance was performed. Based on the data available for the study, no grounds were found for modifying the potentiometric surfaces. Therefore, the mass balance for the Lower Mannville-Rundle and the Wabamun-Winterburn aquifer systems could not be closed within reasonable limits.

The values of hydraulic conductivity presented in table 18 were used subsequently in numerical simulations of steady-state natural flow of formation waters in the Swan Hills study area, and of deep injection in selected aquifers. The set of parameters is consistent to the extent permitted by the available data.

Because the numerical model is based on the principle of mass conservation for subsurface flow (equation 6), it was expected that the match between computed and observed potentiometric surfaces would be good for those aquifers for which the mass balance closed within reasonable limits, and poorer for the Lower Mannville-Rundle and Wabamun-Winterburn aquifer systems.

Calibration of the numerical model

For modelling purposes it is necessary to define a bounded three-dimensional region with appropriate boundary conditions for fluid flow. Because the present investigation was directed at the feasibility of deep injection of liquid wastes at a specific site, the model region must be generally centered around the injection site and include the prospective injection aquifers and the stratigraphic succession which could be affected. With the possible effects of injection being unknown, it was decided in the preliminary phase to simulate fluid flow in the entire hydrostratigraphic succession beneath the Lower Cretaceous Base of Fish Scales Zone. As presented previously, there are eight aquifer and eight aquitard systems in the area, neglecting the Nordegg aquifer and Fernie aquitard which are found only in the southwest corner of the study area.

In the Swan Hills study area there are no hydraulic boundaries for the groups of aquifers and aquitards below the top of the bedrock. Only geometric boundaries separate different hydrostratigraphic units, accompanied by changes in the values of the hydraulic

parameters. The boundary values of the hydraulic head along the lateral boundaries of the hydrostratigraphic units were obtained from the potentiometric surfaces defined previously. Due to lack of data there was no potentiometric surface for the Grosmont aquifer. The hydraulic heads at the top of the system were considered to be those at the water table. By comparison with the Cold Lake area (Basin Analysis Group 1985) a value of 6.7×10^{-3} mm/a was prescribed as natural replenishment at the top of the bedrock, while the Precambrian basement was considered as an impervious boundary.

In order to circumvent the problem of lack of boundary conditions for the Grosmont aquifer and also to reduce the number of hydrostratigraphic units for modelling, it was decided to choose a model area immediately west of the boundary of the Grosmont Formation, and east of the Jurassic boundary (figure 38). The model area covers 4250 km^2 of the hydrostratigraphic succession listed in table 18.

The model area was divided into 109 surface elements with a total of 128 surface nodes. The areal distribution of surface nodes and elements was transformed into a three-dimensional structure with nodes along vertical axes from the surface, resulting in a discrete system of 1413 volume elements defined by 1779 nodes. The computation of the solution of steady-state natural flow described by equation (7) took 1 h, 47 min, 11 s CPU time on a VAX-11/750 computer with a floating point accelerator.

The results, in terms of hydraulic heads, were compared with values of the observed potentiometric surfaces at the same locations, and were also plotted as computed potentiometric surfaces for visual comparison. The average of the relative differences between computed and observed hydraulic heads for each aquifer varies between 0.8% for the Basal Cambrian aquifer and 10% for the Lower Mannville-Rundle aquifer system. The maximum relative difference between computed and observed hydraulic heads for each aquifer is 2% for the Basal Cambrian aquifer, 21% for the Lower Mannville-Rundle aquifer system, 16% for the Wabamun-Winterburn aquifer system, and varies between 4 and 7% for all the others. The reason for relatively poor matching of computed and observed hydraulic heads for the Lower Mannville-Rundle and Wabamun-Winterburn aquifer systems resides in large mass imbalances for the observed flow in these aquifers as discussed in the previous section.

In order to check the accuracy of the numerical simulation and the sensitivity of the model to the grid size, the number of surface elements was increased from 109 to 164, and the number of surface nodes correspondingly increased from 128 to 187. The increase in the number of surface nodes and elements translates into an increase in the number of nodes and volume elements in the three-dimensional structure to 2604 and 2127, respectively. In this case, it took 3 h, 49 min, 47 s CPU time to obtain a solution, confirming the general rule that the increase in CPU time is proportional to the square of the increase in the number of nodes. No improvement of the solution, however, was obtained using the denser grid. The average and maximum errors between computed and observed hydraulic heads varied within 2% of the previous case. These differences can be attributed to approximations and errors in transforming the different grid distributions of computed hydraulic heads into a regular grid distribution, rather than to an increase in the accuracy of the solution. Because a twofold increase in the computational effort was not justified by an improvement of 1 to 2% in the solution, it was decided to retain the initial distribution of nodes and elements.

The match between computed and observed hydraulic heads in the small model area is considered acceptable. Actually, it is good for all the aquifer systems except the Lower Mannville-Rundle and Wabamun-Winterburn, but there is nothing that can be done with respect to these, for reasons discussed previously.

Another parameter which could influence the numerical solution is the hydraulic conductivity appearing in equation (7). For any consistent set of values for the hydraulic conductivity tensor, $\bar{K}$, however, the resulting distribution of hydraulic heads, H, depends only on the boundary conditions. For the same boundary conditions of prescribed hydraulic heads, different sets of hydraulic conductivities will

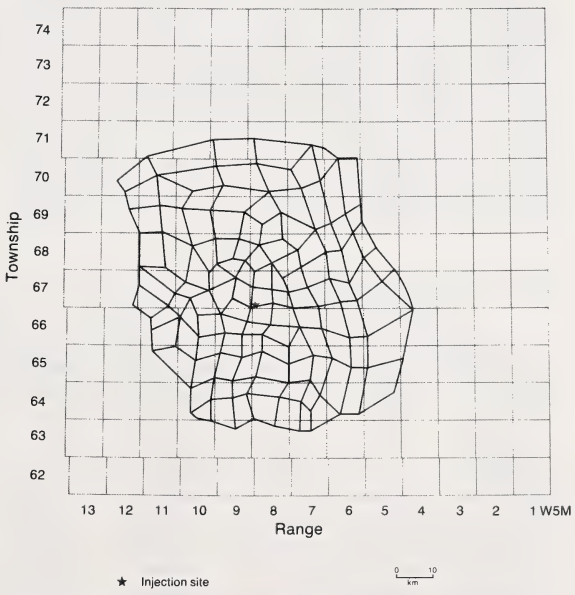

Figure 38. Distribution of nodes and elements in the small model area (4250 km^2).

produce, at least in theory, identical distributions of the hydraulic heads. Possible differences are due only to numerical approximations and truncation errors. The only real difference between results obtained with different sets of hydraulic parameters is in fluxes, which, for given hydraulic gradients, change in direct relation with the hydraulic conductivity, according to Darcy's law (equation 1). Because no fluxes were measured, and injection/pumping data were not available, it was not possible to check such results against reality in order to decide which set of data best characterizes the multilayer hydrostratigraphic system in the model area. Therefore, a sensitivity analysis of the influence of hydraulic conductivity on the steady-state natural flow was not relevant to the study.

Besides the grid size and the hydraulic parameters, the results of a fluid-flow model are sensitive, in general, to the type and values of boundary conditions. In this study, however, there are no other boundary conditions except prescribed hydraulic heads, the values of which are determined from the potentiometric surfaces of each aquifer system. Therefore, the influence of the boundary conditions could not be analyzed and assessed.

Numerical simulation of deep waste injection

The main purpose of this study was to check the feasibility of deep injection of liquid wastes at the Swan Hills injection site, with respect to the fluid flow in the host and surrounding aquifers. Therefore, the first step was the selection of the possible injection aquifers. As discussed previously, the uppermost aquifer systems in Cretaceous strata have to be eliminated due to possible contamination of potable groundwater resources. That leaves as potential injection aquifers the aquifer systems below the Exshaw-Lower Banff aquitard.

The first objective of the numerical simulation was to check if the effects of injection in the prospective aquifers propagate through the system, and to what extent. The proposed amount of 90 000 t/a for deep injection represents a rate of 225 m^3/d, considering a fluid density of 1100 kg/m^3. Numerical simulations of injecting 225 m^3/d in the Basal Cambrian, Cambro-Devonian, Beaverhill Lake or Wabamun-Winterburn aquifer systems were carried out for the case of average hydraulic conductivities, as well as for the extreme case of hydraulic conductivities equal to the minimum value measured in the respective aquifer. These cases represent the most probable and the worst scenarios of injection, respectively, on a regional scale. The numerical model, FE3DGW, is deterministic and incapable of taking into consideration statistical variability of hydraulic parameters for aquifers or aquitards. While an average value still characterizes a given distribution, the use of a minimum value in a deterministic model represents an unreal case, theoretically, the worst case for fluid flow and hydraulic head buildup. The results of numerical simulation of fluid injection were compared with the computed potentiometric surfaces of steady-state natural flow prior to injection. Everything was the same (geometry, hydraulic parameters, boundary conditions) except the source of the fluid at the injection site.

It can be seen from table 19, that only the host aquifer is really affected by injection. When the injection takes place in the Wabamun-Winterburn aquifer system, the increase in hydraulic head is only about 30 m in the injection aquifer itself, with practically no effects in the Beaverhill Lake aquifer system below, and in the Lower Mannville-Rundle aquifer system above. This is due to the geometry of the host aquifer and surrounding aquitards. The Wabamun-Winterburn aquifer system is very thick (380 m at the injection site), so the hydraulic head buildup is small. This small hydraulic head buildup is attenuated upward through the thin Exshaw-Lower Banff aquitard (35 m at the injection site). Below, the thick Ireton aquitard (330 m) does not allow for propagation of hydraulic head buildup in the Beaverhill Lake aquifer system.

Table 19. Steady-state effects of injection of 225 m^3/d in selected aquifers: small model area.

Hydrostratigraphic unit	Natural flow	Injection in Wabamun-Winterburn aquifer system			Injection in Basal Cambrian aquifer		
	Hydraulic head at injection site (m)	Average change (%)	Maximum change (%)	Hydraulic head at injection site (m)	Average change (%)	Maximum change (%)	Hydraulic head at injection site (m)
Viking aquifer	620.2	0.0	0.0	620.2	0.0	0.0	547.47
Upper Mannville aquifer system	549.2	0.0	0.0	549.2	0.0	0.0	528.23
Lower Mannville-Rundle aquifer system	446.1	0.16	0.33	447.7	0.0	0.0	486.61
Wabamun-Winterburn aquifer system	460.5	0.82	6.20	489.1	0.0	0.0	426.66
Beaverhill Lake aquifer system	812.1	0.0	0.1	812.1	0.0	0.0	528.67
Cambro-Devonian aquifer	793.6	0.0	0.0	793.6	0.29	0.91	469.66
Basal Cambrian aquifer	843.9	0.0	0.0	843.9	7.32	35.6	1144.25

Injection in the Beaverhill Lake aquifer system brings, at steady-state, a higher hydraulic head buildup at the injection site than in the case of the Wabamun-Winterburn aquifer system, due to the reduced thickness and reduced hydraulic conductivity. However, no effects are felt in the Wabamun-Winterburn aquifer system, the thick and tight Ireton aquitard acting as an effective barrier. The highest hydraulic head buildup (approximately 570 m) occurs in the Cambro-Devonian aquifer system, if injection takes place in this aquifer. This is due to the fact that the aquifer is very thin (18 m) at the injection site. In the case of injection in the Basal Cambrian aquifer, the hydraulic head buildup is still significant (about 300 m), but not so high as in the case of injection in the Cambro-Devonian aquifer system because, although their thicknesses are about the same, the Basal Cambrian aquifer has a higher value of hydraulic conductivity.

The extreme cases of minimum hydraulic conductivity in the host aquifer were simulated considering (1) a horizontal hydraulic conductivity, K_H, of 1.6×10^{-4} m/d for the Wabamun-Winterburn aquifer system, and (2) a horizontal hydraulic conductivity, K_H, of 1.4×10^{-3} m/d for the Basal Cambrian aquifer (table 8). It should be noted that for the case of minimum hydraulic conductivity in the Wabamun-Winterburn aquifer system, the hydraulic conductivities of all the hydrostratigraphic units above had to be reduced by approximately the same factor in order to have a consistent estimation of hydraulic parameters (see the previous discussion). It was not necessary to modify the hydraulic conductivities in the pre-Ireton succession because the cross-formational flow through the Ireton aquitard is not a major component in the mass balance. In the case of simulation with minimum hydraulic conductivity in the Basal Cambrian aquifer, it was shown that this aquifer is quite independent of all the others and there was no need to readjust the hydraulic parameters in the rest of the succession. The results of these simulations are shown in table 20.

It can be seen that even in these extreme cases of minimum hydraulic conductivity in the host aquifer, the hydraulic head buildup does not effectively propagate into the surrounding aquifers due to the tightness and thickness of the aquitards confining the injection aquifer. The above cases are actually unrealistic, and of theoretical value only, because these hydraulic head buildups will not be attained in the respective aquifers.

Once the fracturing threshold is reached, the rock will fracture due to mechanical stresses, thereby increasing the hydraulic conductivity of the injection aquifer. Because the development of these fractures is most likely to be vertical, surrounding aquitards might be affected. Further study beyond the scope of this project is necessary to assess accurately the potential for these effects on other aquifers in the system. However, it is very unlikely that fractures caused by injection in the Basal Cambrian aquifer will propagate upward through the thick Middle Cambrian and Ireton aquitards. Similarly, for injection into the Wabamun-Winterburn aquifer system, it is unlikely that downward fracturing of the thick Ireton aquitard will propagate to the Beaverhill Lake aquifer system.

Throughout this bulletin, cross-formational flow has only been considered in terms of the natural hydrostratigraphy. However, it must be noted that there is also a potential for cross-formational flow as a result of poor cement jobs in existing and abandoned wells.

One of the main conclusions of the simulations presented so far is that the thick Ireton aquitard acts, for all practical purposes, as an impervious layer between the pre-Ireton and post-Ireton hydrostratigraphic successions. As a result, the two successions can be decoupled, and the effects of injection studied separately. It is also clear that the effects of injection do not propagate into the uppermost layers of the succession and, therefore, the post-Mannville succession (above the Joli Fou Formation) does not have to be considered in simulations, except with respect to downward flow required by the mass balance of the system. In terms of computer resources, the reduction

Table 20. Steady-state effects of injection of 225 m^3/d in selected aquifers considering minimum hydraulic conductivity: small model area.

Hydrostratigraphic unit	Natural flow	Injection in Wabamun-Winterburn aquifer system			Injection in Basal Cambrian aquifer		
	Hydraulic head at injection site (m)	Average change (%)	Maximum change (%)	Hydraulic head at injection site (m)	Average change (%)	Maximum change (%)	Hydraulic head at injection site (m)
Viking aquifer	620.2	0.0	0.0	620.2	0.0	0.0	620.2
Upper Mannville aquifer system	549.2	0.1	0.9	554.1	0.0	0.0	549.2
Lower Mannville-Rundle aquifer system	446.1	13.6	18.8	530.0	0.0	0.0	446.1
Wabamun-Winterburn aquifer system	460.5	80.6	456.2	2561.4	0.0	0.0	460.5
Beaverhill Lake aquifer system	812.1	0.1	0.2	813.9	0.0	0.1	812.5
Cambro-Devonian aquifer system	793.6	0.0	0.0	793.6	0.4	2.1	810.5
Basal Cambrian aquifer	843.9	0.0	0.0	843.9	95.3	626.3	6128.9

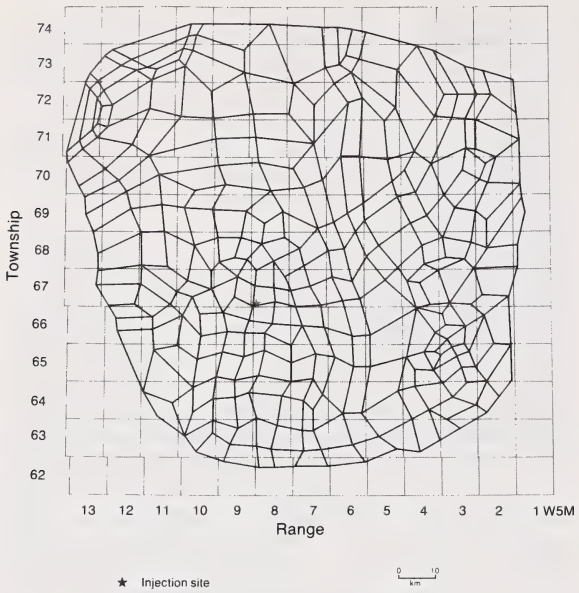

Figure 39. Distribution of nodes and elements in the large model area (10 952 km^2).

in the number of layers in a simulation means fewer nodes and elements, and therefore less CPU time. Or, for the same limits on model size and computer resources, either the model area or the node density can be increased.

It was shown previously that an increase in the node density does not improve the accuracy of the results. Consequently, the model area was expanded to a larger size, covering 10 952 km^2 (figure 39). The area was divided into 279 surface elements defined by 307 nodes. By comparing the results of numerical simulations on the small and large model areas, it was possible to assess the influence of the model boundaries and the radius of influence of the injection well.

Numerical simulations were carried out, first for the pre-Ireton succession, with a total of 1804 nodes and 1384 volume elements. Due to changes in the computer configuration, a typical run took only 54 min, 43 s CPU time. The natural steady-state flow was simulated for the entire area, with average differences between computed and observed hydraulic heads varying between 1.7 and 2.4%, and maximum differences up to 10%.

The effects of injection are the same in the case of the large model area and the small model area. For example, in the case of the Basal Cambrian aquifer, for the regional values of hydraulic conductivity, the freshwater hydraulic head increases at the injection site from 843.9 to 1144.3 m in the Basal Cambrian aquifer and from 793.6 to 800.4 m in the Cambro-Devonian aquifer system, with no change in the Beaverhill Lake aquifer system. The area of influence is slightly elongated to the northeast and reduced to the southwest due to decreasing thickness of the host aquifer from southwest to northeast. The fluid velocity at the node representing the injection site increases from 1.05 cm/a in natural conditions to 14.6 cm/a in the case of steady injection.

For the succession above the Ireton Formation to the top of the Mannville Group, the large model area includes the Grosmont aquifer, separated from the Wabamun-Winterburn aquifer system by the Upper Ireton aquitard. Because a potentiometric surface was not available to define the hydraulic heads along the boundary of the Grosmont aquifer, three observed values were used as boundary conditions. The Lower Mannville and Rundle Groups were considered separate aquifers with different hydraulic conductivities. The total number of nodes in the succession is 2222, defining 1803 volume elements. A simulation took 1 h, 47 min, 27 s CPU time.

With respect to hydraulic head buildup, and for the given injection rate of 225 m^3/d, the effects of injection are, for practical purposes, not propagated beyond the injection aquifer due to the tightness and thickness of the underlying and overlying aquitards. Depending on the geometry and properties of the injection aquifer and adjacent aquitards, however, cross-formational flow will be affected. Calculations shown in table 21 indicate that the pattern of cross-formational flow between two neighboring aquifers may be altered significantly when the injection aquifer has a reduced injectivity, resulting in a higher hydraulic-head buildup. Figure 40a shows the steady-state specific discharge through the Muskeg aquitard. For injection at 225 m^3/d in the thick overlying Beaverhill Lake aquifer system, the downward natural cross-formational flow is enhanced by only 10% (figure 40b). However, for injec-

Table 21. Cross-formational flow at steady state between aquifers, before and after injection at 225 m^3/d.

Aquifer or aquifer system	Natural lateral input (m^3/d)	Natural cross-formational flow (m^3/d)	Cross-formational flow at steady state after injecting 225 m^3/d			
			Wabamun-Winterburn	Beaverhill Lake	Cambro-Devonian	Basal Cambrian
Wabamun-Winterburn	1860	13.8	13.6	14.6	13.9	13.8
Beaverhill Lake	600	-155.8	-155.6	-170.9	-98.0	-155.8
Cambro-Devonian	127	148.5	148.5	162.8	61.5	167.1
Basal Cambrian	124	-6.5	-6.5	-6.5	12.6	-25.1

Note: negative sign means flow leaving the aquifer.

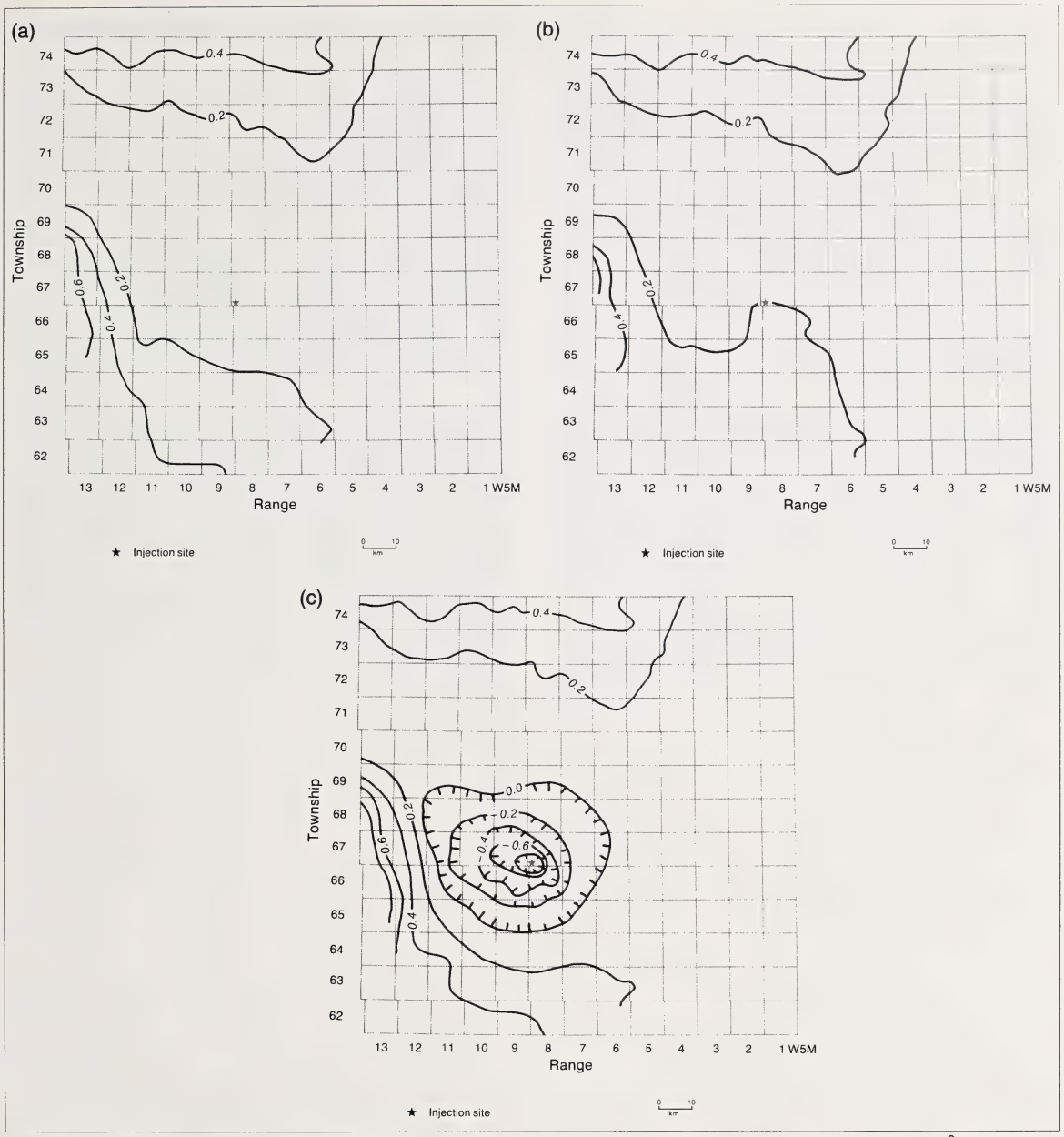

Figure 40. Specific discharge (m/d) through the Muskeg aquitard, a) natural steady state, b) after injection at 225 m^3/d in the overlying Beaverhill Lake aquifer system, c) after injection at 225 m^3/d in the underlying Cambro-Devonian aquifer (from Sauveplane et al. 1986).

tion at the same rate in the thin underlying Cambro-Devonian aquifer, the natural cross-formational flow around the injection site is actually reversed, bringing about an overall reduction of 40% in the net cross-formational flow (figure 40c). The pattern and strength of the cross-formational flow are changed mostly around the injection well.

Generally, the numerical simulations of injecting 225 m^3/d in selected aquifers at the Swan Hills waste disposal site have shown that, assuming representative values for the hydraulic conductivity, the practical effects of injection do not propagate beyond the host aquifer due to the tightness and thickness of the adjacent aquitards. The shape of the hydraulic head

build-up cone is strongly influenced by the geometry of the injection aquifer. For the thick Wabamun-Winterburn and Beaverhill Lake aquifer systems, where the variation in aquifer thickness around the injection well is relatively small, the effects of injection are essentially radial. For thinner aquifers, variations in thickness are important and the effects of injection are no longer strictly radial. Injection, even at rates as low as 225 m^3/d, will not only induce cross-formational fluxes in thin aquitards, but may result in reversal of the natural flow conditions.

Numerical simulations of transient phenomena indicate the way perturbation effects develop and propagate in a system, and how long it takes to reach steady-state, if this state can be reached at all. The study indicates that the recommended injection aquifer is the Wabamun-Winterburn aquifer system. Steady-state numerical simulations for the most probable set of conditions in this aquifer system show an increase in the hydraulic head at the injection site from 460.5 to 489.1 m. This increase of 6.2% is of the same order of magnitude as the total of all the errors and approximations involved in the study, and well within the range of values in the natural system. Therefore, it was decided that a numerical simulation of the transient phenomena in this case was not needed.

The influence of hydraulic conductivity and of the injection rate was checked only for the Wabamun-Winterburn aquifer system, because it was the one recommended for deep waste disposal. Using a horizontal hydraulic conductivity of 1.5×10^{-3} m/d, which represents a more reasonable case of low permeability compared with the average value, the resulting hydraulic head buildup at the node representing the injection site was 276.7 m. Even in this case, however, there are no effects in the overlying or underlying aquifers. This is a direct result of the fact that the entire flow system has to be internally balanced, as discussed previously. At the node representing the injection site, there is an increase in the Darcy velocity from 1.1 to 1.7 cm/a in the case of an assumed horizontal hydraulic conductivity of 1.5×10^{-2} m/d, and an increase from 0.1 to 0.7 cm/a in the case of an assumed horizontal hydraulic conductivity of 1.5×10^{-3} m/d.

A test run was performed for the case of a tenfold increase of the injection rate (2250 m^3/d) in the case of injection in the Wabamun-Winterburn aquifer system. For the average hydraulic conductivity, K, of 1.5×10^{-2} m/d, the corresponding increase in the hydraulic head is 295 m; this is about a tenfold increase over that for the given rate of 225 m^3/d. The final hydraulic-head buildup due to injection is directly proportional to the rate of injection and inversely proportional to the hydraulic conductivity and the effective thickness of the injection aquifer.

Summary and recommendations

The objective of this study was to make recommendations to the Alberta Special Waste Management Corporation regarding the most suitable aquifer for environmentally safe disposal of waste water from treatment processes at their Swan Hills site (13-6-67-8-W5M).

Between the Badheart Formation (Upper Cretaceous) and the Precambrian basement, seven major aquifers or aquifer systems have been identified at the injection site on the basis of the examination and interpretation of stratigraphic and hydrogeological information from 3276 wells, 635 drillstem tests, 3477 core analyses and 645 formation water analyses.

The three uppermost aquifers (Viking, Upper Mannville and Lower Mannville-Rundle) are not suitable for injection because of their relative proximity to ground surface. Disposal should not take place in the Beaverhill Lake aquifer system because of possible contamination of the producing Mitsue and Swan Hills oil fields. The Cambro-Devonian aquifer system should not be considered either because of its potential for exploitation of commercial brines. The two remaining aquifers at the injection site are the Basal Cambrian aquifer (depths between 2843 and 2861 m) and the Wabamun-Winterburn aquifer system (depths between 1647 and 2028 m).

Numerical simulations were conducted to study the long-term effects of injecting 225 m^3/d into both these potential injection aquifers. The hydraulic-head buildup is almost negligible in the Wabamun-Winterburn aquifer system (30 m over an aquifer thickness of 380 m at the injection site). For the much thinner Basal Cambrian aquifer, the hydraulic-head buildup is approximately 300 m.

The recommended injection aquifer was thus the Wabamun-Winterburn aquifer system. Although the numerical simulations were carried out for injection at the base of this aquifer, in practical terms it does not make any difference if the wastes are injected anywhere in the lower half (depths 1800 to 2030 m) of this thick hydrogeological unit.

References

Aggarwal, P.K., R.W. Hull, W.D. Gunter and Y.K. Kharaka (1986): SOLMNEQF: A computer code for geochemical modeling of water-rock interactions in sedimentary basins; *in* Proceedings of Third Canadian/American Conference on Hydrogeology: Hydrogeology of Sedimentary Basins: Application to Exploration and Exploitation (Brian Hitchon, Stefan Bachu and Claude M. Sauveplane, editors), National Water Well Association, Dublin, Ohio, pp.196-203.

Aitken, J.D. (1966): Middle Cambrian to Middle Ordovician cyclic sedimentation, southern Rocky Mountains of Alberta; Bulletin of Canadian Petroleum Geology, v. 14, no. 4, pp. 405-441.

—— (1968): Cambrian sections in the easternmost southern Rocky Mountains and the adjacent subsurface, Alberta; Geological Survey of Canada, Paper 66-23.

Bachu, S., B. Hitchon and P. Mortensen (1986): Preliminary analysis of transport processes in the Basal Cambrian aquifer of south-central Alberta; *in* Proceedings of Third Canadian/American Conference on Hydrogeology: Hydrogeology of Sedimentary Basins: Application to Exploration and Exploitation (Brian Hitchon, Stefan Bachu and Claude M. Sauveplane, editors), National Water Well Association, Dublin, Ohio, pp.118-126.

Bachu, S., C.M. Sauveplane, A.T. Lytviak and B. Hitchon (1987): Analysis of fluid and heat regimes in sedimentary basins; Techniques for use with large data bases; American Association of Petroleum Geologists Bulletin, v. 71, no. 7, pp. 822-843.

Baillie, A.D. (1956): Granite wash in the Clear Hills area; Journal of the Alberta Society of Petroleum Geologists, v. 4, pp. 206-212.

Basin Analysis Group (1985): Hydrogeology of the Cold Lake study area, Alberta Canada; Consultant report prepared for Alberta Environment.

Bear, J. (1972): Dynamics of fluids in porous media; American Elsevier, New York, 764 pp.

Belyea, H.R. (1964): Upper Devonian, Part II – Woodbend, Winterburn and Wabamun Groups; *in* Geological history of western Canada (R.G. McCrossan and P.R. Glaister, editors), pp. 66-88; Calgary; Alberta Society of Petroleum Geologists.

Boethling, F.C. (1976): Viking Formation, Alberta [abstract]; American Association of Petroleum Geologists Bulletin, v. 60, no. 8, p. 1391.

Bredehoeft, J.E. and M.S. Hanshaw (1968): On the maintenance of anomalous fluid pressures: I. Thick sedimentary sequences; Geological Society of America Bulletin, v. 79, pp. 1097-1106.

Burwash, R.A., H. Baadsgaard, Z.E. Peterman and G.H. Hunt (1964): Precambrian; *in* Geological history of western Canada (R.G. McCrossan and R.P. Glaister, editors), pp. 14-19; Calgary; Alberta Society of Petroleum Geologists.

Caldwell, W.G.E. – editor (1975): The Cretaceous System in the Western Interior of North America; Geological Association of Canada, Special Paper 13.

—— (1984): Early Cretaceous transgressions and regressions in the southern Interior plains; *in* The Mesozoic of Middle North America (D.F. Stott and D.J. Glass, editors), Canadian Society of Petroleum Geologists, Memoir 9, pp. 173-203.

Cameron, E.M. (1968): A geochemical profile of the Swan Hills reef; Canadian Journal of Earth Sciences, v. 5, pp. 287-309.

Cant, D.J. (1983): Spirit River Formation – a stratigraphic-diagenetic gas trap in the Deep Basin of Alberta; American Association of Petroleum Geologists Bulletin, v. 67, no. 4, pp. 577-587.

Carrigy, M.A. (1971): Lithostratigraphy of the uppermost Cretaceous (Lance) and Paleocene strata of the Alberta plains; Research Council of Alberta, Bulletin 27.

Davies, P.B. (1987): Modeling areal, variable density, ground-water flow using equivalent head-analysis of potentially significant errors; *in* Proceedings of the NWWA/IGWMC Conference – Solving groundwater problems with models; pp. 888-903, Dublin, Ohio; National Water Well Association.

Davies, G.R. and S.D. Ludlam (1973): Origin of laminated and graded sediments, Middle Devonian of Western Canada; Geological Society of America Bulletin, v. 84, pp. 3527-3546.

De Wiest, R. (1965): Geohydrology; John Wiley and Sons, 366 pp.

Ethier, V.G. (1975): Application of Markov analysis to the Banff Formation (Mississippian), Alberta; Journal of the International Association of Mathematical Geology, v. 7, pp. 47-61.

Exploration Staff, Chevron Standard Limited (1979): The geology, geophysics and significance of the Nisku reef discoveries, West Pembina area, Alberta, Canada; Bulletin of Canadian Petroleum Geology, v. 27, no. 3, pp. 326-359.

Fischbuch, N.R. (1968): Stratigraphy, Devonian Swan Hills reef complexes of central Alberta; Bulletin of Canadian Petroleum Geology, v. 16, no. 4, pp. 444-556.

Frind, E.O. (1980): Seawater intrusion in continuous coastal aquifer-aquitard systems; paper presented at the Third International Conference on Finite

Elements in Water Resources, Univ. Miss. Oxford, May 1980.

Fritz, P. and S.K. Frape – editors (1987): Saline water and gases in crystalline rocks; Geological Association of Canada, Special Paper 33.

Fuller, J.G.C.M. and J.W. Porter (1969): Evaporite formations and petroleum reservoirs in Devonian and Mississippian of Alberta, Saskatchewan and North Dakota; American Association of Petroleum Geologists Bulletin, v. 53, pp. 909-926.

Grayston, L.D., D.F. Sherwin and J.F. Allan (1964): Middle Devonian; *in* Geological history of western Canada (R.G. McCrossan and R.P. Glaister, editors), pp. 49-59; Calgary; Alberta Society of Petroleum Geologists.

Green, R. (1982): Geological map of Alberta; scale 1:1 267 000; Alberta Geological Survey, Alberta Research Council.

Gupta, S.K., C.R. Cole and F.W. Bond (1979): Finite-element three-dimensional groundwater (FE3DGW) flow model formulation, program listings and users' manual; Pacific Northwest Laboratory, Richland, Washington.

Gupta, S.K., C.R. Cole and G.F. Pinder (1984): A finite-element three-dimensional groundwater (FE3DGW) model for a multiaquifer system; Water Resources Research, v. 20, no. 5, pp.553-563.

Hackbarth, D. (1985): Ground water and surface water monitoring program, Alberta Special Waste Management Corporation; *in* Proceedings, Second Canadian/American Conference on Hydrogeology (Brian Hitchon and Mark Trudell, editors), National Water Well Association, Dublin, Ohio, pp. 113-114.

Halbertsma, H.L. (1959): Nomenclature of Upper Carboniferous and Permian strata in the subsurface of the Peace River area; Alberta Society of Petroleum Geologists Journal, v. 7, pp. 109-118.

Hamilton, W.N. (1971): Salt in east-central Alberta; Bulletin 29; Edmonton, Alberta Research Council.

—— (1982): Salt and gypsum in Alberta; Canadian Institute of Mining Bulletin, October, pp. 73-89.

Havard, C. and A. Oldershaw (1976): Early diagenesis in back-reef sedimentary cycles, Snipe Lake reef complex, Alberta; Bulletin of Canadian Petroleum Geology, v. 24, no. 1, pp. 27-69.

Hitchon, B. (1963): Composition and movement of formation fluids in strata above and below the pre-Cretaceous unconformity in relation to the Athabasca oil sands; *in* The K.A. Clark Volume (M.A. Carrigy, editor), pp. 63-74; Information Series 45; Edmonton; Alberta Research Council.

—— (1964): Formation fluids; *in* Geological history of western Canada (R.G. McCrossan and R.P. Glaister, editors) pp. 201-217; Calgary; Alberta Society of Petroleum Geologists.

—— (1969a): Fluid flow in the Western Canada Sedimentary Basin. 1. Effect of topography; Water Resources Research, v. 5, no. 1, pp. 186-195.

—— (1969b): Fluid flow in the Western Canada Sedimentary Basin. 2. Effect of geology; Water Resources Research, v. 5, no. 2, pp. 460-469.

—— (1984a): Geothermal gradients, hydrodynamics, and hydrocarbon occurrences, Alberta, Canada; American Association of Petroleum Geologists Bulletin, v. 68, no. 6, pp. 713-743.

—— (1984b): Formation waters as a source of industrial minerals in Alberta; *in* The Geology of Industrial Minerals in Canada (G.R. Guillet and W. Martin, editors), pp. 247-249; Canadian Institute of Mining and Metallurgy, Special Volume 29.

—— (1985): Graphical and statistical treatment of standard formation water analyses, *in* Proceedings of First Canadian/American Conference on Hydrogeology: Practical Applications of Ground Water Geochemistry (Brian Hitchon and E.I. Wallick, editors), National Water Well Association, Dublin, Ohio, pp. 225-236.

Hitchon, B., G.K. Billings and J.E. Kloven (1971): Geochemistry and origin of formation waters in the western Canada sedimentary basin – III. Factors controlling chemical composition; Geochimica et Cosmochimica Acta, v. 35, no. 6, pp. 567-598.

Hitchon, B. and M.E. Holter (1971): Calcium and magnesium in Alberta brines; Economic Geology Report 1; Edmonton; Alberta Research Council.

Hitchon, B. and H.R. Krouse (1972): Hydrogeochemistry of the surface waters of the Mackenzie River drainage basin, Canada – III. Stable isotopes of oxygen, carbon and sulphur; Geochimica et Cosmochimica Acta, v. 36, pp. 1337-1357.

Hitchon, B., A.A. Levinson and M.K. Horn (1977): Bromide, iodide, and boron in Alberta formation waters; Economic Geology Report 5; Edmonton; Alberta Research Council.

Hitchon, B., C.M. Sauveplane, S. Bachu and A.T. Lytviak (1985): The Swan Hills facility of Alberta Special Waste Management Corporation: evaluation for deep waste disposal; *in* Proceedings, Second Canadian/American Conference on Hydrogeology: Hazardous Wastes in Ground Water: A Soluble Dilemma (Brian Hitchon and Mark Trudell, editors), National Water Well Association, Dublin, Ohio, pp. 115-122.

Jackson, P.C. (1984): Paleogeography of the Lower Cretaceous Mannville Group of Western Canada; *in* Elmworth – Deep Basin gas field (J.A. Masters, editor), American Association of Petroleum Geologists, Memoir 38, pp. 49-77.

James, N.P. (1984): Shallowing-upward sequences in carbonates; *in* Facies Models, 2nd. edition (R.G.

Walker, editor), Geoscience Canada Reprint Series 1, pp. 213-228.

Jansa L.F. and N.R. Fischbuch (1974): Evolution of a Middle and Upper Devonian sequence from a clastic coastal plain-deltaic complex into overlying carbonate reef complexes and banks, Sturgeon-Mitsue area, Alberta; Geological Survey of Canada, Bulletin 234.

Klingspor, A.M. (1969): Middle Devonian Muskeg evaporites of western Canada; American Association of Petroleum Geologists Bulletin, v. 53, pp. 927-948.

Klovan, J.E. (1974): Development of Western Canadian Devonian reefs and comparison with Holocene analogues; American Association of Petroleum Geologists Bulletin, v. 58, no. 5, pp. 787-799.

Koster, E.H. and P.J. Currie (1987): Upper Cretaceous coastal plain sediments at Dinosaur Provincial Park, southeast Alberta; *in* 'Decade of North American Geology' Commemorative Fieldguide Volume, (S.S. Beus, editor), v. 2, pp. 9-14, Rocky Mountain Section, Geological Society of America.

Kramers, J.W. and G.B. Mellon (1972): Upper Cretaceous-Paleocene coal-bearing strata, northwest-central Alberta plains; *in* Proceedings, First Geological Conference on Western Canadian coal (G.B. Mellon, J.W. Kramers and E.J. Siegel, editors), Research Council of Alberta, Information Series No. 60, pp. 109-124.

Lavoie, D.H. (1958): The Peace River Arch during Mississippian and Permo-Pennsylvanian time; Journal of Alberta Society of Petroleum Geologists, v. 6, pp. 69-73.

Lerand, M.M. (1982): Sedimentology of Upper Cretaceous fluviatile, deltaic and shoreline deposits; American Association of Petroleum Geologists Annual Convention, June 1982, Guidebook to Canadian Society of Petroleum Geologists Trip No. 8.

Lusczynsky, N.J. (1961): Head and flow of ground water of variable density; Journal of Geophysical Research, v. 54, no. 12, pp. 4247-4256.

Macauley, G. (1958): Late Paleozoic of Peace River area, Alberta; *in* Jurassic and Carboniferous of western Canada (A.J. Goodman, editor), American Association of Petroleum Geologists, pp. 289-308.

Macauley, G., D.G. Penner, R.M. Procter and W.H. Tisdall (1964): Carboniferous; *in* Geological history of western Canada (R.G. McCrossan and R.P. Glaister, editors), pp. 89-102; Calgary; Alberta Society of Petroleum Geologists.

Macqueen, R.W. and C.A. Sandberg (1970): Stratigraphy, age, and interregional correlation of the Exshaw Formation, Alberta Rocky Mountains; Bulletin of Canadian Petroleum Geology, v. 18, no. 1, pp. 32-66.

Martin, R. (1966): Paleogeomorphology and its application to exploration for oil and gas (with examples from western Canada); American Association of Petroleum Geologists Bulletin, v. 50, pp. 2277-2311.

Masters, J.A. – editor (1984): Elmworth – case study of a deep basin gas field; American Association of Petroleum Geologists, Memoir 38.

McCamis, J.G. and L.S. Griffith (1967): Middle Devonian facies relationships, Zama area, Alberta; Bulletin of Canadian Petroleum Geology, v. 15, no. 4, pp. 434-467.

McCrossan, R.G. and R.P. Glaister – editors (1964): Geological history of western Canada; Calgary; Alberta Society of Petroleum Geologists.

McGugan, A., H.K. Roessingh and W.R. Danner (1964): Permian; *in* Geological history of western Canada (R.G. McCrossan and R.P. Glaister, editors), pp. 103-112; Calgary; Alberta Society of Petroleum Geologists.

Miall, A.D. (1984): Principles of sedimentary basin analysis; New York; Springer Verlag.

Naqvi, I.H. (1972): The Belloy Formation (Permian), Peace River area, northern Alberta and northeastern British Columbia; Bulletin of Canadian Petroleum Geology, v. 20, no. 1, pp. 58-88.

Nelson, S.J., R.P. Glaister and R.G. McCrossan (1964): Introduction; *in* Geological history of western Canada (R.G. McCrossan and R.P. Glaister, editors), pp. 1-13; Calgary; Alberta Society of Petroleum Geologists.

Nurkowski, J.R. and R.A. Rahmani (1984): An Upper Cretaceous fluvio-lacustrine coal-bearing sequence, Red Deer area, Alberta, Canada; *in* Sedimentology of coal and coal-bearing sequences (R.A. Rahmani and R.M. Flores, editors), International Association of Sedimentologists, Special Publication 7, pp. 163-176.

Oliver, T.A. and N.W. Cowper (1965): Depositional environments of Ireton Formation, central Alberta; American Association of Petroleum Geologists Bulletin, v. 49, pp. 1410-1425.

Parrish, J.T., G.C. Gaynor and D.J.P. Swift (1984): Circulation in the Cretaceous Western Interior Seaway of North America, a review; *in* The Mesozoic of Middle North America (D.F. Stott and D.J. Glass, editors), Canadian Society of Petroleum Geologists, Memoir 9, pp. 221-231.

Parsons, W.H. (1973): Alberta; *in* The future petroleum provinces of Canada – their geology and potential (R.G. McCrossan, editor); pp. 73-120; Canadian Society of Petroleum Geologists, Memoir 1.

Porter, J.W., R.A. Price and R.G. McCrossan (1982): The Western Canada Sedimentary Basin; Philosophical Transactions of the Royal Society of London, Series A, v. 305, pp. 169-192.

Price, R.A. (1981): The Cordilleran foreland thrust and fold belt in the southern Canadian Rocky Mountains; *in* Thrust and nappe tectonics (K. McClay and N.J. Price, editors), Geological Society of London, Special Paper 9, pp. 427-448.

—— (1984): Mesozoic geotectonic setting of the Western Canadian Sedimentary Basin [abstract]; *in* The Mesozoic of Middle North America (D.F. Stott and D.J. Glass, editors), Canadian Society of Petroleum Geologists, Memoir 9, pp. 560-561.

Procter, R.M. and G. Macauley (1968): Mississippian of Western Canada and Williston Basin; American Association of Petroleum Geologists Bulletin, v. 52, pp. 1956-1968.

Pugh, D.C. (1973): Subsurface Lower Paleozoic stratigraphy in northern and central Alberta; Geological Survey of Canada, Paper 72-12.

—— (1975): Cambrian stratigraphy from western Alberta to northeastern British Columbia; Geological Survey of Canada, Paper 74-37.

Rahmani, R.A. (1984): Estuaries on mesotidal shorelines of a Late Cretaceous epicontinental seaway, Canadian Western Interior, Alberta; *in* The Mesozoic of Middle North America (D.F. Stott and D.J. Glass, editors), Canadian Society of Petroleum Geologists, Memoir 9, p. 561.

Reeder, S.W., B. Hitchon and A.A. Levinson (1972): Hydrogeochemistry of the surface waters of the Mackenzie River drainage basin, Canada – I. Factors controlling inorganic composition; Geochimica et Cosmochimica Acta, v. 36, pp. 825-865.

Rosenthal, L. and R.G. Walker (1984): Anatomy of a prograding wave and storm dominated delta shoreline complex, the Chungo Sandstone (Milk River–Eagle equivalent) in the southern Alberta Foothills [abstract]; *in* The Mesozoic of Middle North America (D.F. Stott and D.J. Glass, editors), Canadian Society of Petroleum Geologists, Memoir 9, pp. 561-562.

Rottenfusser, B. (1982): Sedimentology and diagenesis of the Gething Formation, Peace River oil sands, northwestern Alberta; CSPG Reservoir, v. 9, no. 11, pp. 2-3.

Rudkin, R.A. (1964): Lower Cretaceous; *in* Geological history of western Canada (R.G. McCrossan and R.P. Glaister, editors), pp. 156-168; Calgary; Alberta Society of Petroleum Geologists.

St. Onge, D.A. and S.H. Richard (1975): Surficial geology – Whitecourt; scale 1:250 000; Map 1367A; Geological Survey of Canada.

Sauveplane, C.M., S. Bachu and B. Hitchon (1986): Comparison of analytical and numerical methods for evaluating cross-formational flow and selecting the preferred injection aquifer, Swan Hills, Alberta, Canada; *in* Proceedings, International Symposium on Subsurface Injection of Liquid Wastes, National Water Well Association, Dublin, Ohio, pp.485-508.

Sheasby, N.M. (1971): Depositional patterns of the Upper Devonian Waterways Formation, Swan Hills area, Alberta; Bulletin of Canadian Petroleum Geology, v. 19, no. 2, pp. 377-404.

Simpson, K.J. (1985): The Alberta system for managing special wastes; *in* Proceedings, Second Canadian/American Conference on Hydrogeology: Hazardous Wastes in Ground Water: A Soluble Dilemma (Brian Hitchon and Mark Trudell, editors), National Water Well Association, Dublin, Ohio, pp. 111-112.

Sloss, L.L. (1963): Sequences in the cratonic interior of North America; Geological Society of America Bulletin, v. 74, pp. 93-113.

Smith, D.G., C.E. Zorn and R.M. Sneider (1984): The paleogeography of the Lower Cretaceous of western Alberta and northeastern British Columbia in and adjacent to the Deep Basin of the Elmworth area; *in* Elmworth – case study of a deep basin gas field (J.A. Masters, editor), American Association of Petroleum Geologists, Memoir 38, pp. 79-114.

Springer, G.D., W.D. MacDonald and M.B.B. Crockford (1964): Jurassic; *in* Geological history of western Canada (R.G. McCrossan and R.P. Glaister, editors), pp. 137-155; Calgary; Alberta Society of Petroleum Geologists.

Stearn, C.W., R.L. Carroll and T.H. Clark (1979): Geological evolution of North America; New York; John Wiley and Sons.

Stoakes, F.A. (1980): Nature and control of shale basin fill and its effect on reef growth and termination: Upper Devonian Duvernay and Ireton Formations of Alberta, Canada; Bulletin of Canadian Petroleum Geology, v. 28, no. 3, pp. 345-410.

Stockwell, C.H. (1969): Tectonic Map of Canada; scale 1:5 000 000; Map 1251A; Geological Survey of Canada.

Stott, D.F. (1983): Late Jurassic – early Cretaceous foredeeps of northeastern British Columbia; Transactions of the Royal Society of Canada, Series IV, v. 21, pp. 143-153.

—— (1984): Cretaceous sequences of the Foothills of Canadian Rocky Mountains; *in* The Mesozoic of Middle North America (D.F. Stott and D.J. Glass, editors), Canadian Society of Petroleum Geologists, Memoir 9, pp. 85-107.

Stott, D.F. and D.J. Glass - editors (1984): The Mesozoic of Middle North America; Canadian Society of Petroleum Geologists, Memoir 9.

Tokarsky, O. (1977): Hydrogeology of the Whitecourt area, Alberta; Report 76-3; Edmonton; Alberta Research Council.

van Hees, H. (1958): The Meadow Lake Escarpment – its regional significance to Lower Paleozoic strati-

graphy; Saskatchewan Geological Society and North Dakota Geological Society, 2nd International Williston Basin Symposium, pp. 70-78.

—— (1959): Middle Cambrian of the southern Alberta plains; 9th Annual Field Conference Guidebook, Alberta Society of Petroleum Geologists, pp.73-85.

van Hees, H. and F.K. North (1964): Cambrian; *in* Geological history of western Canada (R.G. McCrossan and R.P. Glaister, editors), pp. 20-33; Calgary; Alberta Society of Petroleum Geologists.

Vogwill, R.I.J. (1978): Hydrogeology of the Lesser Slave Lake area, Alberta; Report 77-1; Edmonton; Alberta Research Council.

Vonhof, J.A. (1965): The Oligocene Cypress Hills Formation and its reworked deposits in southwestern Saskatchewan; Alberta Society of Petroleum Geologists, 15th Annual Guidebook Part 1, Cypress Hills Plateau, pp. 142-161.

Walker, R.G. – editor (1982): Clastic units of the Front Ranges, Foothills and Plains in the area between Field, B.C. and Drumheller, Alberta; 11th Congress of International Association of Sedimentologists, August 1982, Guidebook to Excursion 21A.

—— – editor (1984): Facies models (2nd. edition); Geoscience Canada, Reprint Series 1.

Williams, G.D. and C.R. Stelck (1975): Speculations on the Upper Cretaceous paleogeography of North America; *in* The Cretaceous System in the Western Interior of North America (W.G.E. Caldwell, editor), Geological Association of Canada, Special Paper 13, pp. 1-20.

Yakowitz, S. and L. Duckstein (1980): Instability in aquifer identification: theory and case studies; Water Resources Research, v. 16, no. 6, pp. 1045-1064.

Appendix A. Results of tests at the injection well (CSL Ethel 13-6-67-8-W5M).

Subsequent to the completion of the work cited in this bulletin, a well (CSL Ethel 13-6-67-8-W5M) was drilled at the site of the special waste treatment plant of the Alberta Special Waste Management Corporation, completed in the lower part of the Nisku aquifer, and prepared for injection.

Geophysical well logs

Figure A1 shows selected geophysical well logs from the injection well, together with the location of drillstem tests and cores, and generalized stratigraphy. With the exception of the top of the Exshaw-Lower Banff aquitard, predicted depths based on extrapolated stratigraphic surfaces through the injection site are generally less than 1% in error from the actual depth; a 6.9% error for the Exshaw-Lower Banff aquitard most probably arose due to lateral discontinuity of the carbonate succession in the Banff Formation shale.

The aquitard overlying the Wabamun-Winterburn aquifer system is 127.5 m thick, but contains within it a carbonate bed 12.5 m thick (1604.0 to 1616.5 m), leaving 34.5 m of continuous aquitard above the Wabamun-Winterburn aquifer system. The authors do not believe this thin carbonate will practically affect the sealing properties of the overlying aquitard, bearing in mind the hydraulic capacity of the injection aquifer and the fact that even the shallowest zone recommended for perforation is more than 175 m below the base of the overlying aquitard.

Only about 16 m of the underlying Ireton aquitard was penetrated, but it is known to be about 330 m thick at the injection site. The well logs indicate that the underlying aquitard is a 'purer' shale, compared to the overlying aquitard, and therefore probably has a lower permeability, as predicted in our evaluation and as used in the numerical simulation.

The Wabamun-Winterburn aquifer system contains three zones of generally higher permeability; the lower two were recommended for perforation. The upper zone (approximately 1743 to 1787 m) is divided into three potential perforation zones, and was neither cored nor tested and could probably be considered as a backup injection zone in the future, if necessary. The two recommended perforation zones are near the base of the Wabamun Group and in the post-Nisku portion of the Winterburn Group. The Nisku Formation was generally less permeable than the recommended perforation zones. The position of the simulated injection in the numerical model was placed at the base of the Wabamun-Winterburn aquifer system (that is, in the Nisku Formation) but there was no reason for re-running the model using the recommended perforation zones.

Drillstem tests

Seven drillstem tests were run in the injection well, the results of which are summarized in table A1. The two successful drillstem tests in the Wabamun aquifer correspond approximately to the upper zone recommended for perforation, and the drillstem test in the Nisku aquifer to the lower zone recommended for perforation. Two drillstem tests run in the Banff carbonate aquifer and the Gething Formation (Lower Mannville aquifer) were not interpreted because they recovered only drilling mud. For the Wabamun-Winterburn aquifer system, the bulk value of permeability as obtained from the regional evaluation of the drillstem test data was $7.3 \times 10^{-15} m^2$. The weighted average permeability (with respect to formation thicknesses) of the three drillstem test results at the injection well is $2.9 \times 10^{-14} m^2$, which is about four times the regional estimate. Similarly, for the hydraulic conductivity the

Table A1. Summary of drillstem tests at CSL Ethel 13-6-67-8-W5M.

Drillstem test	1	2	3	4	5	6	7
Stratigraphic unit	Nisku Fm.	Wabamun Gp.	Wabamun Gp.	Wabamun Gp.	Wabamun Gp.	Banff Fm.	Gething Fm.
Depths (m)	1925-1945	1853-1873	1853-1873	1853-1873	1830-1853	1498-1526	1435.5-1450
Recovery	640 m gassy sw no GTS	Misrun	Misrun	684 m gassy sulf sw, no GTS	796 m muddy H_2S cut sw, no GTS	15 m mud no GTS	110 m watery mud no GTS
Samples	Formation water (table A3)			Formation water (table A3)	Formation water (table A3)	–	–
Permeability ($x10^{-14}$ m^2)	4.9			1.8	2.7		
Hydraulic conductivity ($x10^{-2}$ m/d)	8.0			2.4	3.6		
Fresh water hydraulic head (m)	509			473	468		

sw = salt water, sulf = sulfurous, GTS = gas to surface

Appendix A. (continued)

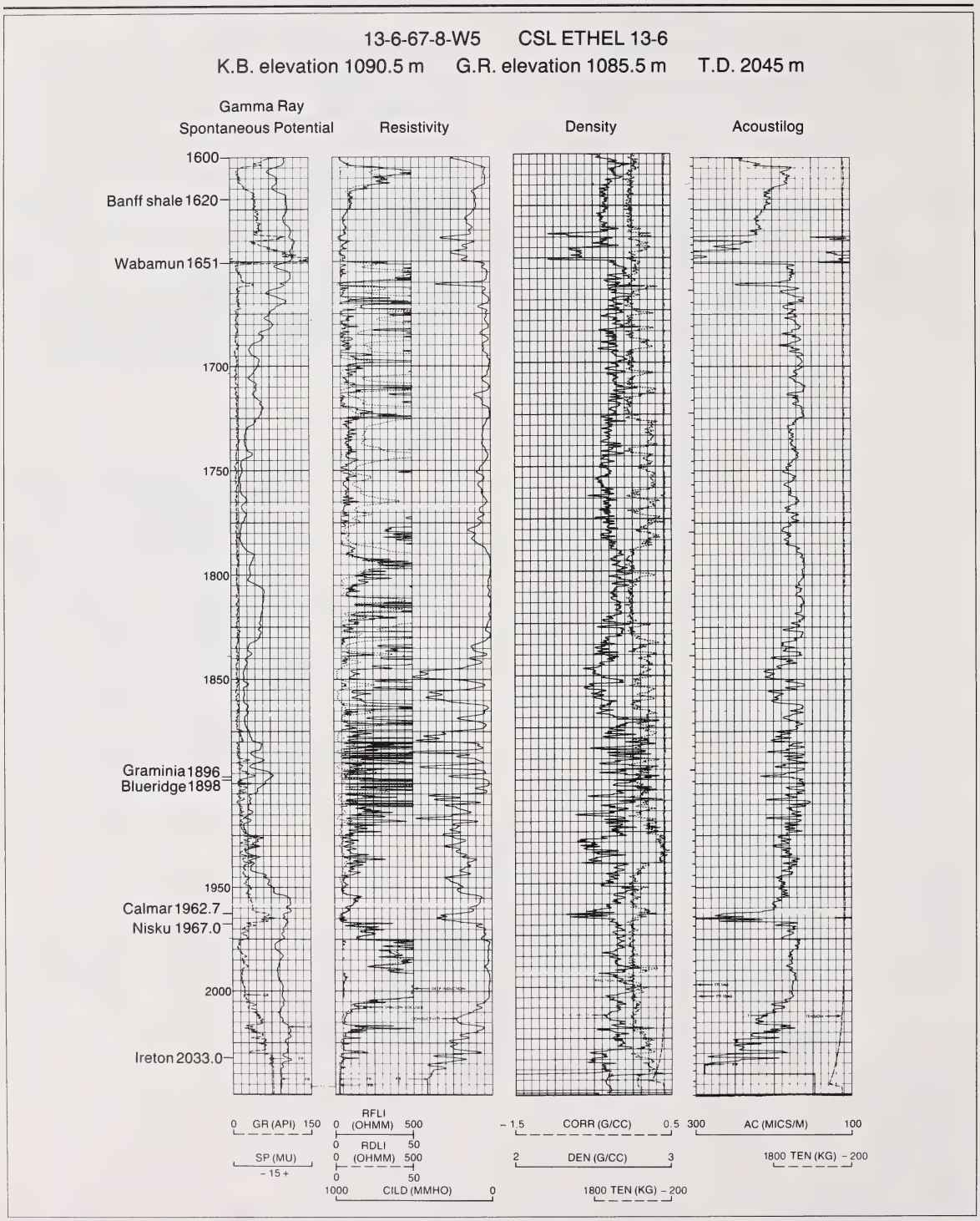

Figure A1. Geophysical well logs at CSL Ethel 13-6-67-8-W5M.

Appendix A. (continued)

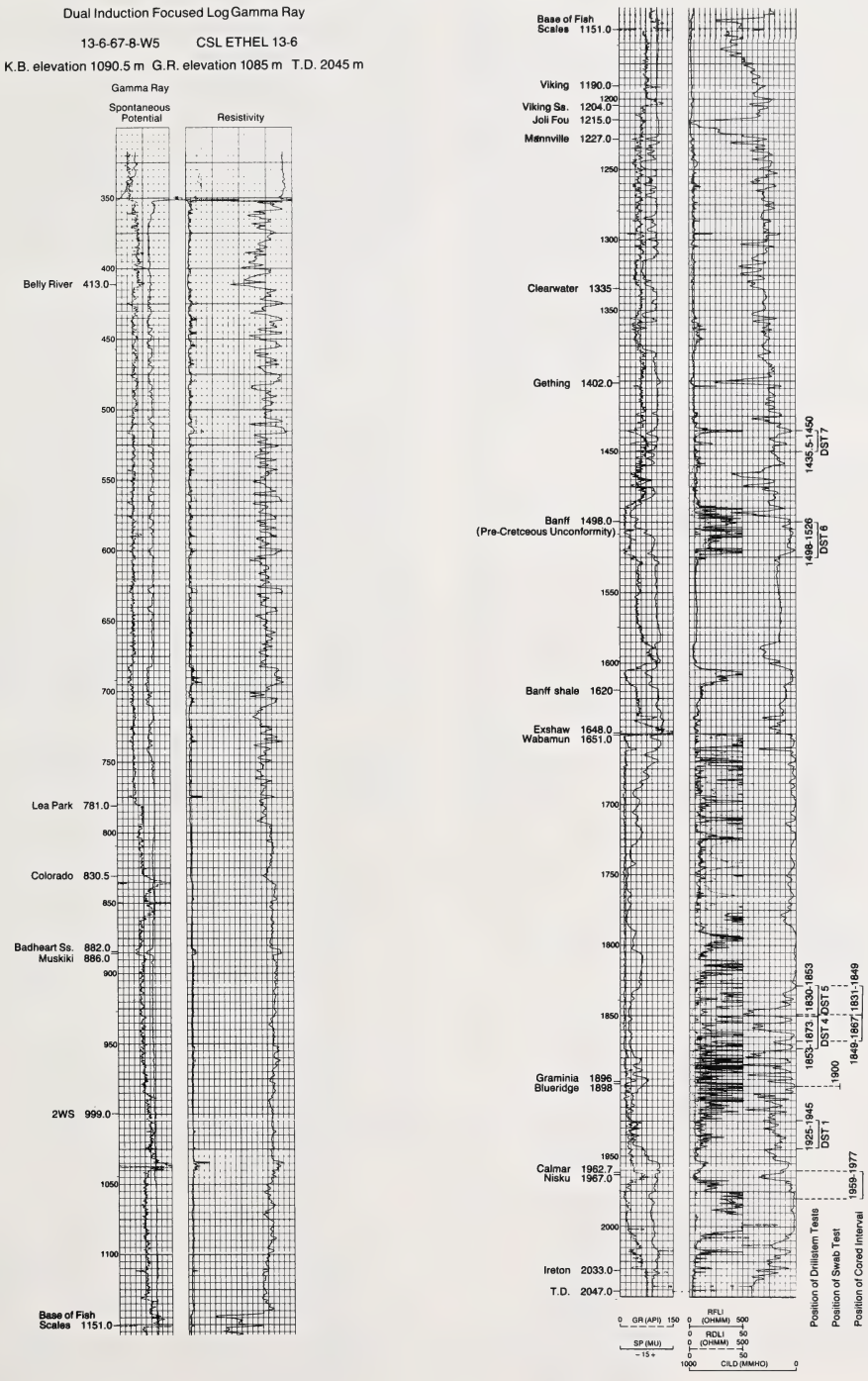

Figure A1. (continued)

Appendix A. (continued)

regional bulk value for the aquifer was $9.9x10^{-3}$ m/d; the corresponding value at the injection well is 4.3 x 10^{-2} m/d, which is 4.3 times higher than the regional value. The comparison between regional and observed values is also instructive when one considers the hydraulic diffusivity (ratio of hydraulic conductivity to specific storage). The regional bulk diffusivity based on drillstem test and core results was 46.9 m^2/d; the value at the injection well is 90.6 m^2/d, which means that the injection capacity of the aquifer is 1.9 times higher than estimated. For the specific storage, the ratio between observed and regional values is 1.6 (the observed value is $3x10^{-4}$ m^{-1}). For hydraulic heads, the prediction is accurate enough; the measured value is about 483 m; the regional grid value at the site was 460 m which shows an error of about 5%.

Core analyses

Three cores were taken in the Wabamun-Winterburn aquifer and the results are reported in table A2. These results show, first, that the length analyzed is only 40%, 32.7% and 6.3% of three cored intervals, respectively; thus, even if the same intervals had been sampled in both drillstem testing and coring, one should not expect the same results; drillstem test results should be more representative. However, for the cored portion of the Wabamun Group (1831 to 1867 m), the average (weighted) hydraulic conductivity from core analyses is $1.2x10^{-2}$ m/d, which should be compared to the value of $3.1x10^{-2}$ m/d obtained by drillstem testing a similar interval (1830 to 1873 m). The former hydraulic conductivity certainly compares very well with the regional core hydraulic conductivity of $1.6x10^{-2}$ m/d estimated for the Wabamun Group. From core analyses, the result for hydraulic diffusivity in the tested Wabamun Group is 28.5 m^2/d, which is very close to the regional value of 28.2 m^2/d.

If one accepts the drillstem test results as more representative than the core results, the value obtained earlier for regional hydraulic conductivity ($4.25 x10^{-2}$ m/d) should then be compared to the value obtained following the mass balance calculations in the numerical simulation. With a value of $1.5x10^{-2}$ m/d for horizontal hydraulic conductivity, it was shown that the steady-state hydraulic head buildup around the well does not exceed 30 m when injecting 225 m^3/d in the Wabamun-Winterburn aquifer system. Admitting that the real thickness of this aquifer at the injection site has been reduced from a predicted 380 m to 316 m (the Nisku Formation is 'tight', as shown from the core results) and that the buildup is roughly inversely proportional to the aquifer thickness and to its hydraulic conductivity, a gross estimate of the hydraulic head buildup can be made without performing any additional numerical simulation of the effects of injection. The result is about 15 m of hydraulic head buildup predicted in the Wabamun-Winterburn aquifer system around the injection site at the end of the transient period.

Formation water analyses

The three drillstem tests in the Wabamun-Winterburn aquifer system effectively recovered only formation water or (in the shallowest test) muddy formation water (table A3). In each test the most representative analysis was that obtained from the downhole sampler. The two contiguous drillstem tests in the Wabamun aquifer yielded formation waters about 20 to 25% more saline than the regional average, but this observation has to be tempered with the fact that there were no data points within four townships of the injection site. These two analyses appear to be internally consistent on first appraisal, inasmuch as all components except HCO_3 show an increase with depth.

With respect to the drillstem test in the Nisku aquifer, the following remarks must be prefaced with the observation that the regional maps of formation water composition show numerous unexplained anomalies. The salinity of the formation water at the injection site is closer to that in a well one township to the south of the site than it is to that in a well about one township to the northwest of the site. As a general observation, salinity increases with depth and it seems likely that the analysis from the injection site (201 000 mg/L TDS) and the well to the south (185 000 mg/L TDS) are representative of the regional pattern in the Nisku aquifer around the site, rather than the 60 000 mg/L TDS in the well to the northwest.

Table A2. Summary of core results at CSL Ethel 13-6-67-8-W5M.

Core	1	2	3
Stratigraphic unit	Nisku Fm.	Wabamun Gp.	Wabamun Gp.
Cored interval (m)	1959-1977	1849-1867	1831-1849
Length analyzed (m)	1.14	5.88	7.18
Effective permeability (m^2)	$8.7x10^{-18}$ ($5.8x10^{-15}$)	$1.4x10^{-14}$ ($1.9x10^{-14}$)	$5.3x10^{-15}$ ($1.9x10^{-14}$)
Hydraulic conductivity (m/d)	$6.8x10^{-5}$ ($4.4x10^{-3}$)	$1.9x10^{-2}$ ($1.6x10^{-2}$)	$7.1x10^{-13}$ ($1.6x10^{-2}$)
Anisotropy	4.6 (11.8)	2.3 (14.6)	4.3 (14.6)
Porosity (%)	0.9 (6.3)	9.2 (18.9)	8.1 (18.9)

Data in parentheses are regional values from table 6

Appendix A. (continued)

Swab test: formation water result

A swab test was carried out on the injection zone and the results of the analysis of representative formation water from the injection aquifer are given in table A4. Before swabbing began, 5 m^2 of freshwater mixed with an oxygen scavenger and biocide (bacteria inhibitor) was pumped downhole. To ensure that a representative sample of the formation water was obtained, a sample was taken from each swab. The pH, conductivity, Cl concentration and temperature were monitored. Sample collection began after the third swab. The results are plotted in figure A2. The time plotted in figure A2 is from the first sample taken. The fluctuation in temperature was due to a delay in analyzing the sample. Once the monitored condition stabilized, two 4-L samples were taken. The sampling point was at a tee just off the casing and the first sample was taken near the end of the 18th swab when the pressure had decreased enough to obtain the sample without excessive foaming. The second sample (the analysis reported in table A4) was taken at the beginning of the 19th swab. More foam appeared in this sample. The following analyses were performed in the field: pH, conductivity, alkalinity titration, total NH_3, total CO_2, total $S^=$ and dissolved oxygen. The technique used for the swabbing procedure may have resulted in depletion of the dissolved gases (NH_3, CO_2 and H_2S).

For the record, chemicals used during the drilling were bentonite, caustic soda, soda ash, lime, $CaCl_2$, DF-19, CMC, Peltex, TF-EX, sawdust, Kwik Seal, SAAP, Separan, feed grit, and lignite (from Technifluids, Calgary).

The results of the SOLMNEQF calculations are presented in table A5. The adjusted pH at reservoir temperature is 6.25, and the analyzed cations and anions balance to within 3.1%. Calculated total dissolved solids are 186 788 mg/L, slightly lower than that reported for the drillstem test results (table A3). Foaming was reported during field sampling, with possible loss of CO_2, and therefore the slight undersaturation with respect to calcite and dolomite may well be an artifact of the sampling problems rather than real undersaturation in a carbonate reservoir. Quartz is at saturation, but the end members of olivine, pyroxenes and amphiboles are all undersaturated, as expected. The absence of a determination for Al precludes calculation of the saturation indices for feldspars and clay minerals. Pyrite shows strong undersaturation.

In the absence of information on the composition of the injected water it was not possible to calculate the effects of mixing on the solution/precipitation of minerals in the injection aquifer. However, the Special Waste Injection Site has been designed so that the treated process liquids are injected deep underground and there is no surface discharge from the facility (Simpson 1985). Because much of the injected water will likely be surface runoff it is possible to determine probable solution/precipitation reactions using information on the mineralogy of the injection aquifer (table A6) and the composition of river water in the

Table A3. Chemical composition (mg/L), physical properties and production data for formation waters at CSL Ethel 13-6-67-8-W5M.

Stratigraphic unit	Nisku Fm.	Wabamun Gp.	Wabamun Gp.
Depth (m)	1925-1945	1853-1873	1830-1853
Source	DST 1	DST 4	DST 5
Recovery	640 m gassy sw	684 m gassy sulf sw	796 m muddy H_2S cut sw
Na	57800	42400	39200
K	880	1030	990
Ca	12200	9800	9600
Mg	2570	2280	2140
Cl	127000	94400	88800
HCO_3	129	257	338
CO_3	<1	<1	<1
SO_4	788	950	119
Fe	6	5.6	34
TDS (ignition)	188030	147210	138440
TDS (calc.)	201307	150992	141049
pH (laboratory) (25°C)	6.6	6.8	6.7
Density (25°C)	1.170	1.123	1.114
Refractive index (25°C)	1.369	1.360	1.357
Resistivity (ohm m, 25°C)	0.051	0.060	0.078

sw = salt water, sulf = sulfurous

Appendix A. (continued)

Swan Hills study area; the nearest complete river water analysis available in published literature is given in table A7.

The chemical effects of waste water injection were investigated using the program SOLMINEQ.87, an updated version of SOLMNEQF. As noted previously, the formation water analysis from the swab test showed low total organic carbon, resulting in slight undersaturation of calcite. The extremely rapid dissolution/precipitation kinetics for calcite make it a very safe assumption that calcite is at equilibrium with the formation water in the reservoir, bearing in mind that calcite comprises about half the formation mineralogy (table A6). Accordingly, a modified formation water analysis was calculated with calcite at equilibrium. Values for dissolved Al were not available for either the swab test formation water (table A4) or the river water sample (table A7). Although a value for Al could be calculated for the formation water, assuming equilibrium with the clay minerals (illite, kaolinite, chlorite or smectite) present in the formation, this was not done because nothing was known about Al-bearing minerals associated with the river water. The value calculated for the formation water would be an equilibrium value so when the formation water was mixed with the river water the amount of Al in solution would decrease. This decrease would be reflected in the saturation indices of the Al-bearing minerals, which

Table A4. Chemical composition, physical properties and production data for formation water produced during a swab test in the injection aquifer (basal Nisku Formation) at CSL Ethel 13-6-67-8-W5M.

Depth (m)	1900	
Source	Swab test	
Well status	Injection well	
Field Analysis		
pH		6.52
Alkalinity		
(ppm HCO_3)		189.5
(ppm $CaCO_3$)		155.2
H_2S	ISE (mg/L)	0.18
NH_3	ISE (mg/L)	76
Total CO_2	ISE (mg/L)	101
Dissolved O_2	(mg/L)	0.8
Conductivity	(mmhos/cm)	172
Laboratory Analysis		
	Analytical Method	
Li	ICP (mg/L)	17
Na	ICP (mg/L)	58000
K	ICP (mg/L)	770
Mg	ICP (mg/L)	1990
Ca	ICP (mg/L)	11400
Sr	ICP (mg/L)	370
Ba	ICP (mg/L)	0.2
Cu	ICP (mg/L)	<100
Zn	ICP (mg/L)	<300
Pb	ICP (mg/L)	<2000
Fe	ICP (mg/L)	12
Mn	ICP (mg/L)	<0.1
Al	ICP (mg/L)	<0.6
H_2AsO_3	AA (as As) (µg/L)	2.5
H_3BO_3	ICP (mg/L)	160.1
PO_4	ICP (as P) (mg/L)	18.4
NH_3	FIA (mg/L)	103
SiO_2	ICP (mg/L)	27.8
Cl	IC (mg/L)	113000
SO_4	IC (mg/L)	745
HCO_3	TIC (mg/L)	50.1
CO_3	TIC (mg/L)	<0.01
Total dissolved solids (calc.)		184881
TIC	(mg/L)	16.5
TOC	(mg/L)	64.7
TC	(mg/L)	81.2
pH		6.76

Trace Elements (mg/L)

Cd	ICP	<100
Cs	AA	<100
Cr	ICP	<300
CN	APP	213
Hg	AA	<20
Ni	ICP	<300
Se	ICP	<400
Ti	ICP	200
V	ICP	<300

Aromatic Hydrocarbons (mg/kg) (headspace)

Benzene	<10
Toluene	<10

Stable Isotopes

$\delta^{18}O$ (‰ SMOW)	0.00
δD (‰ SMOW)	-47.6

AA = atomic absorption, APP = automated pyridine pyrozolone, FIA = flow injection analysis, IC = ion chromatography, ICP = inductively coupled plasma, ISE = ion selective electrode, TC = total carbon, TIC = total inorganic carbon, TOC = total organic carbon
Analyst: Bernice Young (Oil Sands and Hydrocarbon Recovery Department, Alberta Research Council)

Appendix A. (continued)

would also decrease as the proportion of river water increased.

The effects of mixing the formation water and the river water on the permeability/porosity of the injection aquifer can be indicated by examining changes in the saturation indices of all possible minerals which can form from these mixtures. If the saturation index (SI) is positive the mineral has a potential for precipitation; if negative, the mineral has a potential for dissolution.

At reservoir temperature and pressure the river water is supersaturated with respect to calcite, dolomite and, to a very minor degree, magnesite. When mixed with up to 25% of the formation water the SI values of these carbonates increase, with calcite reaching an SI of 0.53. Mixing with more than 25% of the formation water results in decreasing SI values for these carbonate minerals. Due to the extremely rapid rate of calcite kinetics and the presence of calcite in the reservoir, the initial supersaturation will result in precipitation of calcite in the injection aquifer. Although calcite will precipitate quickly, the amount will be small; expected volumes range from 0.00025 cc/L of river water to a maximum of 0.00079 cc/L of river water.

In the formation water, at reservoir conditions, quartz is supersaturated due to the presence of clay minerals and K-feldspar, and this supersaturation is maintained because of the extremely slow kinetics of quartz precipitation. Cristobalite shows a minor degree of supersaturation, but no other silica minerals are supersaturated. Mixtures with less than 25% river water result in decreased supersaturation and quartz precipitation is not expected.

Table A5. Results of SOLMNEQF calculations on formation water (table A4) produced during a swab test in the injection aquifer (basal Nisku Formation) at CSL Ethel 13-6-67-8-W5M.

Cations (anal., meq/L)	3044.3
Anions (anal., meq/L)	2952.0
Cations/Anions	1.031
Cations (calc., meq/L)	2973.1
Anions (calc., meq/L)	2882.6
Total solids (calc., mg/L)	186788
pH (calc., reservoir temperature)	6.25 (65°C)
Density (calc., reservoir temperature)	1.1370
Saturation Indices (ΔG_{diff})	
Calcite	-0.166
Dolomite	-0.334
Halite	-1.738
Anhydrite	-0.455
Barite	-1.421
Celestite	-0.595
Siderite	-1.924
Quartz	0.631
Apatite (chlor)	41.848
Diopside	-1.479
Enstatite	-3.015
Fayalite	-5.352
Forsterite	-9.552
Pyrite	-70.734
Tremolite	8.349

It is concluded that modification of the permeability/porosity of the reservoir will be small due to mineral precipitation and should not have a significant effect over the time span of injection. It would be prudent, however, to carry out similar calculations once the composition of the actual injection water is known.

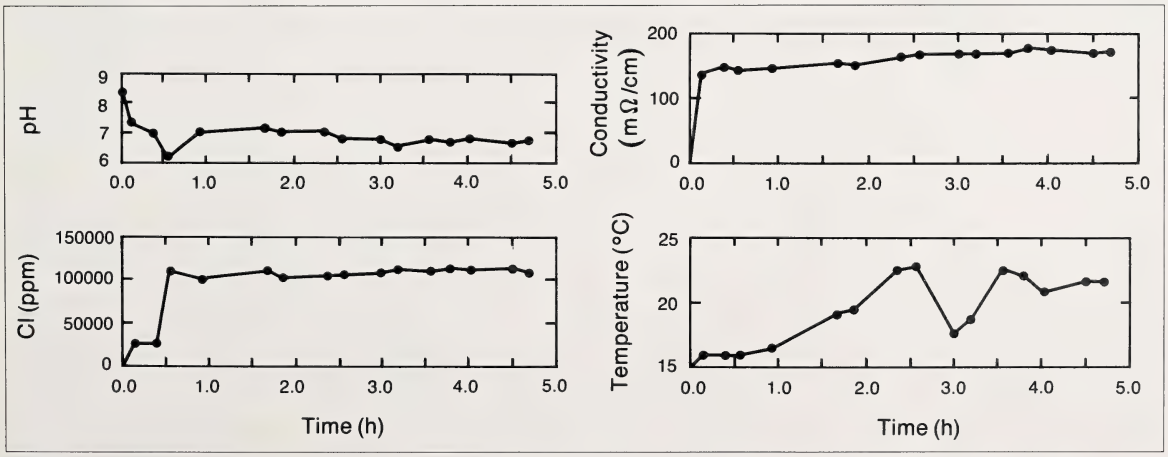

Figure A2. Variations of pH, Cl, conductivity and temperature with time during the swab test at CSL Ethel 13-6-67-8-W5M.

Appendix A. (continued)

Table A6. Normalized X-ray diffraction peak heights for core samples from the Nisku Formation at CSL Ethel 13-6-67-8-W5M.

Depth (m)	Calcite	Dolomite	Quartz	Illite± Illite/Smectite	Kaolinite	Chlorite	Swelling Clay (Smectite)	K-feldspar
1963.5	37	18	37	4	2			2
1968.2	48	38	10	1	1		1	1
1971.0	59	31	8	1		<1		1

Table A7. Composition of the Athabasca River at Whitecourt (14-34-59-12-W5M) used to simulate mixing reactions in the injection aquifer at CSL Ethel 13-6-67-8-W5M

Field Analysis				
pH		8.2		
Temperature (°C)		8.3		
Conductivity (mmhos/cm)		261.6		
Laboratory Analysis				
Li	(µg/L)		Trace Elements	
Na	(mg/L)	4.5		
K	(mg/L)	0.5	Ni (µg/L)	<2
Mg	(mg/L)	10.8	U (µg/L)	0.5
Ca	(mg/L)	43.1		
Sr	(mg/L)	0.34		
Cu	(µg/L)		Stable Isotopes	
Zn	(µg/L)	<1		
Fe	(mg/L)	0.07	$\delta^{18}O$ (‰ SMOW) (water)	-18.0
Mn	(µg/L)	<1	$\delta^{34}S$ (% meteorite troilite) (SO_4)	+11.8
H_3BO_3	(µg/L)	80		
PO_4	(ortho., fltd., mg/L)	<0.01		
PO_4	(Σ inorg., fltd., mg/L)	<0.01		
PO_4	(Σ, unfltd., mg/L)	0.04	Other Properties	
SiO_2	(mg/L)	3.7		
F	(mg/L)	0.11	Colour	20
Cl	(mg/L)	3.1	Turbidity	4.8
SO_4	(mg/L)	35.9	Suspended matter (mg/L)	1.4
HCO_3	(mg/L)	144		
NO_3	(mg/L)	0.19		
TOC	(mg/L)	<2		

From Reeder et al. (1972, table 3, M-67), Hitchon and Krouse, (1972, table 1, M-67).

Appendix B. Chemical composition, physical properties and production data for formation waters from the Swan Hills study area.

It is important in studies of water-rock interaction and diagenesis, that detailed analyses of both formation waters and the rock matrix be carried out. Modelling, using computer codes such as SOLMNEQF (Aggarwal et al. 1986), requires this information. All formation water analyses used in the regional evaluation of the hydrogeology of the Swan Hills study area originated from the files of the ERCB. The limitations of these analyses are described in Hitchon (1985) and the methods of data processing in Bachu et al. (1987). None of these analyses is suitable for water-rock interaction studies for a variety of reasons.

In the early 1970s, samples of about one thousand formation waters were collected across Alberta through a cooperative program with the ERCB. All were from drillstem tests of then currently drilled wells, and the produced formation waters were subsampled for the Alberta Research Council. In addition to selected major element determinations by the ERCB, the samples were sent to the Alberta Research Council, filtered and preserved, and selected minor and trace elements determined by a variety of techniques, including AA and ICP. Bearing in mind the vicissitudes of drillstem tests, and the need for appropriate field procedures if reliable formation water composition is to be achieved, it is believed that the analyses resulting from the cooperative program with the ERCB are reasonably representative of in situ formation water composition; certainly they are more representative than conventional standard analyses, but not so representative as if sampled and preserved in the field. With this caveat in mind, the analysis file from the cooperative program was searched for data from the Swan Hills study area and these analyses are given in tables B1 to B6; in addition, table B1 contains a previously published analysis (W-F, Hitchon et al. 1971) and an analysis of formation water (D-41) from the Beaverhill Lake B Pool at the Carson Creek North Field in which the sample was filtered and preserved in the field. All analyses in tables B1 to B6 were evaluated using the computer code SOLMNEQF (Aggarwal et al. 1986) and the results are reported in the sections of this bulletin dealing with their respective aquifers. It was beyond the scope of this study to determine the detailed mineralogy of the individual aquifers. Therefore, comments on the mineralogical composition relevant to these formation water analyses were obtained from the literature, as appropriate. Table B7 contains additional trace element data for the samples reported in tables B1 to B6.

Appendix B. (continued)

Table B1. Chemical composition (mg/L), physical properties and production data for formation waters from the Beaverhill Lake aquifer.

Sample Number	D-41	W-F+	RCAH 22-1274B	RCAH 7-676A	RCAH 37-175B	RCAH 4-175A
Location	16-5-62-12-W5M	12-28-63-11-W5M	10-33-64-12-W5M	2-6-65-12-W5M	12-23-67-11-W5M	10-32-67-11-W5M
Depth (m)	2654.2-2659.1	2776.1-2778.8	2696.3-2731.0	2756.9-2769.1	2677.7-2692.9	2628.9-2700.5
Source	Separator (flowing)	Wellhead (tubing)	DST 1	DST 1	DST 1	DST 3
Recovery	–	–	1935 m gsy sw 310 m gsy mud GTS 255 m^3/d	1074 m sw 437 m oil 9 m mc oil gas TSTM	73 m gc sw 113 m gc oil 55 m gc/oc mud gas TSTM	1070 m sw 110 m msw 762 m wc
Well status	Oil well	Oil well	Abandoned	Oil well	Abandoned	Abandoned
Li	19	26.4	82	39	27	83
Na	28700	65000	58800	72000	58500	57400
K	456	1560	5370	1890	754	4610
Mg	186	607	3000	400	656	2000
Ca	1880	4690	17700	2990	4240	24300
Sr	59	232	683	137	191	524
Ba	0.3	–	3.6	1.1	1	2.7
Cu	0.2	0.13	*	*	*	0.6
Ag	0.5	–	*	*	1.1	1.4
Zn	*	0.06	3.5	*	1.5	3.5
Pb	1.5	–	63	1	4.4	27
Fe	2	42	1.6	*	*	1
Mn	0.1	0.13	12	1.8	1.2	20
Al	*	–	*	*	*	*
H_2AsO_3	*	–	*	*	*	*
H_3BO_3	223	703	850	758	422	528
PO_4	9	–	42	*	12	39
NH_3	101	–	281	424	191	181
SiO_2	36	–	15	4.6	14	14
F	–	–	2.6	3.1	4.2	4.3
Cl	46600	113000	135800	117700	102000	136600
Br	116	291	449	322	242	388
I	12	28	13	41	27	7
SO_4	1660	914	470	1390	774	706
HCO_3	298	218	109	225	146	95
Total solids (calc.)	80392	187112	223499	198227	168040	227348
Total solids (110°C)	83300	191800	250600	205500	172400	260100
Total solids (ignition)	78600	183900	214200	191700	167600	220800
Cations (anal., meq/L)	1303.0	2883.9	3532.4	3072.7	2642.5	3685.9
Anions (anal., meq/L)	1268.3	2924.7	3503.0	3018.3	2682.8	3524.9
Cations (calc., meq/L)	1279.2	2774.8	3403.8	2963.9	2563.9	3553.8
Anions (calc., meq/L)	1249.5	2819.2	3378.8	2913.1	2606.4	3398.0
pH (laboratory)	7.50	6.90	6.47	7.30	6.2	6.53
pH (calc., reservoir temp.)	6.77 (87.8°C)	6.43 (96.0°C)	6.04 (91.1°C)	6.59 (81.0°C)	5.91 (79.5°C)	6.09 (93.3°C)
Density (15.56°C)	1.0543	1.1238	1.1495	1.1333	1.116	1.1564
Refractive index (25°C)	1.3509	1.3616	1.3688	1.3641	1.3608	1.3707
Resistivity (ohm m, 25°C)	–	0.062	–	–	0.069	–

– = not determined, * = below detection, + from Hitchon et al. (1971)

Appendix B. (continued)

Table B2. Chemical composition (mg/L), physical properties and production data for formation waters from the Wabamun-Winterburn aquifer system.

Sample number	RCAH 111-274	RCAH 69-576A
Stratigraphic unit	Winterburn Gp. Blueridge Fm.	Wabamun Gp.
Location	2-30-63-4-W5M	6-8-63-2-W5M
Depth (m)	1316.7-1325.3	1038.1-1060.7
Source	DST 2	DST 3
Recovery	975 m sw	640 m sul sw 61 m mud
Well status	Abandoned	Abandoned
Li	30	23
Na	32000	26400
K	1010	411
Mg	1390	819
Ca	6850	3050
Sr	159	218
Ba	2.8	0.6
Cu	*	0.2
Ag	1.1	0.5
Zn	*	7.3
Pb	3.1	1.4
Fe	1.6	0.5
Mn	1.3	5.6
Al	*	0.03
H_2AsO_3	*	2.4
H_3BO_3	214	163
PO_4	25	5.6
NH_3	114	99
SiO_2	22	8
F	–	2.2
Cl	63300	53500
Br	192	177
I	14	14
SO_4	698	27
HCO_3	482	635
Total solids (calc.)	106448	85362
Total solids (110°C)	118700	89500
Total solids (ignition)	99000	85300
Cations (anal., meq/L)	1794.6	1318.1
Anions (anal., meq/L)	1711.7	1459.3
Cations (calc., meq/L)	1728.2	1312.2
Anions (calc., meq/L)	1645.3	1453.4
pH (laboratory)	7.8	7.2
pH (calc., reservoir temp.)	7.57 (40.7°C)	7.08 (35.0°C)
Density (15.56°C)	1.078	1.060
Refractive index (25°C)	1.3520	1.3472
Resistivity (ohm m, 25°C)	0.072	0.092

– = not determined, * = below detection

Table B3. Chemical composition (mg/L), physical properties and production data for formation waters from the Upper Banff and Pekisko aquifers.

Sample number	RCAH 32-376A	RCAH 195-174
Stratigraphic unit	Banff Fm.	Pekisko Fm.
Location	10-22-68-8-W5M	7-16-62-10-W5M
Depth (m)	1417.6-1448.1	1526.4-1542.9
Source	DST 1	DST 5
Recovery	829 m sw	152 m gc sl sulf sw 27 m sl gc wc mud 15 m mud
Well status	Abandoned	Abandoned
Li	3.7	7.7
Na	3970	10600
K	55	211
Mg	19	396
Ca	152	1130
Sr	20	70
Ba	1.3	0.3
Cu	*	*
Ag	*	0.3
Zn	*	*
Pb	*	0.7
Fe	*	0.1
Mn	*	0.2
Al	*	*
H_2AsO_3	*	*
H_3BO_3	39	73
PO_4	*	2.9
NH_3	–	–
SiO_2	10	14
F	2	1.1
Cl	6030	19100
Br	14	15
I	4	1
SO_4	95	891
HCO_3	181	210
Total solids (calc.)	10593	32763
Total solids (110°C)	10800	34000
Total solids (ignition)	8830	32600
Cations (anal., meq/L)	181.7	538.4
Anions (anal., meq/L)	172.6	539.2
Cations (calc., meq/L)	181.4	536.9
Anions (calc., meq/L)	172.3	538.4
pH (laboratory)	8.1	7.93
pH (calc., reservoir temp.)	7.80 (46.6°C)	7.61 (50.5°C)
Density (15.56°C)	1.008	–
Refractive index (25°C)	1.3347	1.3378
Resistivity (ohm m, 25°C)	0.549	–

- = not determined, * = below detection

Appendix B. (continued)

Table B4. Chemical composition (mg/L), physical properties and production data for formation waters from the Lower Mannville aquifer.

Sample Number	RCAH 41-1074A	RCAH 110-274	RCAH 12-675	RCAH 400-475B	RCAH 39-475A
Stratigraphic unit	Glauconitic Ss	Gething Fm.	Ostracode Zone	Glauconitic Ss.	Ostracode Zone
Location	7-26-62-4-W5M	2-30-63-4-W5M	6-27-63-8-W5M	7-13-64-1-W5M	7-13-64-1-W5M
Depth (m)	1025.3-1039.4	981.5-990.6	1286.3-1311.9	813.8-827.2	912.6-916.2
Source	DST 5	DST 3	DST 2	DST 2	DST 1
Recovery	223 m sw GTS 2548 m^3/d	183 m sw	666 m sw 122 m sl stnd gc mdy sw	357 m sw 18 m mud	283 m sw 9 m mud
Well status	SI gas well (Viking and Gething)	Abandoned	Abandoned	Gas well (Viking)	Gas well (Viking)
Li	6.6	7.1	13	13	19
Na	15300	11400	17500	20400	23800
K	117	126	133	190	369
Mg	365	304	314	253	641
Ca	881	857	731	1840	1840
Sr	110	92	120	144	132
Ba	7.7	1.6	169	3.1	9.2
Cu	*	*	0.1	*	0.1
Ag	0.3	*	*	*	*
Zn	1	*	4.7	*	*
Pb	0.6	0.9	0.4	1.5	1.7
Fe	0.2	*	*	*	0.2
Mn	*	*	0.4	1.3	0.2
Al	*	*	0.3	0.06	0.9
H_2AsO_3	*	*	*	3.8	3.8
H_3BO_3	50	37	56	62	140
PO_4	3.2	6.4	3.4	6.3	6.8
NH_3	–	–	–	37	53
SiO_2	5.1	15	7.4	14	16
F	0.6	–	1	1.1	1.4
Cl	25000	18900	28300	38000	42800
Br	82	55	68	120	130
I	9	8	10	14	14
SO_4	78	54	*	161	189
HCO_3	710	928	830	342	830
Total solids (calc.)	42633	32711	48127	61488	70806
Total solids (110°C)	44400	34500	–	66800	72300
Total solids (ignition)	40300	31700	–	61530	67100
Cations (anal., meq/L)	721.4	553.7	804.4	971.9	1145.4
Anions (anal., meq/L)	693.7	532.6	781.3	1039.6	1170.7
Cations (calc., meq/L)	719.7	552.5	801.0	969.0	1140.9
Anions (calc., meq/L)	692.1	531.5	777.9	1036.8	1166.4
pH (laboratory)	7.7	7.4	7.1	7.1	6.9
pH (calc., reservoir temp.)	7.53 (37.6°C)	7.30 (36.7°C)	6.96 (48.8°C)	7.01 (33.4°C)	6.80 (35.2°C)
Density (15.56°C)	1.032	1.026	1.0321	1.044	1.050
Refractive index (25°C)	1.3402	1.3380	1.3404 (21°C)	1.3436	1.3450
Resistivity (ohm m, 25°C)	0.152	0.182	0.155	0.142	0.132

– = not determined, * = below detection

Appendix B. (continued)

Table B4. (continued)

Sample number	RCAH 47-874B	RCAH 211-174B	RCAH 22-876	RCAH 21-876A	RCAH 7-175	RCAH 24-374A
Stratigraphic unit	Glauconitic Ss	Gething Fm.	Ostracode Zone	Ostracode Zone	Ellerslie Fm.	Gething Fm.
Location	11-36-64-12-W5M	6-33-65-5-W5M	10-23-66-2-W5M	10-23-66-2-W5M	7-29-69-1-W5M	10-23-71-4-W5M
Depth (m)	1509.4-1517.3	1055.8-1060.1	748.0-755.9	771.1-781.5	704.1-711.1	716.3-722.4
Source	DST 2	DST 1	DST 2	DST 1	DST 1	DST 2
Recovery	384 m blk sul sw 235 m brk wtr 18 m mud	38 m sw 18 m mdy sw no GTS	146 m mdy sw no GTS	335 m sw 30 m mud gas 14 m^3/d	381 m sw	381 m sw
Well status	Abandoned	Abandoned	Abandoned	Abandoned	Abandoned	Abandoned
Li	34	10	8.4	9.7	7.9	5.3
Na	25600	17200	15500	19500	15300	10600
K	1120	152	135	197	161	98
Mg	1360	366	364	401	357	190
Ca	6490	572	721	841	741	304
Sr	220	105	82	88	51	1
Ba	0.7	8.9	0.8	78	2.3	5.8
Cu	*	*	*	*	*	0.2
Ag	*	*	*	*	0.2	0.2
Zn	*	*	2.8	0.3	0.2	*
Pb	1.8	0.3	*	*	0.7	1.1
Fe	0.3	0.1	*	*	*	0.2
Mn	3.2	0.3	1.9	0.1	*	*
Al	0.6	*	*	*	*	0.5
H_2AsO_3	*	1.4	*	1.5	*	4.1
H_3BO_3	219	90	62	108	99	108
PO_4	5.8	2.4	*	*	5.9	6.1
NH_3	105	–	–	–	–	–
SiO_2	12	7.9	8.2	9.1	4.9	12
F	1.5	–	0.5	0.6	–	–
Cl	55000	27200	26200	32900	26000	16400
Br	117	12	79	97	72	39
I	10	1	12	16	15	9
SO_4	1310	23	143	104	8	16
HCO_3	270	420	952	1440	1380	1120
Total solids (calc.)	91858	46169	44167	55507	44032	28910
Total solids (110°C)	99900	53800	48200	59600	44600	29200
Total solids (ignition)	88900	49100	41300	52900	42200	25400
Cations (anal., meq/L)	1519.0	787.2	719.9	894.0	712.7	481.9
Anions (anal., meq/L)	1502.5	747.4	729.8	911.5	729.4	468.0
Cations (calc., meq/L)	1510.4	785.8	719.2	892.9	711.0	481.2
Anions (calc., meq/L)	1495.5	746.0	729.2	910.4	727.6	467.3
pH (laboratory)	6.9	7.85	7.4	6.8	7.2	8.0
pH (calc., reservoir temp.)	6.68 (48.8°C)	7.70 (35.3°C)	7.36 (30.0°C)	6.77 (30.5°C)	7.13 (29.3°C)	7.90 (29.5°C)
Density (15.56°C)	1.065	1.0404	1.033	1.040	1.032	1.022
Refractive index (25°C)	1.3488	1.3407	1.3393	1.3412	1.3406	1.3378
Resistivity (ohm m, 25°C)	0.141	–	0.156	0.130	0.153	0.297

Appendix B. (continued)

Table B5. Chemical composition (mg/L), physical properties and production data for formation waters from the Upper Mannville aquifer.

Sample Number	RCAH 5-375B	RCAH 12-275B	RCAH 91-274A	RCAH 69-474
Location	11-32-70-2-W5M	10-31-71-2-W5M	6-22-71-4-W5M	10-34-71-1-W5M
Depth (m)	422.5-426.7	441.4-450.5	508.4-530.4	636.4-639.8
Source	DST 2	DST 2	DST 2	DST 1
Recovery	30 m sw, 12 m mud GTS 1240 m^3/d	265 m sw, 18 m mud	219 m sw, 73 m mud GTS 450 m^3/d	18 m sw GTS 51 m^3/d
Well status	Abandoned	Abandoned	SI gas well (Bluesky)	SI gas well
Li	3.7	2.2	3.7	4.6
Na	9000	8520	8750	8000
K	65	46	36	59
Mg	77	122	101	97
Ca	109	83	156	130
Sr	13	6.4	25	13
Ba	0.4	1.6	2	3.9
Cu	*	*	*	*
Ag	*	*	*	*
Zn	0.4	*	*	*
Pb	*	0.7	*	*
Fe	0.1	*	*	*
Mn	*	*	*	*
Al	*	*	*	*
H_2AsO_3	*	1.9	*	9
H_3BO_3	36	56	75	85
PO_4	478	91	*	*
NH_3	319	–	*	–
SiO_2	26	19	5.1	6.3
F	13	0.4	0.5	1.4
Cl	15900	12700	12500	11000
Br	44	49	29	26
I	11	8	7	6
SO_4	146	64	26	21
HCO_3	619	390	430	1320
Total solids (calc.)	26829	22107	22111	20749
Total solids (110°C)	28000	21800	21800	19500
Total solids (ignition)	27000	19800	20600	16600
Cations (anal., meq/L)	411.5	377.8	390.4	356.1
Anions (anal., meq/L)	457.3	358.4	351.9	324.4
Cations (calc., meq/L)	411.4	377.4	390.1	355.6
Anions (calc., meq/L)	457.2	358.0	351.5	323.9
pH (laboratory)	7.15	7.2	7.8	8.2
pH (calc., reservoir temp.)	7.15 (25.5°C)	7.16 (25.9°C)	7.73 (27.3°C)	8.08 (28.1°C)
Density (15.56°C)	1.0226	1.015	1.015	1.017
Refractive index (25°C)	1.3382	1.3364	1.3366	1.3362
Resistivity (ohm m, 25°C) –	0.299	0.333	0.355	

– = not determined, * = below detection

Appendix B. (continued)

Table B6. Chemical composition (mg/L), physical properties and production data for formation waters from the Viking aquifer.

Sample Number	RCAH 17-176A	RCAH 12-976	RCAH 21-1175	RCAH 60-1176A	RCAH 14-376B
Location	10-36-62-3-W5M	7-8-62-5-W5M	7-2-62-7-W5M	7-23-62-11-W5M	7-10-67-3-W5M
Depth (m)	740.7-754.4	860.1-880.0	972.3-981.5	1359.1-1376.2	551.7-570.0
Source	DST 1	DST 1	DST 1	DST 1	DST 1
Recovery	407 m sw	137 m sw, 24 m oil	671 m sw	521 m sw 18 m oc sw 9 m oil	199 m sw 18 m mud
	GTS 2549 m^3/d	GTS 14923 m^3/d		GTS 1189 m^3/d	GTS TSTM
Well status	Abandoned	Abandoned	Abandoned	Abandoned	SI gas well (Mannville)
Li	7.4	4.6	3.9	2.3	6.3
Na	16800	11900	9860	6920	14700
K	70	127	32	22	74
Mg	461	102	76	25	312
Ca	1100	311	248	102	855
Sr	107	38	25	9.3	90
Ba	135	78	2.4	16	118
Cu	*	0.1	0.1	*	*
Ag	*	*	*	*	0.3
Zn	0.9	*	*	*	*
Pb	1.6	1.1	0.8	0.5	1.1
Fe	*	*	*	*	0.2
Mn	*	*	*	*	*
Al	*	*	*	*	0.1
H_2AsO_3	*	*	*	*	*
H_3BO_3	34	39	35	63	29
PO_4	5.6	2.8	*	*	5.3
NH_3	29	–	–	–	27
SiO_2	6.9	13	7.3	8.1	9.7
F	0.8	0.6	0.5	0.8	0.8
Cl	29400	18200	15500	9860	25000
Br	130	545	51	53	182
I	22	17	14	15	1
SO_4	16	14	54	16	16
HCO_3	1370	1710	2100	2090	140
Total solids (calc.)	49520	32494	27867	19096	41400
Total solids (110°C)	52500	33500	28800	20500	45200
Total solids (ignition)	48500	30800	26700	16300	40800
Cations (anal., meq/L)	801.5	529.8	435.3	301.3	694.3
Anions (anal., meq/L)	821.0	523.5	457.5	304.7	686.3
Cations (calc., meq/L)	799.5	529.0	434.2	300.0	694.1
Anions (calc., meq/L)	819.0	522.6	456.4	303.5	686.1
pH (laboratory)	7.6	7.5	7.5	7.9	7.47
pH (calc., reservoir temp.)	7.49 (30.3°C)	7.43 (32.7°C)	7.41 (34.9°C)	7.67 (42.0°C)	7.45 (26.5°C)
Density (15.56°C)	1.036	1.025	1.020	1.016	1.0322
Refractive index (25°C)	1.3412	1.3386	1.3372	1.3362	1.3404
Resistivity (ohm m, 25°C)	0.143	0.241	0.246	0.364	–

– = not determined, * = below detection

Appendix B. (continued)

Table B6. (continued)

Sample Number	RCAH 144-475	RCAH 10-375B	RCAH 89-274A
Location	6-36-67-4-W5M	7-1-68-4-W5M	6-22-71-4-W5M
Depth (m)	591.3-621.8	584.6-595.6	463.3-502.0
Source	DST 1	DST 1	DST 1
Recovery	40 m sw 13 m mdy sw 68 m mud, no GTS	113 m sw 37 m wc mud 18 m mud, no GTS	268 m mc sw
Well status	Abandoned	Abandoned	SI gas well (Mannville)
Li	5	5.8	3.3
Na	13100	13300	11500
K	67	186	47
Mg	277	328	156
Ca	565	541	360
Sr	70	61	49
Ba	17	73	57
Cu	*	0.1	*
Ag	*	0.3	*
Zn	*	0.3	*
Pb	0.2	0.9	0.3
Fe	*	0.1	*
Mn	0.1	0.1	0.3
Al	*	*	*
H_2AsO_3	*	*	*
H_3BO_3	32	32	38
PO_4	2.5	3.8	*
NH_3	–	–	–
SiO_2	17	9.1	5.1
F	0.6	0.4	–
Cl	22000	22500	18400
Br	66	66	50
I	14	17	9
SO_4	51	41	12
HCO_3	370	268	222
Total solids (calc.)	36603	37366	30857
Total solids (110°C)	36700	38200	42800
Total solids (ignition)	35000	35100	–
Cations (anal., meq/L)	606.8	622.1	521.0
Anions (anal., meq/L)	609.7	621.6	509.3
Cations (calc., meq/L)	605.9	621.3	520.6
Anions (calc., meq/L)	608.8	620.8	508.9
pH (laboratory)	8.2	7.9	7.9
pH (calc., reservoir temp.)	8.07 (27.4°C)	7.80 (27.1°C)	7.84 (25.0°C)
Density (15.56°C)	1.028	1.026	1.024
Refractive index (25°C)	1.3387	1.3392	1.3382
Resistivity (ohm m, 25°C)	0.188	0.154	0.243

Appendix B. (continued)

Table B7. Additional trace element determinations (mg/L) for formation waters.

Table No.	Sample Number	Co	Cr	Mo	Ni	Ti	V
B1	D-41	0.2	0.4	*	0.4	0.2	0.3
B1	W-F+	0.015	*	-	0.042	-	-
B1	RCAH 22-1274B	*	2.7	2.3	2.3	0.5	1.2
B1	RCAH 7-676A	*	1.0	*	1.6	*	*
B1	RCAH 37-175B	0.6	1.0	1.2	1.1	0.3	0.7
B1	RCAH 4-175A	0.6	2.1	1.2	1.2	0.5	0.9
B2	RCAH 111-274	0.8	1.8	*	*	0.4	0.9
B2	RCAH 69-576A	0.3	0.5	*	0.5	0.2	0.4
B3	RCAH 32-376A	*	*	*	*	*	*
B3	RCAH 195-174	0.1	0.3	*	*	0.1	0.2
B4	RCAH 41-1074A	0.1	0.4	*	0.4	0.1	0.2
B4	RCAH 110-274	0.3	0.5	*	*	0.1	0.3
B4	RCAH 12-675	0.2	0.1	*	0.3	*	*
B4	RCAH 40-475B	*	0.3	0.5	*	*	*
B4	RCAH 39-475A	*	0.2	0.5	*	*	*
B4	RCAH 47-874B	*	0.5	0.5	0.4	0.1	0.2
B4	RCAH 211-174B	0.1	0.2	*	0.2	*	0.1
B4	RCAH 22-876	*	0.1	*	*	*	*
B4	RCAH 21-876A	*	0.1	0.2	0.2	*	*
B4	RCAH 7-175	*	0.1	*	*	*	*
B4	RCAH 24-374A	0.2	0.3	0.7	0.3	0.1	0.2
B5	RCAH 5-375B	*	*	*	*	*	*
B5	RCAH 12-275B	*	*	0.5	*	*	*
B5	RCAH 91-274A	*	*	*	*	*	*
B5	RCAH 69-474	*	*	1.1	*	*	*
B6	RCAH 17-176A	0.2	0.2	0.7	*	*	*
B6	RCAH 12-976	0.5	0.2	*	0.3	*	0.1
B6	RCAH 21-1175	*	*	*	*	*	*
B6	RCAH 60-1176A	*	*	*	*	*	*
B6	RCAH 14-376B	0.2	0.2	0.4	0.3	*	0.1
B6	RCAH 144-475	*	0.1	0.2	*	*	*
B6	RCAH 10-375B	0.2	0.2	*	0.3	0.1	0.2
B6	RCAH 89-274A	0.1	0.2	0.2	0.2	0.1	0.1

* = below detection, + = Rb 2 mg/L, Be and Cd were below detection in all samples, Se was reported in 8 samples (range 0.4-7.8 mg/L), Sn was reported in 3 samples (range 1.6-1.9 mg/L)